



UNIVERSITY OF AGDER

DESIGN, MODELLING AND SIMULATION
OF
Electro-Hydraulic Self-Contained Cylinders
BASED ON
Digital Hydraulics

A Master's Thesis
IN
MECHATRONICS ENGINEERING
SPRING 2018

BY
Hamza Albaidaq
Olav Palmer Taksdal Bjørnarå

SUPERVISOR
ASST. PROF. **Damiano Padovani**

This Master's Thesis is carried out as a part of the education at the University of Agder and is therefore approved as a part of this education. However, this does not imply that the University answers for the methods that are used or the conclusions that are drawn.

UNIVERSITY OF AGDER, 2018
FACULTY OF TECHNOLOGY AND SCIENCE
DEPARTMENT OF ENGINEERING SCIENCES

Abstract

Nowadays, hydraulic cylinders are mostly powered by a separate HPU and controlled by conventional servo and proportional valves. New trends have been under development the last years. The first trend is self-contained designs where the power unit is integrated in the cylinder design. Digital hydraulics is the second new trend where conventional flow control methods are replaced by simple ON/OFF valves and digital displacement pumps.

A totally novel design would be a combination of the two mentioned trends. Designing a hydraulic cylinder that combines both the self-contained method and digital hydraulics is expected to results in many gained advantages. It would be a totally new system that has never been investigated earlier. It was not possible in the project period to find any existing products or publications related to this idea.

In this master thesis, different approaches are proposed for designing an electro-hydraulic self-contained cylinder, based on digital hydraulics. The start is a literature review of relevant publications about digital hydraulics and self-contained hydraulic cylinders. Benefits of digital hydraulics and the self-contained designs are presented.

The design process is divided into two main stages. The first is designing different concepts of the hydraulic architecture of an electro-hydraulic self-contained cylinder based on digital hydraulics that includes both ON/OFF valves and digital displacement pumps. The second stage is to develop different control approaches that can implemented on the hydraulic architectures designed in the first stage. The most significant hydraulic components used in the hydraulic design are modelled in MATLAB-Simulink. The proposed control algorithms are also built in MATLAB-Simulink models.

Five combinations of hydraulic architectures and control approaches are selected to cover all the proposed hydraulic and control systems. The combinations are then simulated with a generic load case to investigate the functionality and controllability of all systems. The most significant results such as accuracy and pressure progression are presented and analysed.

Lastly, a kinematic model of a single boom crane standing in the laboratory of the University of Agder has been implemented as a load case for one of the combinations. The goal was to investigate the possibility to drive the crane by one of the systems designed in this thesis. The results ware sufficient and indicated the feasibility of such a solution.

The results achieved in this thesis give a clear indication that an electro-hydraulic self-contained cylinder design is achievable with digital hydraulics. Many advantages are gained, such as reliability and load holding capability. A last hydraulic architecture is proposed at the end for future work to enhance the efficiency and enable the possibility of recovering energy.

Preface

This Master thesis is the final written work of our study at The Faculty of Engineering and Science, at the University of Agder in Grimstad. We would like to give a special thanks to our supervisor Asst. Prof. Damiano Padovani for the excellent support and guidance throughout this thesis.

This work has been performed by:

Hamza Albaidaq

Hamza Albaidaq

Signature

24.05.2018

Date

Olav Palmer Taksdal
Bjørnara

Olav Bjørnara

Signature

24.05.2018

Date

Abbreviations & Nomenclatures

Abbreviations

CTRL	-	Control System
DDP	-	Digital Displacement Pump
DEHC	-	Digital Electro Hydraulic Cylinder
DFCU	-	Digital Flow Control Unit
EHA	-	Electro Hydrostatic Actuator
EHC	-	Electro hydraulic Cylinder
EMC	-	Electro Mechanical Cylinder
HP	-	High Pressure
HPU	-	Hydraulic Power Unit
HYD	-	Hydraulic System
LP	-	Low Pressure
PCM	-	Pulse Code Modulation
PNM	-	Pulse Number Modulation
PWM	-	Pulse Width Modulation
SHA	-	Servo Hydraulic Actuator
SHLD	-	Servi Hybrid Linear Drive

Nomenclatures

Q_{max}	- Maximum required flow	$[\frac{m^3}{s}]$
v_{max}	- Maximum cylinder velocity	$[\frac{m}{s}]$
Q_N	- Nominal flow	$[\frac{m^3}{s}]$
Δp_N	- Nominal pressure drop	$[Pa]$
ΔV	- Working Volume	$[m^3]$
p_1	- Minimum Working Pressure	$[Pa]$
p_0	- Pre-charged Pressure (Normally $\approx 90\%$ of p_1)	$[Pa]$
p_2	- Maximum Working Pressure	$[Pa]$
n	- Polytrophic Exponent (1 for Isotherm and 1.4 for Adiabatic process)	$[-]$
Δp	- Pressure drop over valves	$[Bar]$
$x_1 \rightarrow x_n$	- 0 or 1 depending on if the valve is open or closed	
Q	- Flow over the smallest valve with 1 Pa pressure drop	$[\frac{m^3}{s}]$
Q_p	- Flow from the pump	$[\frac{m^3}{s}]$
Q_t	- Flow to the tank	$[\frac{m^3}{s}]$
A	- Cylinder A side area	$[m^2]$
A_r	- Cylinder B side area	$[m^2]$
U_p	- Opening combination of pump DFCU	$[-]$
U_t	- Opening combination of tank DFCU	$[-]$
v	- Cylinder Velocity	$[\frac{m}{s}]$
F	- Cylinder Force	$[N]$
$K_{v1} \rightarrow K_{vn}$	- Flow coefficient of different orifice/valve combinations	$[m^3 \cdot \sqrt{\frac{m}{kg}}]$
m	- Load mass	$[Kg]$
a	- Acceleration	$[\frac{m}{s^2}]$
p_a	- Pressure in piston side	$[Bar]$
p_b	- Pressure in rod side	$[Bar]$
F_f	- Friction force	$[N]$
F_{Load}	- Load force	$[N]$
f_v	- Coeff. of viscous friction for piston	$[\frac{kg}{s}]$
f_c	- Coulomb friction force	$[N]$
f_s	- Static friction time constant	$[\frac{s}{m}]$
τ_s	- Static friction time constant	$[\frac{s}{m}]$
γ	- Approximation for friction force	$[-]$
k_{lower}	- Lower Spring force	$[\frac{N}{m}]$
k_{upper}	- Upper Spring force	$[\frac{N}{m}]$
c_{lower}	- Lower Damper force	$[\frac{N \cdot s}{m}]$
c_{upper}	- Upper Damper force	$[\frac{N \cdot s}{m}]$
L	- Length of cylinder	$[m]$
Q_A	- Flow into cylinder chamber A	$[\frac{m^3}{s}]$
Q_B	- Flow out of cylinder chamber B	$[\frac{m^3}{s}]$
v	- Cylinder velocity	$[\frac{m}{s}]$
x	- Cylinder position	$[m]$
V_{A0}	- Dead volume chamber A	$[m^3]$
V_{B0}	- Dead volume chamber B	$[m^3]$
β	- Oil bulk modulus	$[Pa]$
\dot{p}_a	- Pressure gradient chamber A	$[\frac{Pa}{s}]$
\dot{p}_b	- Pressure gradient chamber B	$[\frac{Pa}{s}]$

C	- Capacitance based accumulator model	$[\frac{m^3}{bar}]$
V_{lp}	- Line volume	$[m^3]$
V_0	- Accumulator gas volume	$[m^3]$
p_{lp}	- Line pressure	$[bar]$
p_0	- Accumulator pre-charge pressure	$[bar]$
N	- Polytropic index	$[-]$
\dot{p}	- Change in pressure	$[Bar]$
Q_{ac}	- Flow to accumulator	$[\frac{l}{min}]$
Re	- Reynolds number	$[-]$
V_{line}	- Fluid velocity	$[\frac{m}{s}]$
D_{line}	- Inner diameter of pipe	$[m]$
ν	- Kinematic viscosity of the oil	$[\frac{m^2}{s}]$
μ	- Dynamic viscosity of the oil	$[\frac{kg}{m \cdot s}]$
L_{line}	- Length of pipe	$[m]$
P_{IN}	- Input power	$[Watt]$
p_p	- Pump pressure	$[Pa]$
$\eta_{Combined}$	- Combined efficiency of motor and pump	$[-]$
P_{OUT}	- Output power	$[Watt]$
M_{eq}	- Equivalent inertial load	$[kg]$
G_{eq}	- Equivalent gravitational load	$[N]$
C_{eq}	- Equivalent Coriolis force	$[\frac{kg}{m}]$
L_{min}	- Retracted cylinder length	$[m]$
J_{cm}	- Inertia around combined center of mass	$[kg \cdot m^2]$
m_{cm}	- Combined mass of boom and payload	$[kg]$

Contents

Abstract	I
Preface	III
Abbreviations & Nomenclatures	V
List of Figures	XI
List of Tables	XIII
1 Introduction	1
1.1 Motivation	1
1.2 Problem Statement	3
1.3 Report Outline	4
2 Theoretical Background	5
2.1 Electro-Hydraulic Actuators	6
2.1.1 Benefits and Advantages	6
2.1.2 Sample Products	7
2.1.3 Potential Applications	8
2.2 Digital Hydraulics	9
2.2.1 ON/OFF Valves	11
2.2.2 Control Methods	13
2.2.3 Comparison of Control Methods	20
2.2.4 Digital Displacement Pumps	23
3 System Design	25
3.1 Hydraulic System 1	25
3.1.1 Power Unit	25
3.1.2 DFCU	26
3.2 Hydraulic System 2	26
3.2.1 Power Unit	27
3.2.2 DFCU	27
3.2.3 Switch	27
3.3 Hydraulic System 3	27
3.3.1 Power Unit	28
3.3.2 DFCU	28
3.3.3 Switch	28
3.4 Hydraulic System 4	28
3.4.1 Power Unit	29
3.4.2 DFCU	29
3.4.3 Switch	29
3.5 Dimensioning of Components	30
4 Control Design	31
4.1 Control System 1	31

4.2	Control System 2	32
4.3	Control System 3	34
4.3.1	Two Edge Control	34
4.3.2	Four Edge Control	40
5	System Modelling	41
5.1	Valves	41
5.1.1	Dimensioning of orifices for valves sizes adjustment	42
5.1.2	Valve delay and response	43
5.2	Cylinder	46
5.3	Accumulator	49
5.4	Line losses	50
5.5	Pump and electrical motor	50
5.6	Pressure relief valve	51
5.7	Cooler and filter	51
5.8	Bulk modulus	51
5.9	Power	51
6	Results	53
6.1	Load case	53
6.2	System simulation and analysis	55
6.2.1	Combination 1	56
6.2.2	Combination 2	59
6.2.3	Combination 3	62
6.2.4	Combination 4	65
6.2.5	Combination 5	68
6.3	Simulation of a single-boom crane	71
6.3.1	Crane kinematic model	71
6.3.2	Simulations results and comparison	74
7	Discussion	77
7.1	Advantages	78
7.2	Challenges	79
8	Conclusion & Future Work	81
8.1	Conclusions	81
8.2	Future Work	82
	Bibliography	86
A	Simulations Parameters	87
B	Sample valve data sheet	89
C	Expressions for load components	97

List of Figures

1.1	Existing electro-mechanical and hydraulic actuators	1
1.2	Target architecture of a DEHC	2
2.1	Topology	5
2.2	Typical simplified HPU supplying different actuators	6
2.3	Sample products from Rexroth and SERVI	7
2.4	Operating principle of SHA-A1	8
2.5	Typical piping on offshore crane	9
2.6	Example for digital flow control unit	10
2.7	Proportional flow compared to discretized flow	10
2.8	The 128 valve manifold	12
2.9	(a) Equally coded valve system prototype (b) Used on/off vales	12
2.10	States combinations in PCM and PNM systems	14
2.11	Flow states with different number of valves in parallel PCM method	15
2.12	Fault effect in a 6 valve PCM coded DFCU	15
2.13	Rearranged valves configuration by faults	16
2.14	Transient uncertainty of 4 valve PCM and 15 valve PNM	17
2.15	Effect of valve delay on the combined valve opening	17
2.16	Different coding schemes for PWM combined with parallel valve control	18
2.17	Hydraulic stepper schematic	19
2.18	Different control methods schematics	20
2.19	20 mm Step response by (a)Bang-Bang (b)PWM (c)Stepping (d)PCM	21
2.20	Digital displacement pump types	23
2.21	Sample products from Rexroth and ARTEMIS	23
3.1	Designed system based on 4 DFCU's	25
3.2	Designed system based on 2 DFCU and 1 4/2 valve	26
3.3	4/2 ways valve represented by 4 ON/OFF valves	27
3.4	Designed system based on 6 binary sized pumps	28
3.5	Designed system based on 3 DFCU and no high pressure accumulator	29
4.1	Block diagram	31
4.2	Detailed block diagram	32
4.3	Block diagram	33
4.4	Detailed block diagram	33
4.5	Two/Four edge control	34
4.6	Simplified block diagram of two edge control	35
4.7	Pressure in cylinder chamber A with different valve openings with $p_p = 120$ Bar, $p_t = 4$ Bar and $F = -10000$ N	36
4.8	Pressure in cylinder chamber B with different valve openings with $p_p = 120$ Bar, $p_t = 4$ Bar and $F = -10000$ N	36
4.9	Cylinder velocity with different valve openings with $p_p = 120$ Bar, $p_t = 4$ Bar and $F = -10000$ N	37
4.10	View on cylinder velocity controllability	37

4.11	Possible velocities with $p_p = 120$ bar $p_t = 4$ bar and $F = -10000$ N when chamber B pressure is wanted to be kept between 50-60 bar	38
4.12	Pressures in chamber B within the range of 50-60 bar with $p_p = 120$ bar $p_t = 4$ bar and $F = -10000$ N	38
4.13	Velocity resolution with $p_p = 120$ bar $p_t = 4$ bar and $F = 10000$ N and chamber B pressure kept within 50-60 bar	39
4.14	Difference in low velocity controllability between two and four edge control with 4-valves DFCU	40
5.1	Flow curves for three different orifice sizes	41
5.2	Orifice adjustment of valves	42
5.3	Simulated valve response with $T_s = 10ms$	44
5.4	Simulink model for valve	44
5.5	Operation modes of a switching valve in case of using digital control methods	45
5.6	Cylinder load case	46
5.7	Measured friction force	47
5.8	Modelled friction based on measured data	48
6.1	Study load case	53
6.2	Position reference and load case	54
6.3	Plots of system response to the 4 DFCU system	56
6.4	Position error by different valve response times in combination 1	58
6.5	Position error by different Bulk modulus in combination 1	58
6.6	Plots of system response to the 4 DFCU system with CTRL 3 with cost function (4.5)	59
6.7	Position error by different valve response times in combination 2	61
6.8	Position error by different Bulk modulus in combination 2	61
6.9	Plots of system response to the 2 DFCU system	62
6.10	Position error by different valve response times in combination 3	64
6.11	Position error by different Bulk modulus in combination 3	64
6.12	Plots of system response to the DDP system	65
6.13	Position error by different valve response times in combination 4	67
6.14	Position error by different Bulk modulus in combination 4	67
6.15	Plots of system response to the DDP system	68
6.16	Position error by different valve response times in combination 5	69
6.17	Position error by different Bulk modulus in combination 5	70
6.18	Picture and main components of test crane	71
6.19	Main dimensions of test crane	71
6.20	Equivalent load components over the length of the cylinder	72
6.21	Hydraulic load sensing system used in the experiment	73
6.22	Performed working cycles	74
6.23	Results comparison for working cycle 1	75
6.24	Results comparison for working cycle 2	75
6.25	Results comparison for working cycle 3	76
6.26	Results comparison for working cycle 4	76
8.1	Proposed hybrid system based on 6 binary sized pumps	82
8.2	Proposed driving and energy recovery modes	83

List of Tables

2.1	Comparison of ON/OFF valves vs traditional Servo/Proportional valves	11
2.2	Commercial ON/OFF valves measurements	13
2.3	Control Methods Comparison	22
4.1	Flow direction controller	32
6.1	Selected and Simulated Combinations	55
6.2	Reference pressure for the load case with cost function (4.5)	59
7.1	System combinations results weighting	77

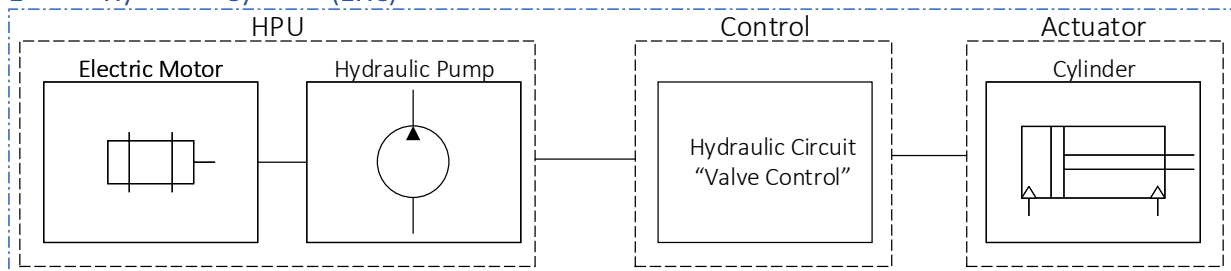
1 | Introduction

1.1 Motivation

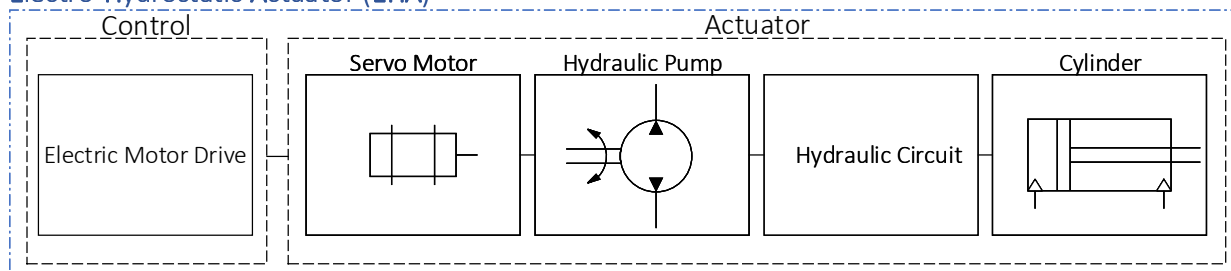
Hydraulics is one of the most used power transmission systems world wide. It is known for its reliability and high power concentration. Hydraulic cylinders are found in a large portion of equipment and instruments in the different areas such as transportation and production. These are known for both high power concentration and high precision when used with corresponding hydraulic control systems. Methodology of controlling cylinders has been developed a lot in the last decades to improve efficiency and precision. However, the main focus remained on treating cylinders and hydraulic control system as two different sections.

Nowadays, different solutions have been developed and some are still under development to compete with and replace the conventional solution of an Electro-Hydraulic Cylinder (EHC). Electro-Hydrostatic Actuator (EHA) and Electro-Mechanical Cylinder are some of the modern alternatives for EHA. Figure 1.1 presents block diagrams with working and controlling principles for the three mentioned actuating systems.

Electro-Hydraulic Cylinder (EHC)



Electro-Hydrostatic Actuator (EHA)



Electro-Mechanical Cylinder (EMC)

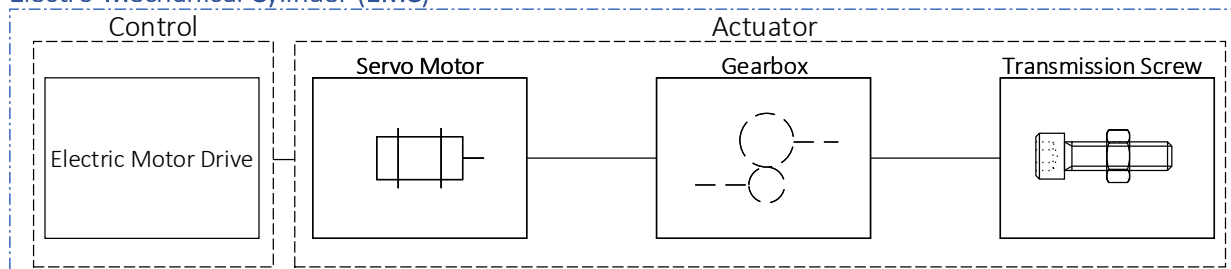


Figure 1.1: Existing electro-mechanical and hydraulic actuators

This thesis will look into developing a novel Digital Electro-Hydraulic Cylinder (DEHC). This means that the unit includes all the components in a conventional system, where these are normally built and installed separately. Additionally, digital hydraulics based on ON/OFF valves and Digital Displacement Pumps (DDP) is used for control. The goal product will only have an electrical connection to the operation base for driving and controlling. This will lead to enhanced flexibility in implementing due to plug and play design. Such a solutions also lowers the threshold for using hydraulic actuators for applications with space limitations for the separate hydraulic power unit (HPU). The installation process would not require special knowledge about hydraulics, and could easily be performed by a mechanical/electrical worker. The main benefits of using digital hydraulics are the expected lower costs, reliability, simplicity and fault tolerance. Earlier research show a large unused potential of digital hydraulics. Figure 1.2 shows a possible architecture of the target DEHC.

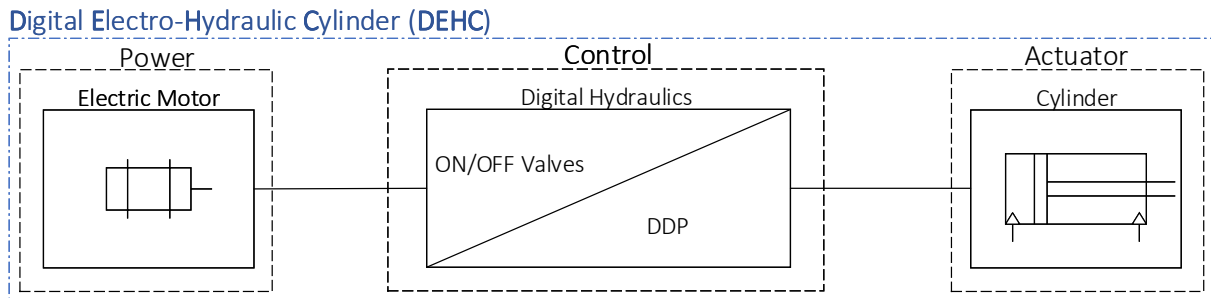


Figure 1.2: Target architecture of a DEHC

1.2 Problem Statement

The main purpose for this thesis is designing, modelling, simulation and control of an electro-hydraulic self-contained cylinder based on digital hydraulics. The thesis is started with the theoretical background and a state of art review. The following tasks are performed:

- Design several hydraulic architecture concepts for the solution based on digital hydraulics.
- Design several control algorithms that can be implemented on the hydraulic systems.
- Model the most significant hydraulic components.
- Select some combination between the hydraulic architectures and control algorithms thus all hydraulic and control concepts are included.
- Simulating all combinations with the same load case and criteria.
- Present all significant results to show the performance of each combination.
- Compare the results of the different combinations against each other.
- Draw a conclusion from the achieved results.
- Present important future work aspects.

1.3 Report Outline

Chapter 1 - Introduction

The introduction includes a brief motivation for the use of self contained cylinders and digital hydraulics. Then the problem statement is presented.

Chapter 2 - Theoretical Background

This chapter starts with a brief look into the self contained cylinders and benefits to this design. A potential application case is also mentioned followed by an introduction to digital hydraulic. The focus is on the key component in digital hydraulics that are ON/OFF valves, digital displacement pumps and the different control methods.

Chapter 3 - System Design

This chapter introduces four different hydraulic designs. These are designed in different ways based on both ON/OFF valves digital displacement pumps.

Chapter 4 - Control Design

Three different control systems are presented. The two first are simple feed forward and feedback controllers based on the flow and velocity relationship of the cylinder. The third is a more advanced method based on the steady state equations of the system.

Chapter 5 - System Analysing and Modelling

In this chapter, the governing equations applied for modelling and simulation are presented with eventual assumptions.

Chapter 6 - Results

The common load case for all systems is presented. Five selected combinations between hydraulic systems and control systems are simulated. Results are presented and discussed. One of the combinations is also tested on a real crane kinematic model and compared with the results of a conventional hydraulic system.

Chapter 7 - Discussion

Results from Chapter 6 are summarized and discussed. The different system combinations are rated related to different criteria.

Chapter 8 - Conclusion & Future Work

A conclusion is drafted from the whole thesis and results. Potential future works are presented.

2 | Theoretical Background

Linear actuators are needed and used in mechanical systems worldwide. These are used to achieve translational movements such as in pressing machines, but also for rotational movements as in lifting equipment. The main types of linear actuators are the following:

- Pneumatic Cylinders that are used for applications with high speed requirements and light loads.
- Hydraulic Cylinders are used for application with high actuation force requirements.
- Electrical Linear Actuators are used for applications with space limitations and where installation simplicity is required.

The focus in this thesis will be on hydraulic cylinders. The goal is to design a compact system (Self Contained) where digital hydraulics is to be implemented instead of conventional hydraulics. In **Figure 2.1** a topology view of different systems is shown. Split systems with external HPU are not considered.

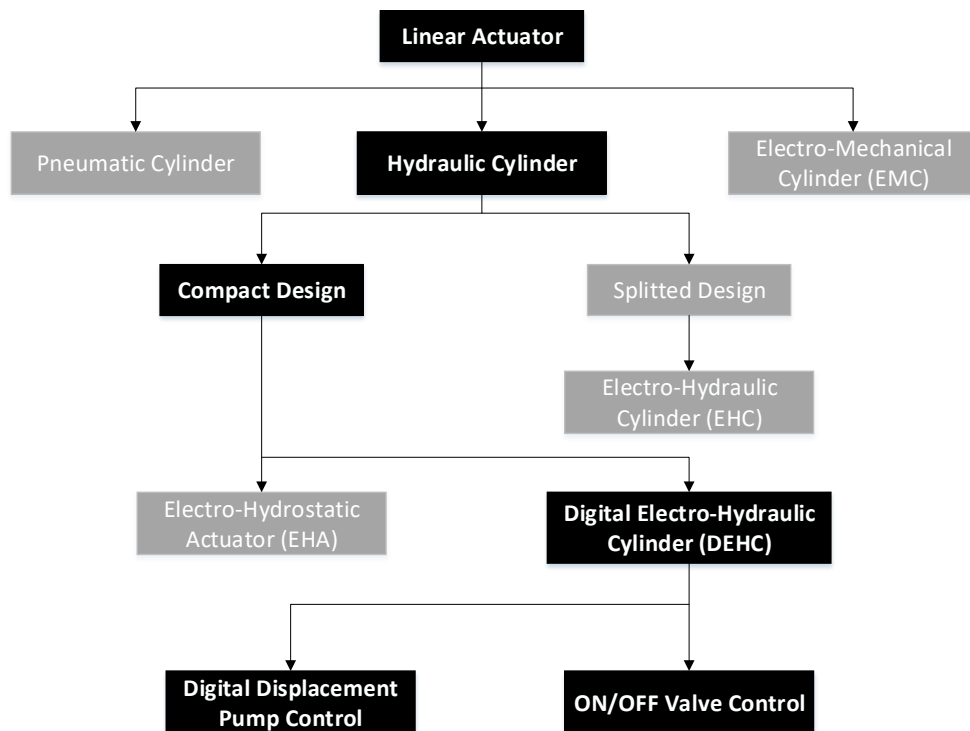


Figure 2.1: Topology

2.1 Electro-Hydraulic Actuators

Conventionally, hydraulic cylinders have always been used in combination with a separate HPU and separate valve block. **Figure 2.2** presents a typical schematics of a simple HPU design supplying different actuators.

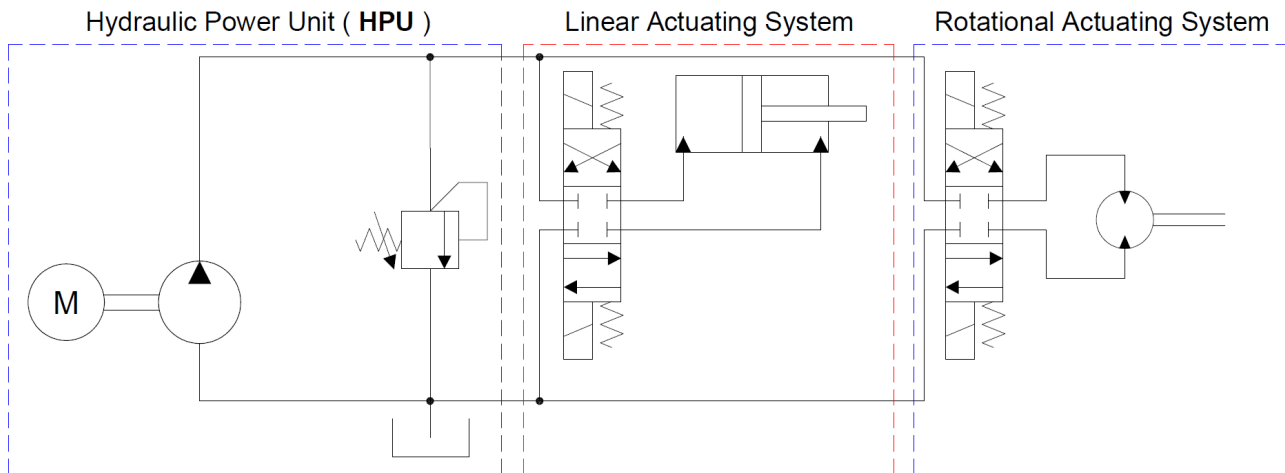


Figure 2.2: Typical simplified HPU supplying different actuators

In a EHA, all the hydraulic components are built in a compact unit with only electrical wiring for control and power supply purposes. There are a few products on the market with different solutions based on a one speed control or electrical drive control. The first solution; has limited controllability and application area, the second solution; has much better controllability however, it has higher costs than conventional solutions. Finally, it is much easier to generate a linear motion with a hydraulic cylinder than a electro-mechanic system.

2.1.1 Benefits and Advantages

There are many benefits to be gained by implementing EHA instead of conventional solutions. Combining hydraulics, electrics and a compact system make it possible to gain the benefits of each system while removing some of the disadvantages.

Benefits of Hydraulics

Hydraulic actuators are known for their high-power concentration which results in a high actuation force. The relative physical size of a hydraulic actuator compared to the produced force is relatively small when compared with other types of actuators. Another advantage of hydraulic cylinder is robustness, durability and relatively long periods without maintenance. Safety is a very important benefit in hydraulic cylinder. It is relatively easy to implement overload protection using pressure relief valves. There is also no need for a holding force as this is achieved by simply closing the valves.

Benefits of Electrics

In a EHA, the actuator has only electrical connection to the operation base. Avoiding long piping and having the flow/pressure source integrated in the actuator itself, helps improving the dynamics and the accuracy of the system. Additionally, it reduces and simplifies the installation and maintenance.

Benefits of System

A EHA system is expected to have significant advantages compared to conventional split solution. Some of the expected advantages are the following:

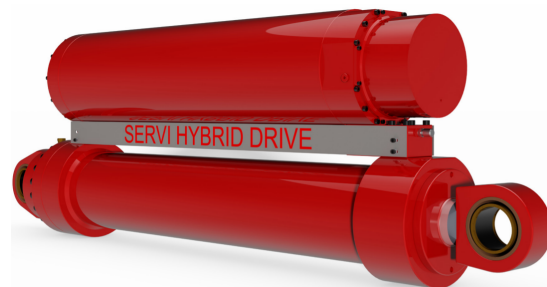
- Simplicity of installation. Few interface connections and compact design simplifies the installation and consequently reduces costs.
- Energy saving by eliminating pressure losses in long pipes and by significantly reducing power losses wasted by idle running of the main HPU.
- EHA requires significantly less consideration when designing the mechanical system where it can be implemented. There is no need for space consideration regarding the HPU, valve blocks and piping.
- Little maintenance due to closed system and no long pipes and hoses.
- As a plug-and-play unit, it lowers the threshold of implementing such a solution significantly.

2.1.2 Sample Products

There are just a few manufacturers developing products with EHA solutions. The Servo-Hydraulic Actuator (SHA) from Bosch Rexroth in **Figure 2.3a** and the Servi Hybrid Linear Drive (SHLD) in **Figure 2.3b** from SERVI are two good examples. Both products are based on a bidirectional hydraulic pump which is driven by a variable speed electrical motor. The basic principle here is to drive the pump in a specific direction and specific speed to achieve the desired extraction or retraction of the hydraulic cylinder. A volume compensator is integrated to compensate for the difference in volume between the piston and the rod side of the cylinder.



(a) Servo-hydraulic actuator (SHA) [1]



(b) Servi hybrid linear drive (SHLD) [2]

Figure 2.3: Sample products from Rexroth and SERVI

The working principle and schematics for SHA-A1 from Rexroth Bosch are shown in **Figure 2.4**. When the cylinder is extracting 2.4a, the pump is displacing the fluid from A to B. The fluid

flows from the rod side X2 to the piston side X1. The difference in volume is compensated from the reservoir into X1. The opposite procedure is run when the cylinder is retracting 2.4b. The pump is displacing the fluid from B-A forcing the piston to retract. The outlet fluid from piston side is distributed between the pump and the reservoir to compensate for volume difference between the cylinders sides. The check valves ensure that the rod side of the cylinder always has higher pressure than the piston side. This is important to achieve the desired functionality of the reservoir.

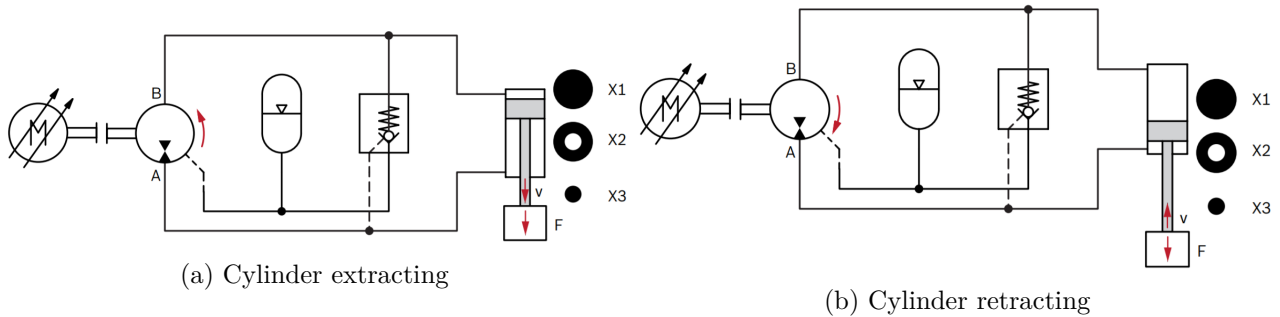


Figure 2.4: Operating principle of SHA-A1 [3]

2.1.3 Potential Applications

Hydraulic cylinders are one of the most used actuator type in the offshore industry because of the reliability, safety, robustness and high-power concentration. Electromechanical Cylinders (EMC) have been under large development in the last decades and as a result, implemented in many different application areas replacing hydraulic cylinders. However, there are still many applications where the EMC have not been implemented or even tested to replace hydraulic cylinders. Applications, that demand a very high grade of power concentration, safety and reliability, are still depending completely on hydraulic cylinders. Also, the high cost and fatal consequences of a function failure are the most used arguments for not implementing EMC in such applications.

The digital electro-hydraulic actuator (DEHC) in this thesis is combining the benefits of the conventional hydraulic cylinder and the advantages of the EMC over hydraulic cylinders. DEHC has basically all the properties of the hydraulic cylinders used today such as safety, reliability and high-power concentration. At the same time, it has the benefits of the EMC specially when considering efficiency and cost reduction.

Large scale cranes are widely used offshore. The working radius of offshore cranes are sometimes over 50 m. Many of these cranes are used in drilling and are designed to fit different tools such as riser yokes and pipe gripper yokes. These tools are normally actuated by hydraulic cylinders. These large-scale cranes with the possibility to fit other tools demand long pipes and hoses from the main HPU out to the crane tip where the tools are connected. Combining this with the pipes and hoses to the actuators, results in large numbers of pipes and hoses to operate the crane. Consequently, the installation and maintenance costs are increased in addition to increased possibility of failure due to corrosion and fatigue. Power loss and increased response time are also critical drawbacks of this solution.



Figure 2.5: Typical piping on offshore crane (yellow marked) [4]

Implementing DEHC on these cranes over today's solutions would have the following advantages:

- Reducing fabrication, installation and maintenance costs by removing a significant amount of piping.
- Increased safety by reduction in area of lines exposed to corrosion and fatigue.
- Simplifying the tools connection process by eliminating all hydraulic lines.
- Free up space in the king by reducing the size of the main HPU.
- Enhanced response and precision by reducing the flexibility in the hydraulic system.
- Improved efficiency through eliminating pressure losses in long pipes and reduction of idle running HPU.

2.2 Digital Hydraulics

Generally, a digital system is a system based on discrete valued components and signals. In the case of hydraulics, discrete values are to be found in the components such as valves and pumps controlling the flow discretely. The core components in digital hydraulic systems are the ON/OFF valves and the digital displacement pumps (DDP). The ON/OFF valves replace the conventional servo and proportional valves to control the flow. A continuous behaviour of the flow coming out from a servo or proportional valve is then replaced with a discretely valued flow through switching the ON/OFF valves between open and closed position. **Figure 2.6** shows a configuration of a digital flow control unit (DFCU) using the ON/OFF valves.

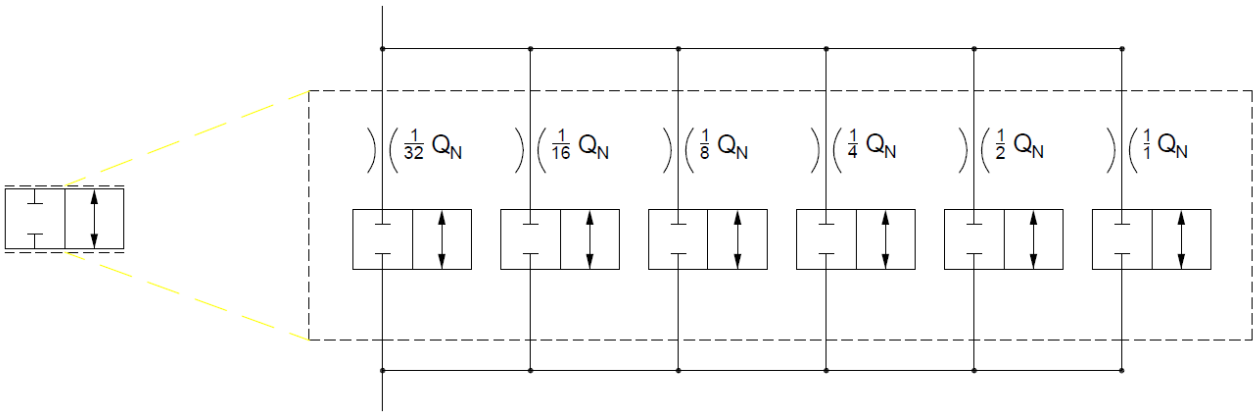


Figure 2.6: Example for digital flow control unit

Flow in servo and proportional valves has a non-linear and proportional relationship to the opening of the valve. A DFCU provides the possibility to get a stepped linear flow. The resolution and the size of the steps depend on the number of the ON/OFF valves in the DFCU. A comparison between a proportional flow and digital flow from two DFCU with different resolution is shown in **Figure 2.7**

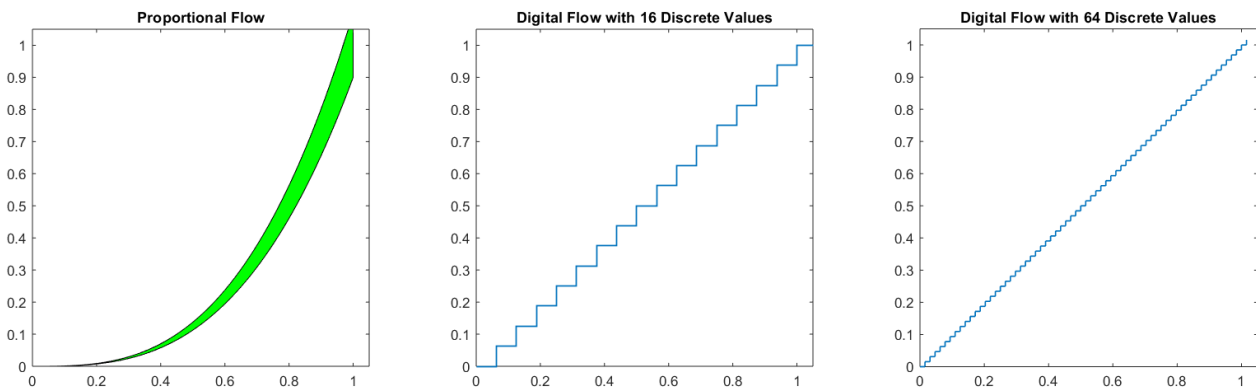


Figure 2.7: Proportional flow compared to discretized flow

Benefits and Advantages

There are numerous benefits of using digital hydraulics over conventional hydraulics according to [5] and some challenges. The benefits include:

- The components can be simpler and more robust, thus have a higher reliability.
- ON/OFF valves can be faster than servo/proportional valves, which could give better performance.
- More energy efficient systems.
- The control system determines the characteristics instead of valve spool.

Challenges

The disadvantages/challenges include:

- Noise and pressure peaks.
- If a high switching frequency of the valves are used (PWM), the lifetime of the valves can suffer significantly.
- The size and price can be high with parallel connected solutions with the valves on the market today.
- The control can be much more complicated than conventional systems.

2.2.1 ON/OFF Valves

To get good results from digital hydraulics the most important component are the ON/OFF valves. A ON/OFF valve is a valve that is either closed or fully opened, it cannot be controlled in between. Thus, to get different amounts of flow, several of these valves can be combined in different structures or a single valve can open and close at high frequencies, these methods will be discussed in the following section. There is a series of properties important for these valves to obtain good results in a digital hydraulic system. These include fast response time, large flow and low uncertainty in response time [6]. Some benefits of the simple ON/OFF valves versus a traditional servo/proportional valve is highlighted in **Table 2.1**, where points in green are assumed better than the opposing point written in red.

Table 2.1: Comparison of ON/OFF valves vs traditional Servo/Proportional valves

ON/OFF Valve	Proportional/Servo Valve
<ul style="list-style-type: none"> • Controllable open or closed • Simple electronics • Loose tolerances • Close to or zero leakage • No need for position sensor • No need for linear solenoid • Cheap • Stable if maximum flow is not exceeded 	<ul style="list-style-type: none"> • Close to Continuous Controllability • Complicated electronics • Tight tolerances • Potential large leakage • Needs position Sensor • Requires linear solenoid • Expensive • Potential instability at certain conditions related to flow, openings and fluid viscosities

Most digital hydraulic systems will need several ON/OFF valves which leads to space challenges. The problem is, ON/OFF valves on the market today are relatively large and slow. However, improvements to these are being made using miniature valves. One such design of a valve package is presented in [7]. In this design 128 same size micro valves are integrated in a manifold shown in **Figure 2.8**.

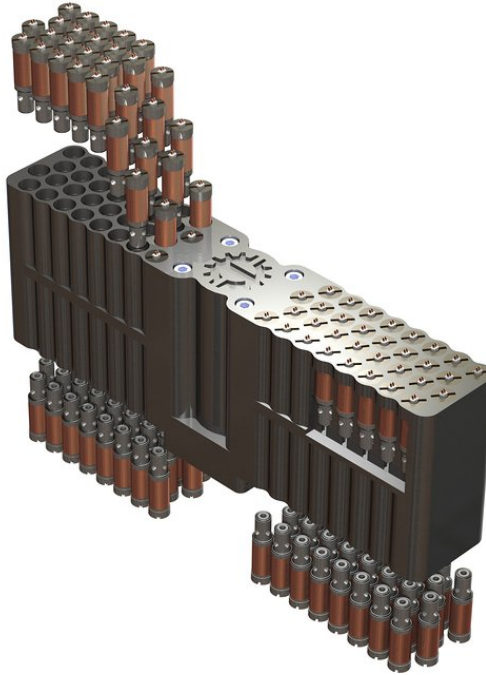


Figure 2.8: The 128 valve manifold [8]

Another example is presented in [9], where 32 miniature valves form the four metering edges. This package is (176x49x72 mm) large and has approximately 30 l/min flow with 5 bar pressure drop and 2 ms response time. This shows that it is possible to get multiple high performance ON/OFF valves integrated in a small component. This is necessary to keep the overall size of the digital hydraulic system down. An prototype example of a similar valve package was also used in [10], however, this package only had 16 valves and can be seen in **Figure 2.9**.

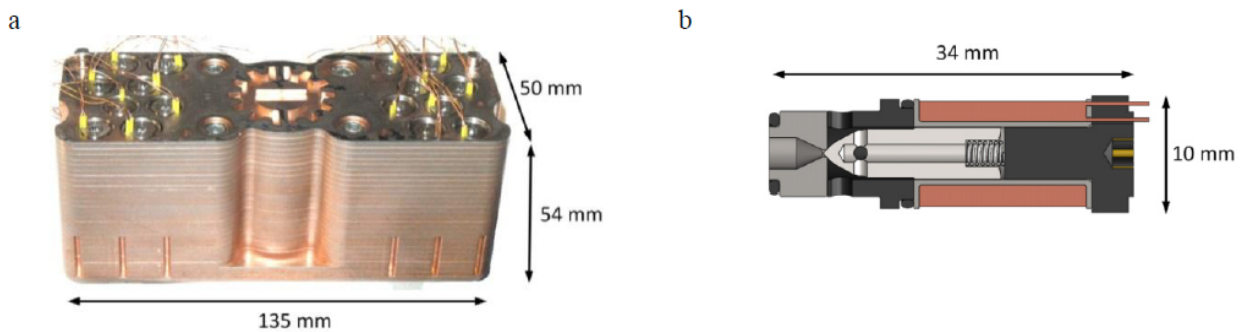


Figure 2.9: (a) Equally coded valve system prototype (b) Used on/off vales [10]

Another important part of the valves in digital hydraulics is the control electronics. It is important that the valves have these specifications according to [5].







- Overvoltage for fast current rise.
- Negative voltage for fast current drop.
- Low voltage to keep the valve position to reduce energy consumption.

The two first points are important because of the need for fast switching of the valves to achieve good controllability and stability of the system. The third point is important because many valves may be used and thus having a low energy consumption on the individual valves is important.

Sample Valves

Increased interest in digital hydraulics has resulted in some development in the ON/OFF valves production. Nowadays, there are some mass production valves in the market that fits the requirements of digital hydraulics. Here, the main criteria is the response time T_s . **Table 2.2** presents an overview of some ready to market valves collected in [11].

Table 2.2: Commercial ON/OFF valves measurements [11]

	SUN DLV	Rexroth SEC6	Rexroth WES	Parker GS02-73	LCM FSVi4.1	Bucher WS22GD
						
T_s	10 ms	7-10 ms	5 ms	5 ms	< 3 ms	5-30 ms
Q_{N5bar}	0,12 l/min	7 l/min	45 l/min	1 l/min	5 l/min	1 l/min
Q_{max}	1 l/min	25 l/min	200 l/min	- l/min	25 l/min	30 l/min
p_{max}	350 bar	420 bar	350 bar	210 bar	300 bar	350 bar
f_{max}	13 Hz	40 Hz	10 Hz	- Hz	200-500Hz	- Hz
€	~100	~600	-	~70	~1500	~150

2.2.2 Control Methods

There are different ways to utilize ON/OFF valves to control a systems motion. Four such methods will be explained in detail in the following sections. First with an explanation of how the method works followed by a comparison of all the methods.

Bang-Bang

There is "Bang-Bang" control, this is the simplest form of control where a valve is simply opened and closed right as the target position is achieved. This will result in a simple control algorithm, however the obvious drawbacks will be poor accuracy, one velocity and pressure peaks.

Parallel Valves System (PNM/PCM)

Parallel connected valves, this idea will also use "Bang-Bang" control, however, by having differently sized or multiple same sized valves in parallel one can achieve different flows. Pulse number modulation (PNM) is when multiple same sized valves are connected in parallel. Assuming 10 same sized valves are connected in parallel and can be opened independently, 10 different flow steps can be generated. So, to generate many different flows a lot of valves are needed. A different approach is pulse code modulation (PCM) here the valves in parallel are sized differently.

One example of 4 valves in parallel where the size ratio of the valves are 1:2:4:8, this will give 15 different flow steps according to **Eq.(2.1)** where n is the number of parallel connected valves.

$$States = 2^n - 1 \tag{2.1}$$

This can be compared to the PNM method like seen in **Figure 2.10** where it is seen that 15 valves are needed to get the same resolution as the PCM method.

Binary DFCU						PNM DFCU																
Net flow	Valve 1, Q	Valve 2, 2Q	Valve 3, 4Q	Valve 4, 8Q	State	Net flow	Valve 1, Q	Valve 2, Q	Valve 3, Q	Valve 4, Q	Valve 5, Q	Valve 6, Q	Valve 7, Q	Valve 8, Q	Valve 9, Q	Valve 10, Q	Valve 11, Q	Valve 12, Q	Valve 13, Q	Valve 14, Q	Valve 15, Q	
0	0	0	0	0	0	0	0	0	0	0	0	0	0	0	0	0	0	0	0	0	0	0
1xQ	1	0	0	0	1	1xQ	1	0	0	0	0	0	0	0	0	0	0	0	0	0	0	0
2xQ	0	1	0	0	2	2xQ	1	1	0	0	0	0	0	0	0	0	0	0	0	0	0	0
3xQ	1	1	0	0	3	3xQ	1	1	1	0	0	0	0	0	0	0	0	0	0	0	0	0
4xQ	0	0	1	0	4	4xQ	1	1	1	1	0	0	0	0	0	0	0	0	0	0	0	0
5xQ	1	0	1	0	5	5xQ	1	1	1	1	1	0	0	0	0	0	0	0	0	0	0	0
6xQ	0	1	1	0	6	6xQ	1	1	1	1	1	1	0	0	0	0	0	0	0	0	0	0
7xQ	1	1	1	0	7	7xQ	1	1	1	1	1	1	1	0	0	0	0	0	0	0	0	0
8xQ	0	0	0	1	8	8xQ	1	1	1	1	1	1	1	1	0	0	0	0	0	0	0	0
9xQ	1	0	0	1	9	9xQ	1	1	1	1	1	1	1	1	1	0	0	0	0	0	0	0
10xQ	0	1	0	1	10	10xQ	1	1	1	1	1	1	1	1	1	1	0	0	0	0	0	0
11xQ	1	1	0	1	11	11xQ	1	1	1	1	1	1	1	1	1	1	1	0	0	0	0	0
12xQ	0	0	1	1	12	12xQ	1	1	1	1	1	1	1	1	1	1	1	1	0	0	0	0
13xQ	1	0	1	1	13	13xQ	1	1	1	1	1	1	1	1	1	1	1	1	1	0	0	0
14xQ	0	1	1	1	14	14xQ	1	1	1	1	1	1	1	1	1	1	1	1	1	1	0	0
15xQ	1	1	1	1	15	15xQ	1	1	1	1	1	1	1	1	1	1	1	1	1	1	1	1

Figure 2.10: States combinations in PCM and PNM systems [12]

More examples of valve resolutions with PCM can be seen in **Figure 2.11**.

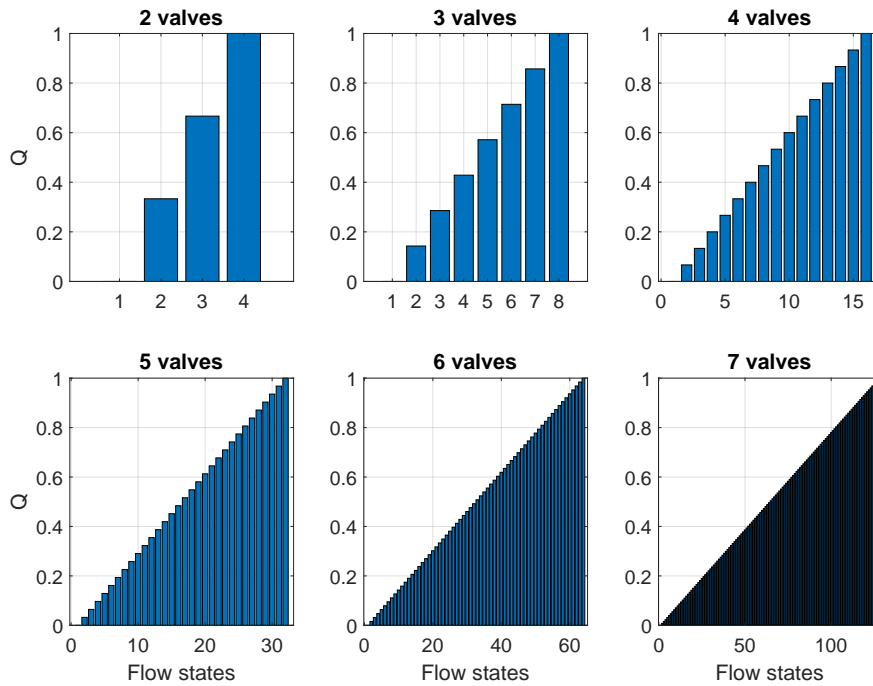


Figure 2.11: Flow states with different number of valves in parallel PCM method

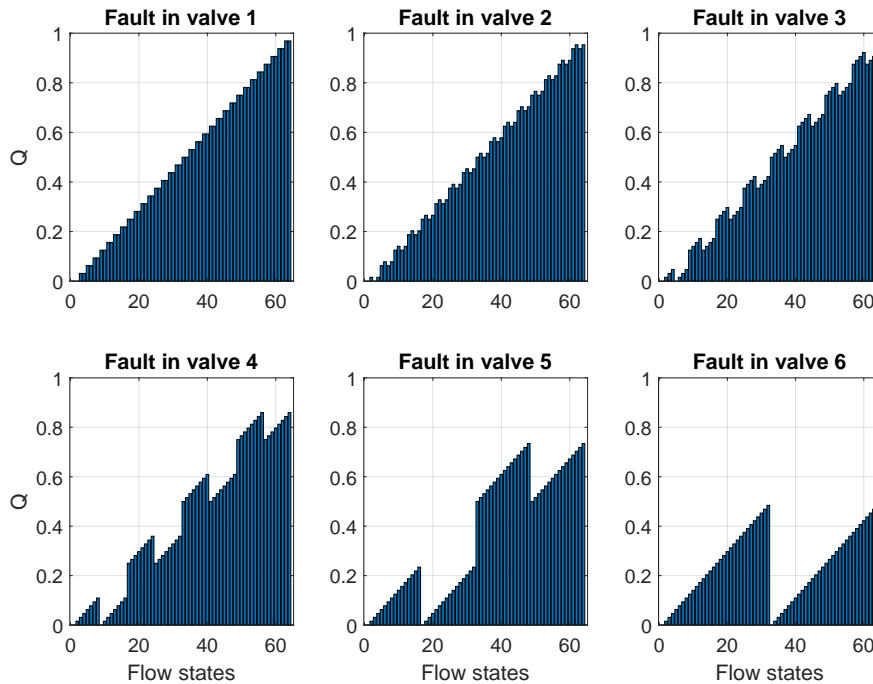


Figure 2.12: Fault effect in a 6 valve PCM coded DFCU

Another interesting feature of the PCM/PNM are the effects of a fault in a valve either not opening or closing. Both cases can be compensated for if the system has implemented some sort of fault detection and software compensation for the given fault. In **Figure 2.12**, the effects of some valves not opening can be seen in a PCM coded DFCU. **Figure 2.13** shows the resorted configuration after fault detection in one of the valve.

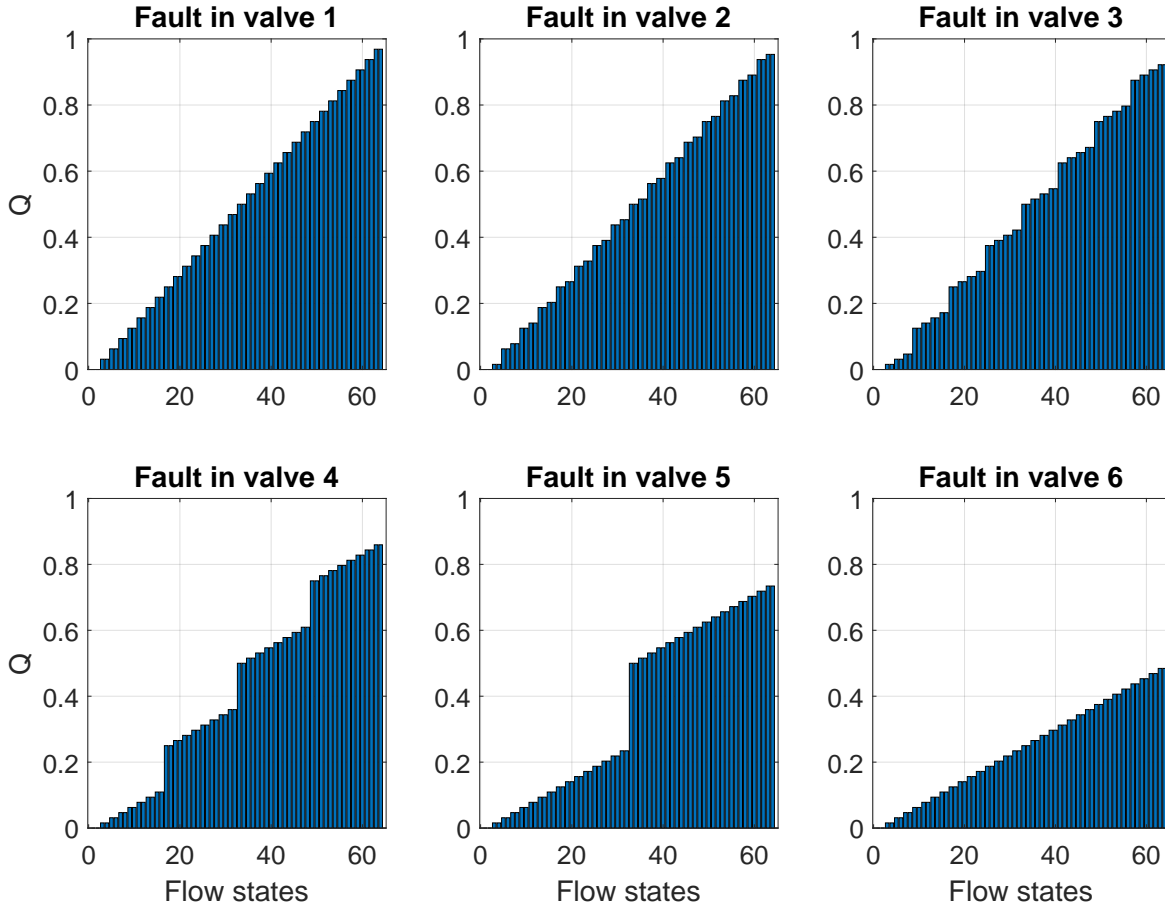


Figure 2.13: Rearranged valves configuration by faults

For the PNM coded DFCU the faults will only reduce the maximum flow by one step regardless of which valve is malfunctioning. Meaning that a fault in only one valve will almost be of no concern if fault detection and compensation is implemented.

Another area where the PNM coded DFCU is more reliable than the PCM coded is related to transient uncertainty. **Figure 2.14** shows the transient uncertainty of the two coding methods. The PCM coded DFCU large uncertainty comes from the fact the valves have different sizes and the fact that during some transitions from one state to the next several valves close while one opens. The largest uncertainty case can be seen where the largest valve opens or closes and all the other valves change state ($[0\ 1\ 1\ 1\ 1\ 1] \leftrightarrow [1\ 0\ 0\ 0\ 0\ 0]$). PNM coded DFCU will only have to open or close valves when it switches from one state to the next. No opening at closing occurs simultaneously. This means the uncertainty in the state is only between the current state and the next one.

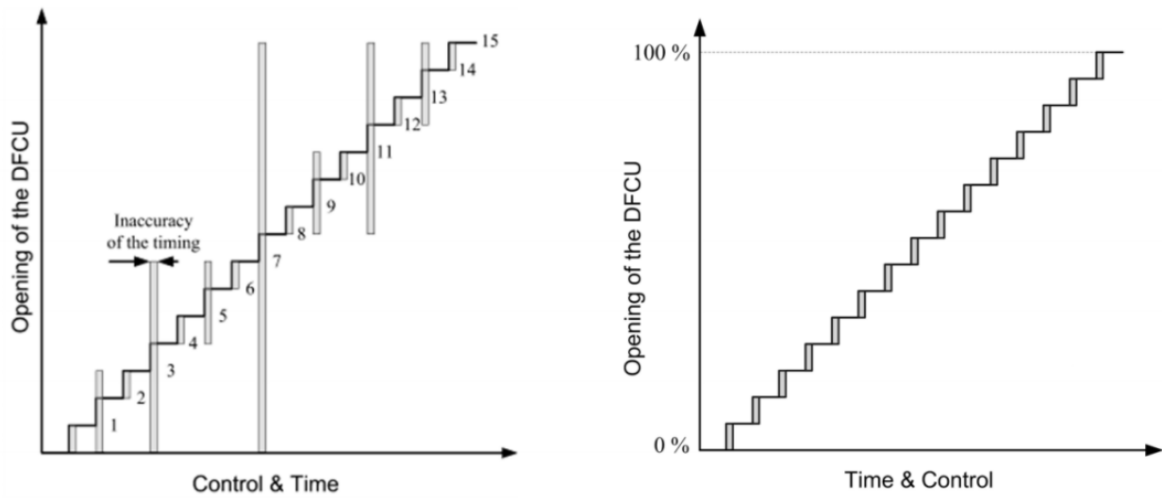


Figure 2.14: Transient uncertainty of 4 valve PCM (left) and 15 valve PNM (right) [5]

Figure 2.15 illustrates the uncertainty problem when some valves have to close as other opens. With two equally sized valves, it is wanted that the combined opening when one valve opens and the other closes to be constant. This can be seen in the first switching. However, when one valve is delayed slightly as shown in the second switching the system will have an opening that is 2 times the one that was wanted for a short time. Similarly, the last switching results in no opening for a moment. This is potentially a big problem for a PCM coded DFCU and thus a big reason for the PNM method to be used.

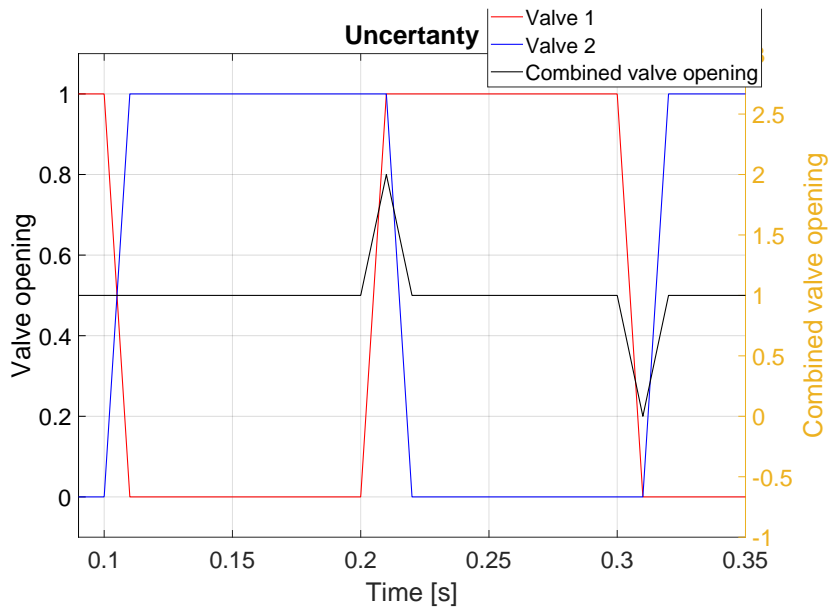


Figure 2.15: Effect of valve delay on the combined valve opening

Pulse Width Modulation (PWM)

Pulse with modulation (PWM) is also an approach that has been studied. Here the mean flow of the valve depends on the ratio between the open and closed time of the valve. So to achieve smoother control, a high switching frequency and low response time of the valve is needed. This results in valves that need to be able to handle large amounts of rapid switching which sets extreme demands to the durability of the valves. This method can also be combined with the parallel valve system. This was done in [13] to increase the control resolution. By doing this a number of different control schemes can be obtained as presented in **Figure 2.16**.

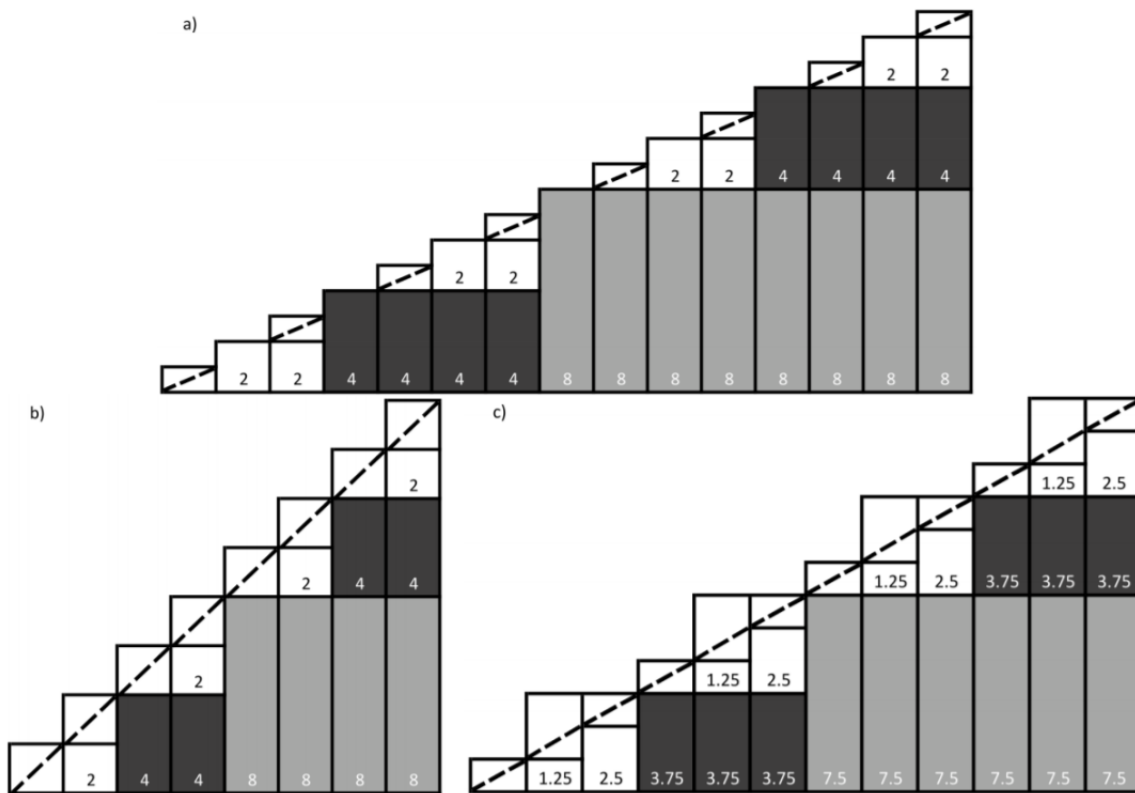


Figure 2.16: Different coding schemes for PWM combined with parallel valve control [13]

System (a) presents a 4-valve system where the smallest valve is controlled by PWM while the 3 larger valves are controlled as a normal PCM system. System (b) also has 4 valves but here the PWM controlled valve has the same size as the smallest PCM controlled valve. System (c) uses 4 valves controlled by PCM. Then the additional two PWM valves are sized, one as the smallest PCM valve and one as the second smallest PCM valve. As can be seen from this, the general goal for all the schemes is to smooth out the transition between one state of the PCM to the next.

Serial Connected System (Stepping)

Serial connected valves with a hydraulic capacitance between such as a flexible hose, pipe or cylinder, make it possible to control the flow stepwise. Firstly the capacitance is charged by opening the first valve while the second valve is closed. When the capacitance is charged, the first valve will close and then, the second opens to release the pressure. The hydraulic actuator will then move stepwise similar to an electrical stepping motor. This method has several benefits, such as high accuracy and no need for feedback systems to measure the actual position of the actuator. A high accuracy sensorless hydraulic stepping actuator based on this idea is presented in [14]. This system has a step size of only $15\mu m$, this results in a high accuracy but with a very limited maximum velocity. The principle of the system is presented in **Figure 2.17**.

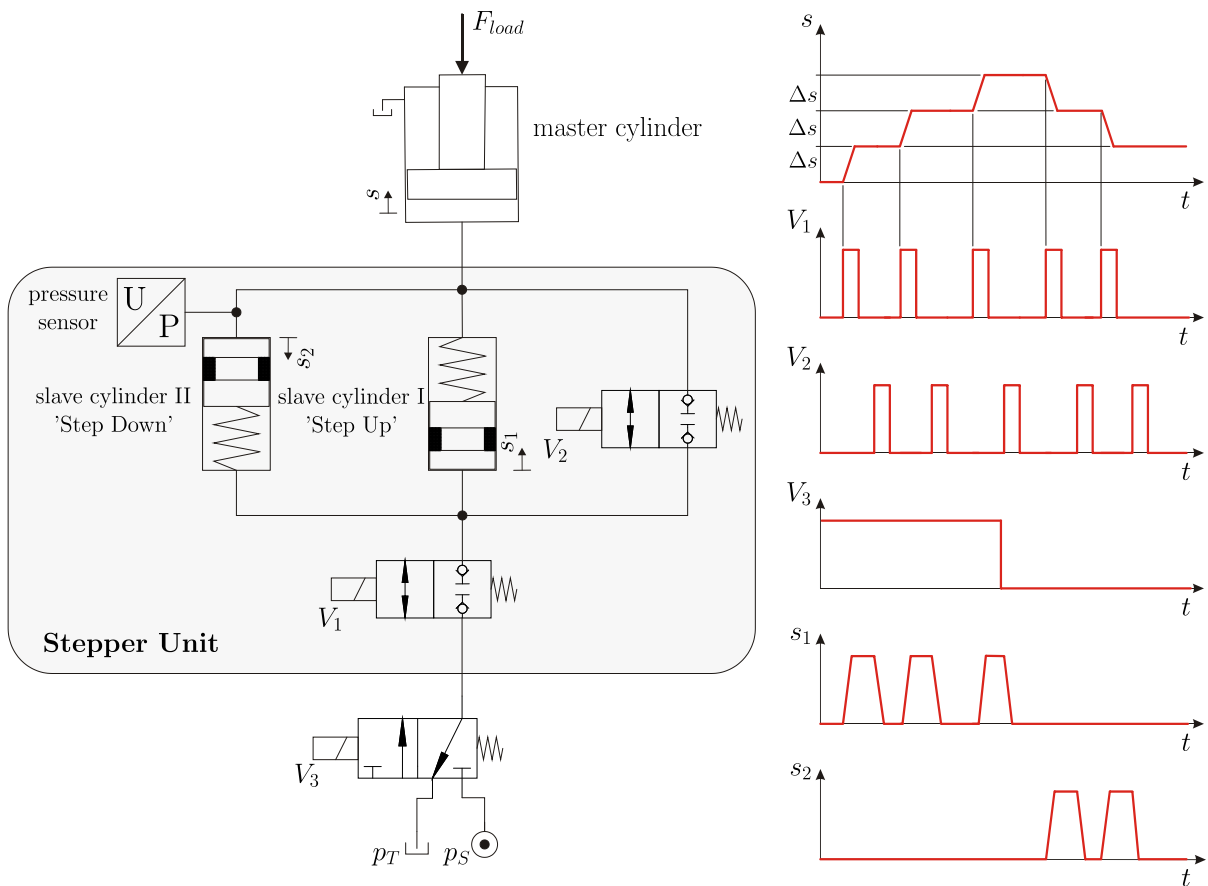


Figure 2.17: Basic hydraulic stepper schematic [14]

2.2.3 Comparison of Control Methods

To examine the behaviour of the different control methods, a simulation study has been performed at Tampere University of Technology in 2003. **Figure 2.18** shows the basic schematics of the different methods using ON/OFF valves.

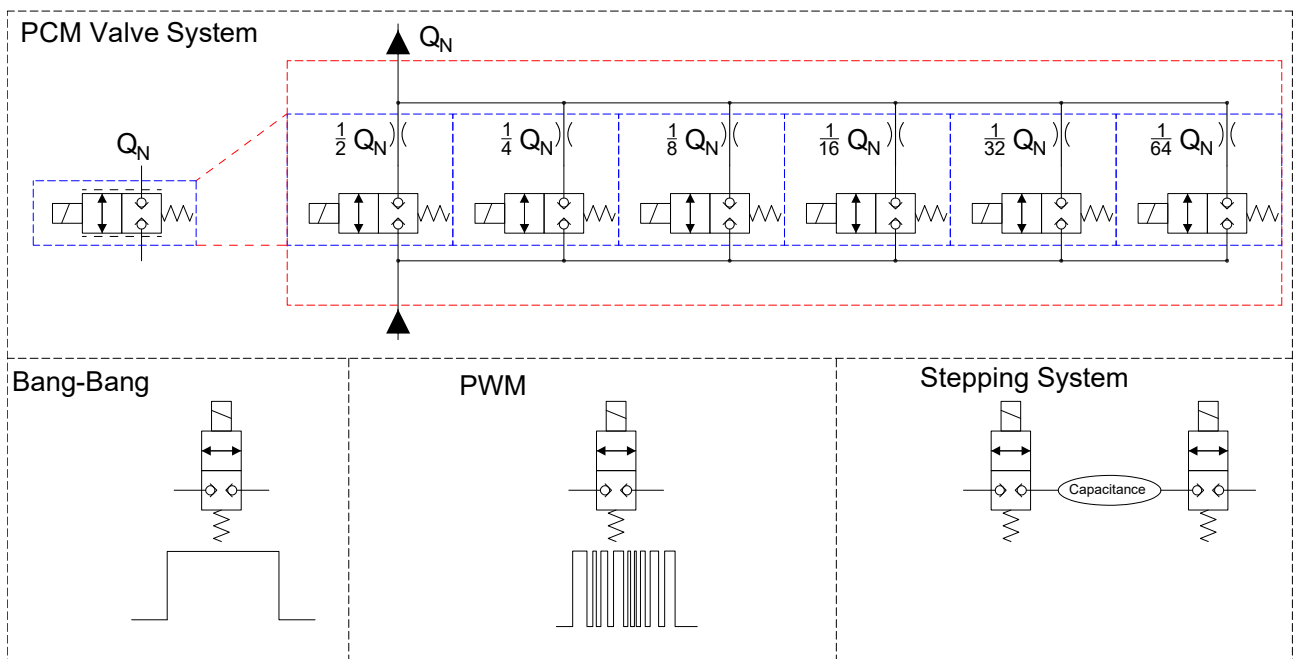


Figure 2.18: Different control methods schematics

The mentioned study consisted of a simple hydraulic system containing a constant pressure source, single acting hydraulic cylinder, vertical load of 100 Kg and control valves. Further parameters and details are described in [15]. Applying a 20 mm step single in the test simulation to each type of control valve, gave the results presented in **Figure 2.19**.

From the results presented in 2.19, obvious characteristics of the different control methods can be drafted. Position error, pressure peaks, motion smoothness and switching frequency are the most critical parameters to evaluate. Generally, pressure peaks lead to shorted life time of the system due to fatigue. It also causes noisy and rough motion. Switching frequency of the valves is directly connected with the durability of these and consequently with costs. At the end, the accuracy of the systems is crucial for the evaluation. Drafted characteristics are summarized in **Section 2.3**.

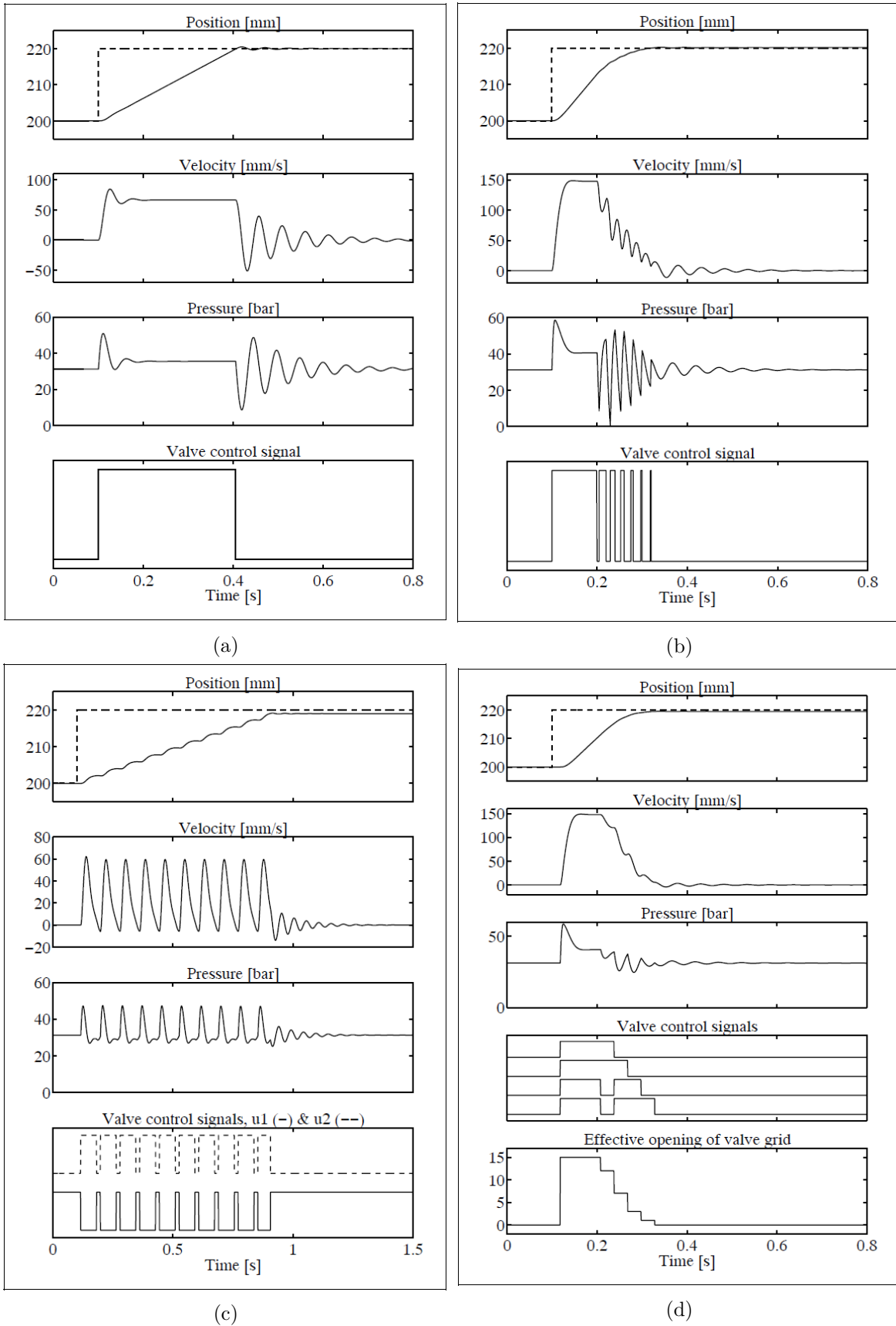


Figure 2.19: 20 mm Step response by (a)Bang-Bang (b)PWM (c)Stepping (d)PCM [15]

Table 2.3: Control Methods Comparison

	Velocity	Motion	Valve Durability	Number of Valves	Pressure
Bang-Bang	<ul style="list-style-type: none"> • Only one possible velocity 	<ul style="list-style-type: none"> • Harsh start & stop • Smooth between start & stop 	<ul style="list-style-type: none"> • Only one switching per motion • High durability 	<ul style="list-style-type: none"> • Only one valve needed 	<ul style="list-style-type: none"> • Large step transitions • Stable in steady state motion • No possibility to damp oscillations
PWM	<ul style="list-style-type: none"> • Velocity control possible • Noisy behaviour 	<ul style="list-style-type: none"> • Smoothness depends on valve's max. frequency • Smooth start & stop 	<ul style="list-style-type: none"> • Demands high switching frequency • Durability suffers 	<ul style="list-style-type: none"> • Only one valve needed 	<ul style="list-style-type: none"> • Pulsating • Stable only when max. flow is required • Possibility to damp oscillations
Stepping	<ul style="list-style-type: none"> • Limited max. velocity • Pulsating behaviour 	<ul style="list-style-type: none"> • Stepwise motion 	<ul style="list-style-type: none"> • Four switching per step • Durability depends on velocity and step size. 	<ul style="list-style-type: none"> • Two valve needed 	<ul style="list-style-type: none"> • Extremely pulsating • Never stable or smooth • Possibility to damp oscillations
PCM	<ul style="list-style-type: none"> • Large range of velocities • Velocity control possible 	<ul style="list-style-type: none"> • Smooth motion depending on number of valves 	<ul style="list-style-type: none"> • Low switching frequency • High durability 	<ul style="list-style-type: none"> • Large number of valve needed 	<ul style="list-style-type: none"> • Least pulsating • Stable by constant speeds • Possibility to damp oscillations

2.2.4 Digital Displacement Pumps

Digital displacement pumps (DDP) are based on multiple, differently or equally sized and independent flow sources. This can be achieved in two different ways. The first alternative is to use parallel connected pumps on the same axis and connect each of the pumps to a valve that either direct the flow to actuator or to tank. The desired flow is achieved by opening the combination of the pumps that gives a corresponding flow. All other pumps are directed to the tank to reduce energy losses. The flow in this solution can be sized in different ways similar to the sizing of the valves system in 2.2.2 . The second alternative is using a radial piston pump and connecting each piston to a valve to direct the flow to the actuator and the tank. This solution is more suitable for pulse number modulation (PNM) coding with existing products. **Figure 2.20** shows the basic schematics of digital pumps.

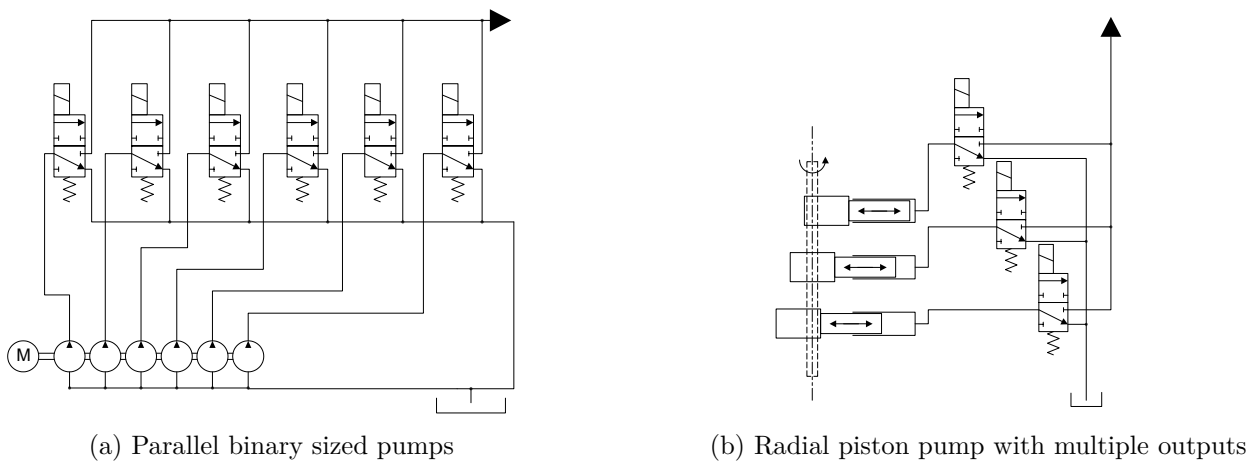


Figure 2.20: Digital displacement pump types

Figure 2.21 presents two pumps configuration from the market. These are corresponding to the configurations presented in **Figure 2.20**. The digital displacement pump from ARTEMIS is already been tested in the wind power industry. The multiple external gear pumps configuration from Rexroth is only an example for pumps that can serve a binary sized pumps configuration. Gerotor pumps are also very good alternative to these due to small size and low cost.

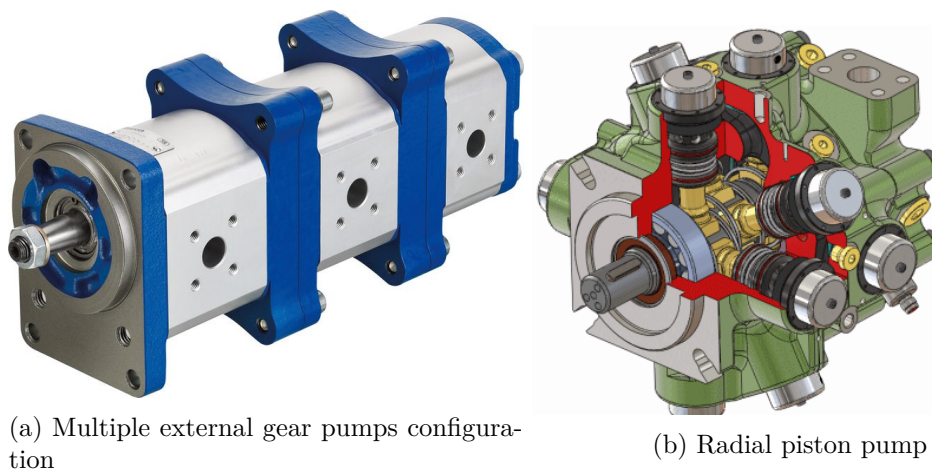


Figure 2.21: Sample products from Rexroth [16] and ARTEMIS [17]

Controlling the flow from a DDP is very similar the method used for controlling parallel connected digital valves. Parallel connected pumps type shown in **Figure 2.20a** has the same control principle as a PCM coded DFCU. It is based on binary sized pumps and depending on the required flow, the corresponding combination of pumps is then directed to the actuation system.

Radial piston pump type with multiple outputs shown in **Figure 2.20b** has a similar flow characteristic as PNM coded DFCU. It is based on equally sized pistons where the required amount of flow is controlling how many pistons are pumping to the actuating system and how many will be directed to tank. However, it is important to mention that the flow from these types of pumps is non-continuous due to phase delay between the pistons. Additionally, the flow from each piston has a sinus curve form in pumping modus since pistons are driven by a cam-shafts.

3 | System Design

In this thesis, several systems have been designed, modelled and analysed to achieve good coverage of the possibilities in designing a DEHC based on digital hydraulics. Considering the properties of different control methods of digital hydraulics listed in **Table 2.3** and availability of components in the market, the main focus will be on designing hydraulic architectures based on PCM coded DFCU and DDP.

3.1 Hydraulic System 1 4 DFCU with High and Low Pressure Accumulators

The first system is a 4 DFCU design presented in **Figure 3.1**. 4 DFCU are used, mainly 2 for each direction the cylinder moves in. All 4 valves can be opened simultaneously if a four edge control approach is wanted as described in **Section 4.3.2**. The design also consists of a high pressure accumulator and a low pressure accumulator.

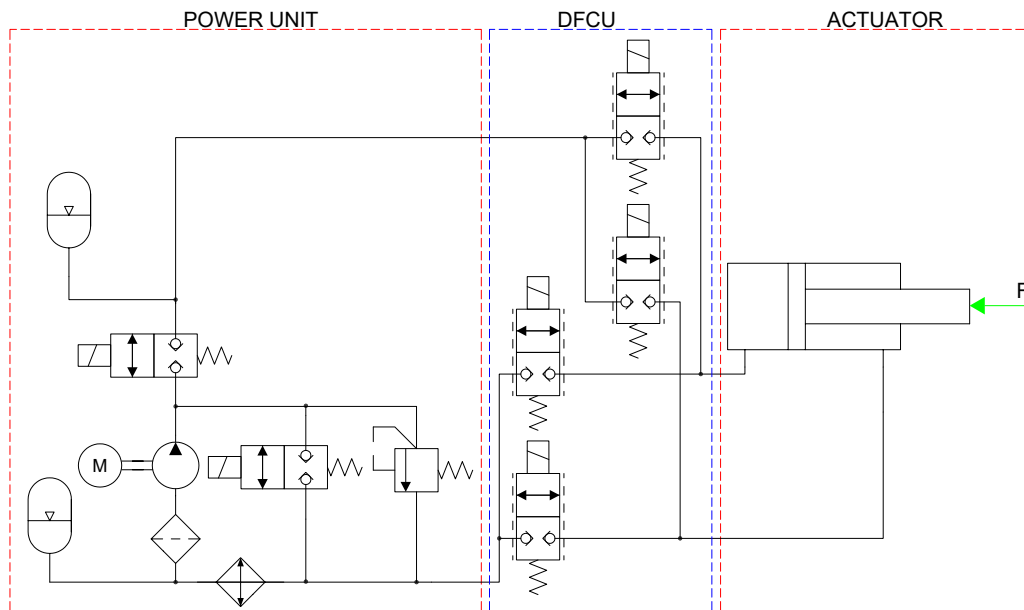


Figure 3.1: Designed system based on 4 DFCU's

3.1.1 Power Unit

The power unit for this system is similar to a conventional HPU design. The major difference and improvement is that the pump is unloaded when the high pressure accumulator has a sufficient pressure. An induction motor is used to drive the pump at a constant speed delivering the maximum required flow at all times. However, the two ON/OFF valves ensure that the pump is unloaded when the high pressure accumulator is charged. This is achieved by installing a pressure transducer at the accumulator to continuously keep the pressure within the settled range. When the pressure in the high pressure accumulator reaches the selected maximum, the

flow is directed to the low pressure accumulator which is used as a closed tank. The power loss in this case is only the power needed to overcome the pressure drop over the valve to the low pressure accumulator. For safety reasons, a pressure relief valve is installed to avoid system damages if both the ON/OFF valves were to be closed at the same time. A filter is installed at the suction port of the pump. A cooler is also installed on the return line to avoid overheating of the system.

3.1.2 DFCU

Four DFCU are used to control the flow from the power unit to the actuator. In this case each DFCU consists of 6 ON/OFF valves. PCM is used to size the valves so the sizes has the ratios $[1, \frac{1}{2}, \frac{1}{4}, \frac{1}{8}, \frac{1}{16}, \frac{1}{32}]$ compared to the original size of the valve. Fixed orifices are used to achieve these modified sizes of valves. Two DFCU are connected to the pressure port of the power unit where each is supplying a different side of the cylinder. The other two DFCU are similarly connected to the tank/return port of the power unit and each to a different side of the cylinder. This design gives large flexibility for the control method that are possible to implement.

3.2 Hydraulic System 2

2 DFCU and 1 Switch with High and Low Pressure Accumulators

The second design is a 2 DFCU design presented in **Figure 3.2**. This design is a simplified version of the previous system. Two of the DFCU are replaced by a single 4/2 valve to switch the direction of the flow. Here it is important that the 4/2 has a similar response time as the valves in the DFCU to keep the performance high. This design will also reduce the number of needed ON/OFF valves especially if the PNM coding method is used, where all the valves provide the same flow. However, the switching frequency of the valves is increased in this design because the number of valves controlling the inflow and outflow is halved. The rest of the architecture is identical to the previous system.

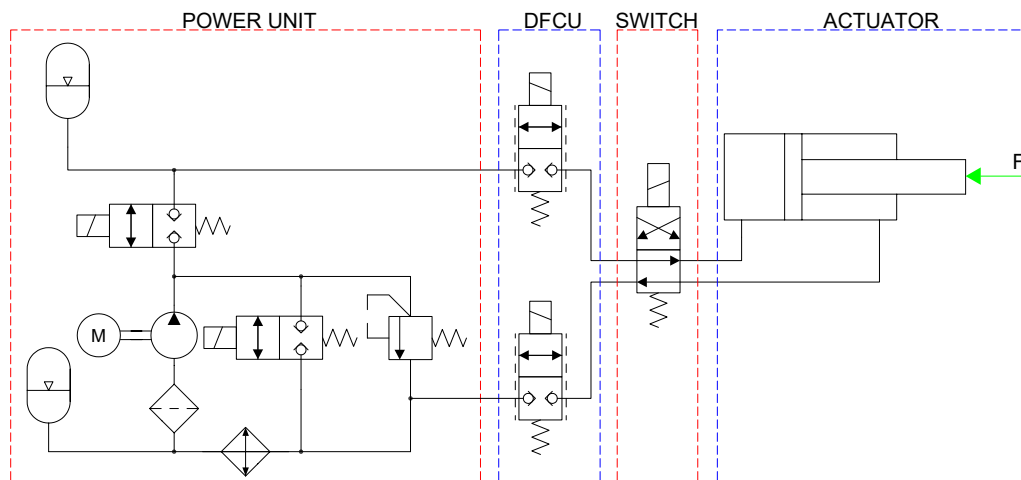


Figure 3.2: Designed system based on 2 DFCU and 1 4/2 valve

3.2.1 Power Unit

The power unit for this system is identical to the power unit in system 1.

3.2.2 DFCU

Two DFCU are used in this system. The first DFCU is only responsible to control the flow from the power unit regardless the motion direction of the cylinder. The second DFCU is responsible for controlling the return flow from the cylinder to the power unit. The total number of ON/OFF valves used in this DFCU for this system is half part the number used in system 1.

3.2.3 Switch

A 4/2 ways directional valve is installed between the DFCU and the cylinder. It is compensating for the two DFCU removed from system 1. For example; when the valve is in position 1, the flow from pressure port is directed to the piston side of the cylinder. Position 2 directs the flow from the pressure port to the rod side of the cylinder. In case of difficulties finding a 4/2 directional valve with similar response time, ON/OFF valves can be used to represent the switch as in **Figure 3.3**.

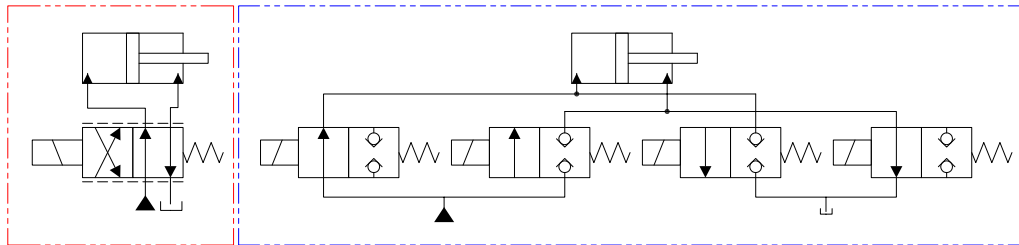


Figure 3.3: 4/2 ways valve represented by 4 ON/OFF valves

3.3 Hydraulic System 3

1 DFCU, 1 Switch, Low Pressure Accumulator and 6 Binary sized Pumps

This design architecture is using several pumps that provide different flows, a schematic can be seen in **Figure 3.4**. Similar to the previous system 2, a 4/2 valve is used to control the direction of pump and tank flow. Tank flow is controlled by a DFCU. The inflow is controlled by six 3/2 ways valves where each is connected to one of the six binary sized pumps. The flow from each pump is either directed to the actuator or the tank depending on required flow from the system.

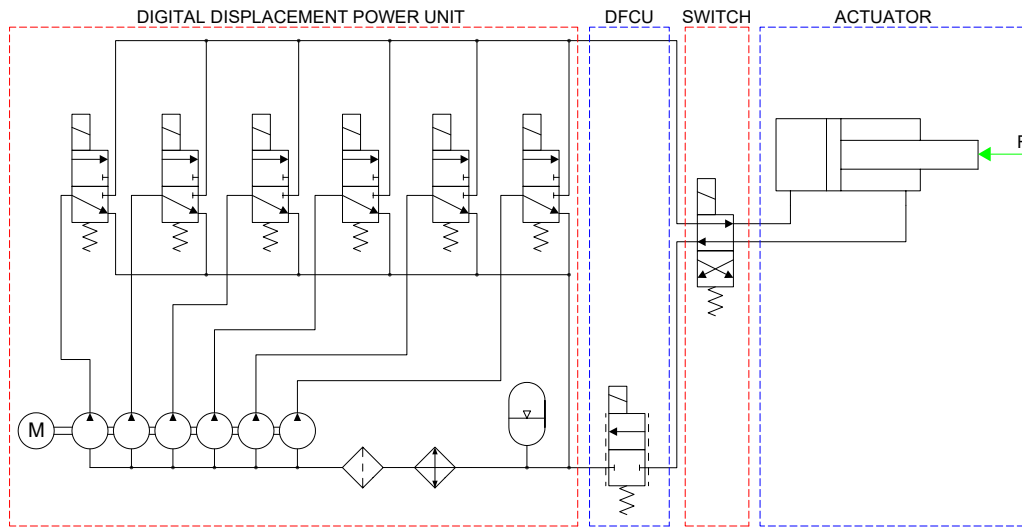


Figure 3.4: Designed system based on 6 binary sized pumps

3.3.1 Power Unit

The power unit is consisting of a motor driving six binary sized external gear pumps at a constant speed. The pumps are supplying continuously and respectively the flows $[\frac{1}{2}, 1, 2, 4, 8, 16] \text{ l/min}$. The flow from each pump is then directed either to the actuator or tank depending on the control signal and amount of flow required. A low pressure accumulator serves as a closed tank. A cooler and a filter are installed on the suction line to avoid overheating and protect the pumps.

3.3.2 DFCU

The DFCU is used for throttling the return flow. This is important to keep a back-pressure in the cylinder chamber connected to tank. This scenario is occurring when the load has the same direction as the velocity of the cylinder. Lack of back pressure could cause uncontrollable motion and vacuum in the cylinder.

3.3.3 Switch

The 4/2 valve in this system has the same functions explained in system 2.

3.4 Hydraulic System 4

3 DFCU and 1 Switch with Low Pressure Accumulator

This design is a 3 DFCU system, presented in **Figure 3.5**. The architecture of the DFCU, switch and actuator are identical to system 2. The major difference is in the power unit. The high pressure accumulator and 2 ON/OFF valves are replaced by a DFCU.

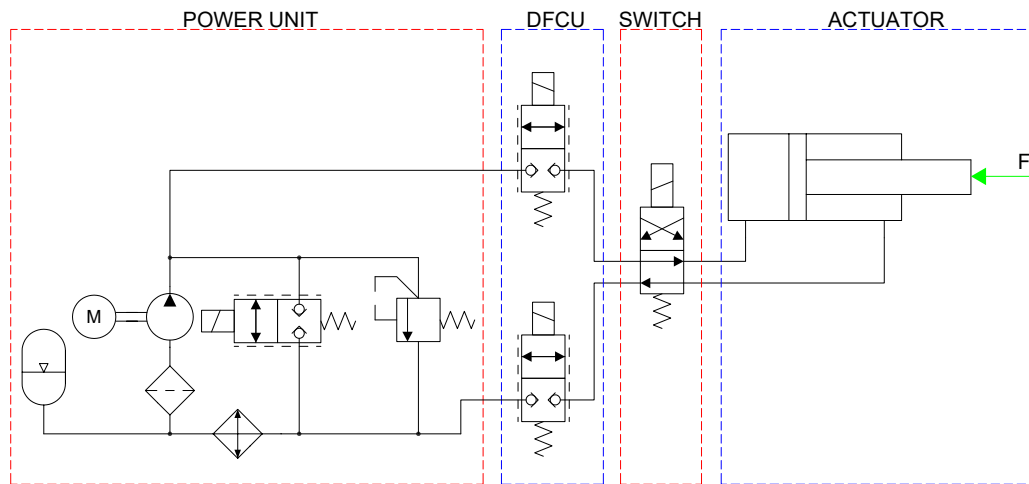


Figure 3.5: Designed system based on 3 DFCU and no high pressure accumulator

3.4.1 Power Unit

The power unit consists of an electrical motor driving a fixed displacement pump at a constant speed. The DFCU is controlling the flow to low pressure accumulator to always keep the pump pressure 15 *Bar* higher than the highest pressure in the actuator. The purpose of this is to have predicted flow through the DFCU that controls the flow from the power unit to the actuator. At the same time, it eliminates unnecessary energy losses caused by unneeded high pump pressure.

3.4.2 DFCU

The two DFCU in this system has an identical function as in system 2.

3.4.3 Switch

The 4/2 valve in this system has the same function explained in system 2.

3.5 Dimensioning of Components

The DEHA is a closed hydraulic system. The different hydraulic diagrams are presented above. All four systems have the same predefined cylinder and the criteria for load and motion. Thus, all four systems require the same flow. The required maximum flow is calculated using **Eq.(3.1)**.

$$Q_{max} = v_{max} \cdot A \quad (3.1)$$

Where:

$$\begin{array}{lll} Q_{max} & - & \text{Maximum required flow} \quad \left[\frac{m^3}{s}\right] \\ v_{max} & - & \text{Maximum cylinder velocity} \quad \left[\frac{m}{s}\right] \\ A & - & \text{Cylinders Piston Area} \quad [m^2] \end{array}$$

From the calculated maximum flow, an equivalent valve size can be found applying **Eq.(3.2)**. The calculated flow coefficient K_v is later used in this thesis to define the size of the valves in a digital flow control unit (DFCU).

$$K_v = Q_N \sqrt{\frac{1}{\Delta p_N}} \quad (3.2)$$

$$\begin{array}{lll} Q_N & - & \text{Nominal flow} \quad \left[\frac{m^3}{s}\right] \\ \Delta p_N & - & \text{Nominal pressure drop} \quad [Pa] \end{array}$$

Pipes are dimensioned according to the recommended values for fluid velocity. These are:

$$\begin{array}{llll} \text{Suction lines} & 0.5 - 2.0 & \left[\frac{m}{s}\right] \\ \text{Pressure lines} & 3.0 - 8.0 & \left[\frac{m}{s}\right] \\ \text{Return lines} & 1.0 - 3.0 & \left[\frac{m}{s}\right] \end{array}$$

The volume of the accumulators is calculated according to **Eq.(3.3)**. The working volume is defined by the difference between the cylinder chamber by full extraction and the rod chamber by full retraction. Both the charging and discharging process are assumed adiabatic.

$$V_0 = \frac{\Delta V \cdot \frac{p_1}{p_0}}{1 - \left(\frac{p_1}{p_2}\right)^{\frac{1}{n}}} \quad (3.3)$$

Where:

$$\begin{array}{lll} V_0 & - & \text{Accumulator Volume} \quad [m^3] \\ \Delta V & - & \text{Working Volume} \quad [m^3] \\ p_1 & - & \text{Minimum Working Pressure} \quad [Pa] \\ p_0 & - & \text{Pre-charged Pressure (Normally } \approx 90\% \text{ of } p_1) \quad [Pa] \\ p_2 & - & \text{Maximum Working Pressure} \quad [Pa] \\ n & - & \text{Polytropic Exponent (1 for Isotherm and 1.4 for Adiabatic process)} \quad [-] \end{array}$$

4 | Control Design

To control the cylinder different approaches were considered. First a simple control algorithm that included position and velocity. Then the addition of pressure measurements were tested. Lastly a more advanced steady state equation model-based control was tested.

4.1 Control System 1 Position Feedback and Velocity Feed Forward

The flow in a hydraulic cylinder has a linear relationship to the extracting/retracting velocity. In this system the reference velocity is used to calculate the reference flow. Since hydraulic systems not always respond identically, a correction feedback is needed. Variation in pressure drop over the valves and variation in load are two examples why a controller with only a feed forward will drift away and never be sufficient enough.

Position feedback is used in this controller as a correction controller. The main value of the control signal will come from the reference velocity and the position feedback controller will serve as a correction controller to achieve sufficient response. A simplified block diagram of the control system is presented in **Figure 4.1**.

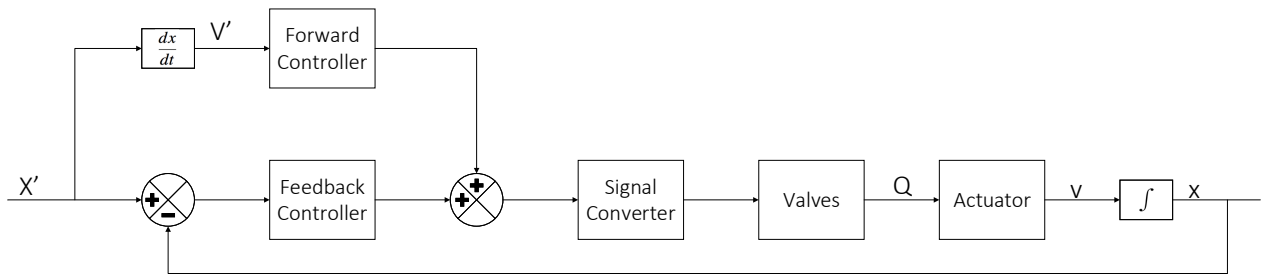


Figure 4.1: Block diagram

In the considered digital hydraulic systems, the flow is controlled by several valves compared to conventional hydraulics where normally only one servo or proportional valve is used. For this cause, it is convenient that the control signal is converted to a binary value and then split to every valve in the DFCU. The flow direction is controlled by the reference velocity and position error to determine the direction of the inflow and outflow. Similarly, the reference flow calculation is changed when the cylinder has to change direction. Difference in effective areas would cause instability if reference flow constantly calculated with the same parameters. The detailed block diagram in **Figure 4.2** shows all the main steps in the controller for this system, and the correlation between the different signals.

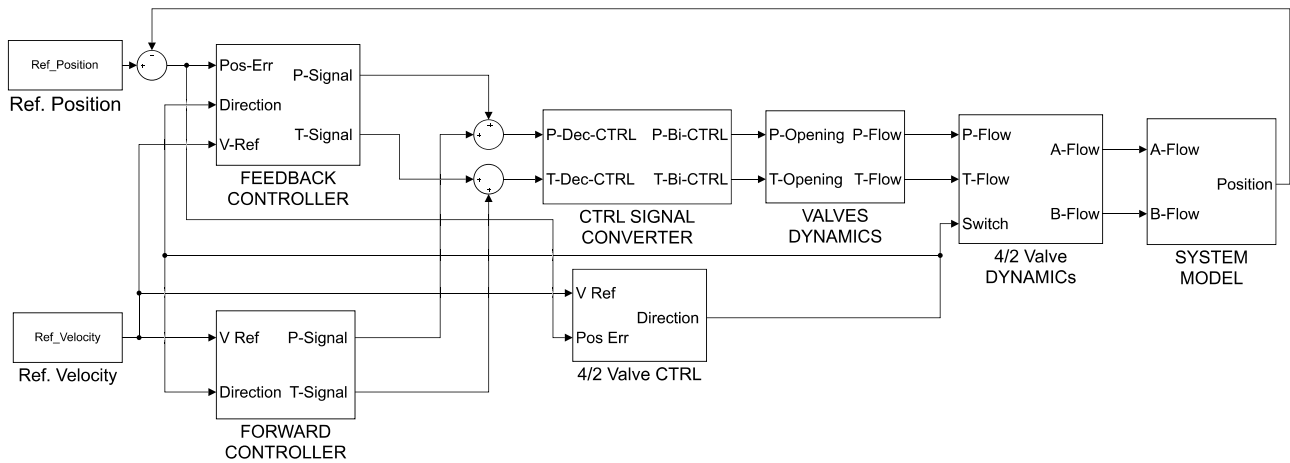


Figure 4.2: Detailed block diagram

The following **Table 4.1** shows all possible states of the switch controlled by the direction of the reference velocity and the direction of the position error. The same table applies for the calculation of the reference flow depending on the active state. Thus, the reference velocity is either multiplied with the piston-side area or the rod-side area.

Table 4.1: Flow direction controller

Direction of Reference Velocity	Direction of Position Error	Pump-side Valves	Tank-side Valves
+	+	$P \rightarrow A$	$B \rightarrow T$
+	-	$P \rightarrow B$	$A \rightarrow T$
-	-	$P \rightarrow B$	$A \rightarrow T$
-	+	$P \rightarrow A$	$B \rightarrow T$

4.2 Control System 2

Position and Pressure Feedback with Velocity Feed Forward

By measuring the pressure in the cylinder and the accumulators, it is expected to achieve more precise and robust control of the cylinder. A basic block diagram is presented in **Figure 4.3**. As in the previous method the required flow to meet the reference velocity is calculated. Additionally, the feedback signal of the pressure is used to select the opening state of the DFCU. A more detailed block diagram is presented in **Figure 4.4**.

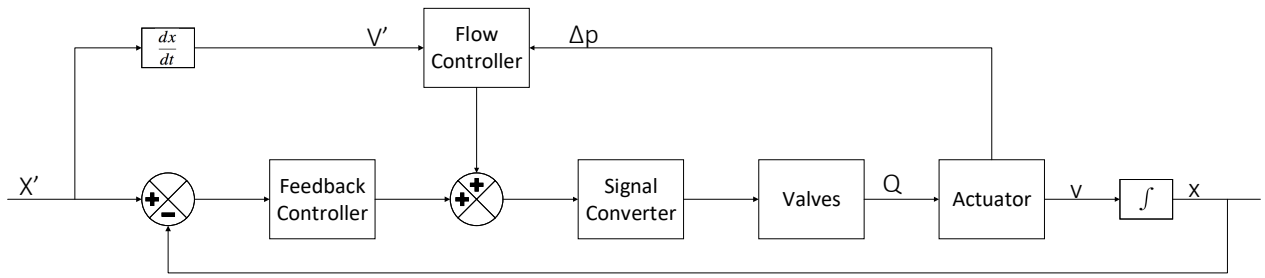


Figure 4.3: Block diagram

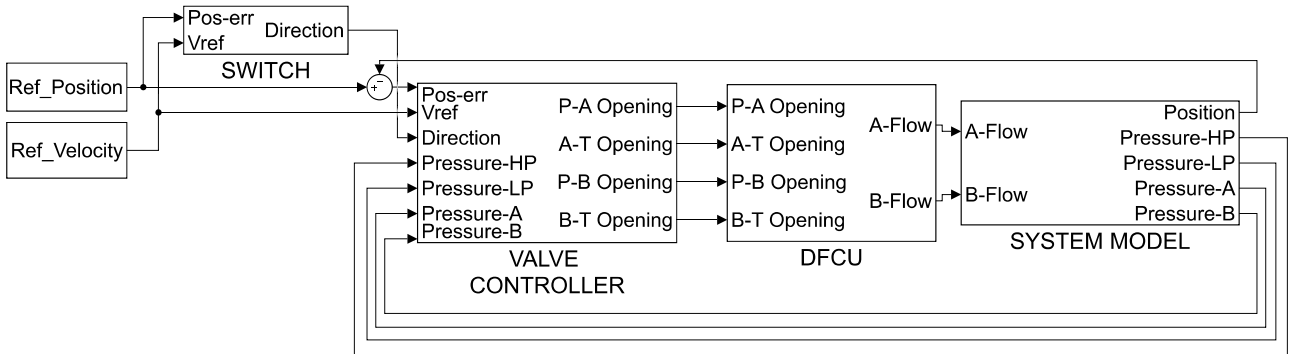


Figure 4.4: Detailed block diagram

From the measured pressure values and the valve flow characteristics, **Eq.(4.1)** is used to calculate the flow for every opening state of the DFCU creating a vector. The position error is then multiplied with a gain and added to the reference velocity. The combination closest to the reference flow can then be selected.

$$Q_{calc} = \sqrt{\Delta p} \cdot (K_{v1} \cdot x_1 + K_{v2} \cdot x_2 + K_{vn} \cdot x_n) \quad (4.1)$$

Where:

- | | | |
|-----------------------------|--|-----------------------------------|
| Δp | - Pressure drop over valves | [Bar] |
| $x_1 \rightarrow x_n$ | - 0 or 1 depending on if the valve is open or closed | |
| $K_{v1} \rightarrow K_{vn}$ | - Flow coefficient of different valves | $[m^3 \cdot \sqrt{\frac{m}{kg}}]$ |

The control signal to the binary converter is the vector index of the closest flow minus 1. As the index of the vector starts at 1 and not zero. This is a simple control algorithm where the key parts is to know the flow dynamics of the valves, and filter the pressure feedback signals. As form the previous controller a rate limit was used to remove noise from the feedback signals.

4.3 Control System 3

Model Control based on Steady State Equation

In **Figure 4.5** a simplified drawing of hydraulic system 1 is presented. An interesting way to control this system is presented in [18] where, the systems steady state equations are used to find the opening states of the DFCU. In this section the idea of this method will be presented and the implementation of it. There are two methods, the simpler method (Two edge control) where only two of the DFCU are operated at a time such as $P \rightarrow A$ and $B \rightarrow T$ to make the cylinder move in the positive direction assuming $p_p > p_a$ and $p_b > p_t$. The other more advanced method (Four edge control) is when it is possible for all four DFCU to be operated at the same time, thus increasing the controllability of the system.

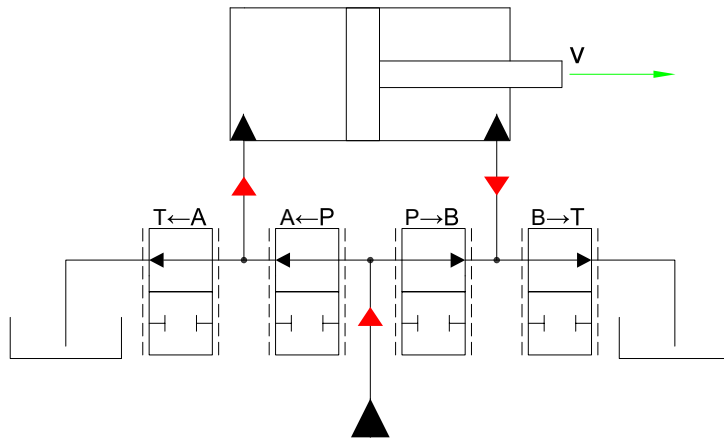


Figure 4.5: Two/Four edge control

4.3.1 Two Edge Control

In **Figure 4.6** a block diagram for two edge control is shown. The system will require feedback signals from the position and the pressure. The reference velocity is used as feed forward signal. To implement this for a four edge control a reduction of search space would have to be added. As the total number of states will be $(2^n)^2$ times as many compared two edge control. Meaning that for a 6 valve DFCU system the four edge control will have 4096 times as many valve combinations resulting in over 16 million combinations.

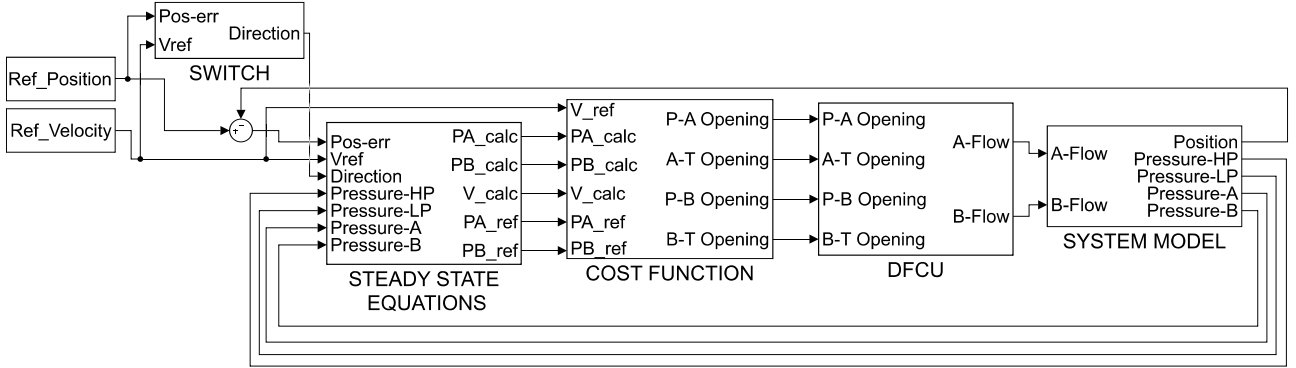


Figure 4.6: Simplified block diagram of two edge control

The idea of the two edge control is based on the steady state equations describing the flow, pressure and velocity for the cylinder. The equations for a cylinder moving in the positive direction is presented in **Eq.(4.2)**, and for the negative direction in **Eq.(4.3)**.

$$\begin{aligned}
 Q_p &= Q \cdot U_p \cdot \sqrt{p_p - p_a} = A \cdot v \\
 Q_t &= Q \cdot U_t \cdot \sqrt{p_b - p_t} = A_r \cdot v \\
 F &= A \cdot p_a - A_r \cdot p_b
 \end{aligned} \quad (4.2)$$

$$\begin{aligned}
 Q_p &= Q \cdot U_p \cdot \sqrt{p_p - p_b} = A_r \cdot v \\
 Q_t &= Q \cdot U_t \cdot \sqrt{p_a - p_t} = A \cdot v \\
 F &= A \cdot p_a - A_r \cdot p_b
 \end{aligned} \quad (4.3)$$

Where:

Q	- Flow over the smallest valve with 1 Pa pressure drop	$\left[\frac{m^3}{s}\right]$
Q_p	- Flow from the pump	$\left[\frac{m^3}{s}\right]$
Q_t	- Flow to the tank	$\left[\frac{m^3}{s}\right]$
p_p	- Pump pressure	$[bar]$
p_t	- Tank pressure	$[bar]$
p_a	- Chamber A pressure	$[bar]$
p_b	- Chamber B pressure	$[bar]$
A	- Cylinder A side area	$[m^2]$
A_r	- Cylinder B side area	$[m^2]$
U_p	- Opening combination of pump DFCU	$[-]$
U_t	- Opening combination of tank DFCU	$[-]$
v	- Cylinder Velocity	$\left[\frac{m}{s}\right]$
F	- Cylinder Force	$[N]$

These equations can be solved analytically for pressure and velocity. For the cylinder moving in the positive direction, the analytical expression is presented in **Eq.(4.4)**.

$$\begin{aligned}
 p_a &= \frac{p_t \cdot A^3 \cdot U_t^2 + p_p \cdot A \cdot A_r^2 \cdot U_p^2 - F \cdot A_r^2 \cdot U_p^2}{A^3 \cdot U_t^2 + A_r^3 \cdot U_p^2} \\
 p_b &= \frac{p_t \cdot A^2 \cdot U_t^2 \cdot A_r + p_p \cdot A_r^3 \cdot U_p^2 + F \cdot A^2 \cdot U_t^2}{A^3 \cdot U_t^2 + A_r^3 \cdot U_p^2} \\
 v &= \frac{Q \cdot U_p}{A} \sqrt{p_p - \frac{p_t \cdot A^2 \cdot A_r \cdot U_t^2 + F \cdot A^2 \cdot U_t^2 + p_p \cdot A_r^3 \cdot U_p^2}{A^3 \cdot U_t^2 + A_r^3 \cdot U_p^2}}
 \end{aligned} \tag{4.4}$$

From these equations the pressure and velocity of the cylinder can be calculated for all the different openings combinations of the DFCU. In the three figures below plots of the pressure in chamber A and B and the velocity of the cylinder with the 64^2 different opening combinations can be seen. This is with a pump pressure of 120 bar and tank pressure of 4 bar and a negative load F of -10000 N.

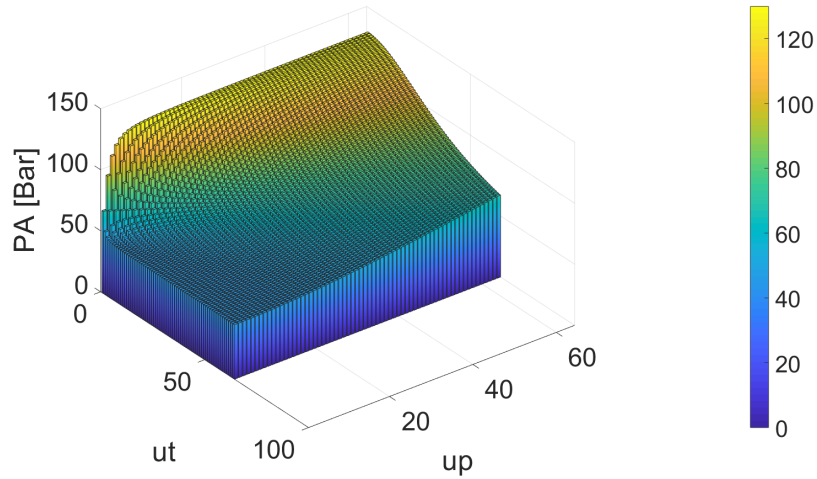


Figure 4.7: Pressure in cylinder chamber A with different valve openings with $p_p = 120$ Bar, $p_t = 4$ Bar and $F = -10000$ N

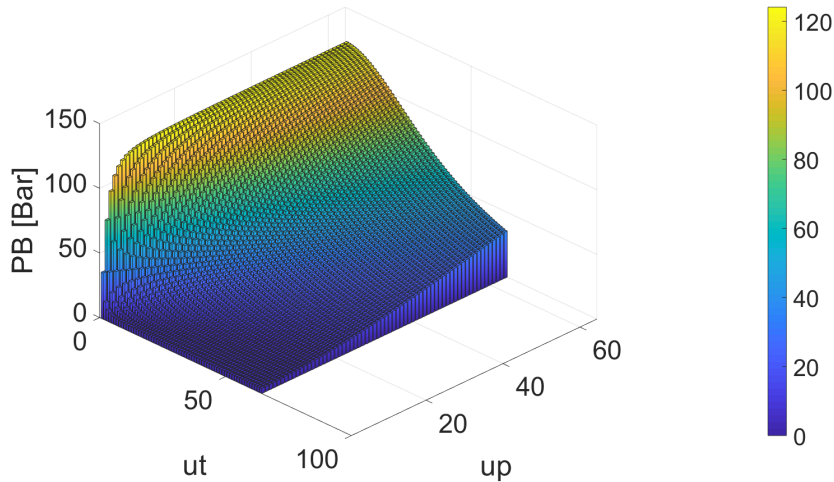


Figure 4.8: Pressure in cylinder chamber B with different valve openings with $p_p = 120$ Bar, $p_t = 4$ Bar and $F = -10000$ N

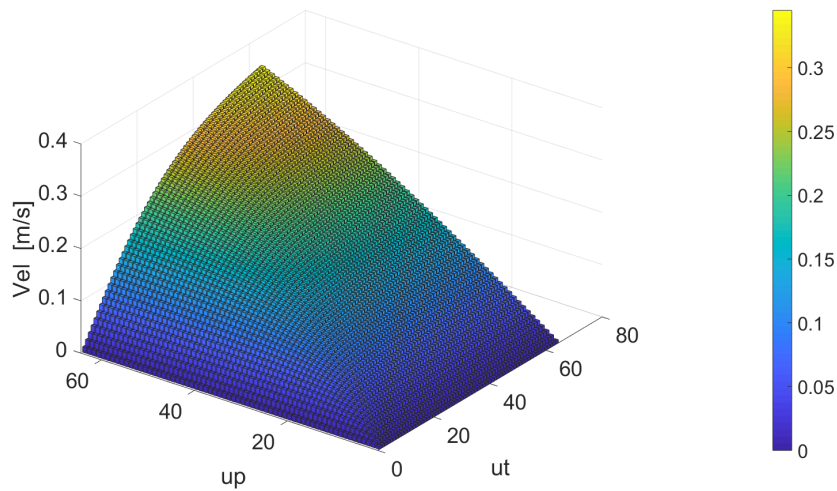


Figure 4.9: Cylinder velocity with different valve openings with $p_p = 120$ Bar, $p_t = 4$ Bar and $F = -10000$ N

Plotting the velocities from **Figure 4.9** by increasing magnitude, as seen in **Figure 4.10** all the achievable velocities are presented. Low resolution at low velocities is observed. The resolution is increasing with the increased velocity. The limited controllability in the lower velocity region is one of the problems with two edge control. However, there are over 2000 combinations that will result in a velocity in the range $0 - 0.15$ m/s which is the range of interest for the considered system.

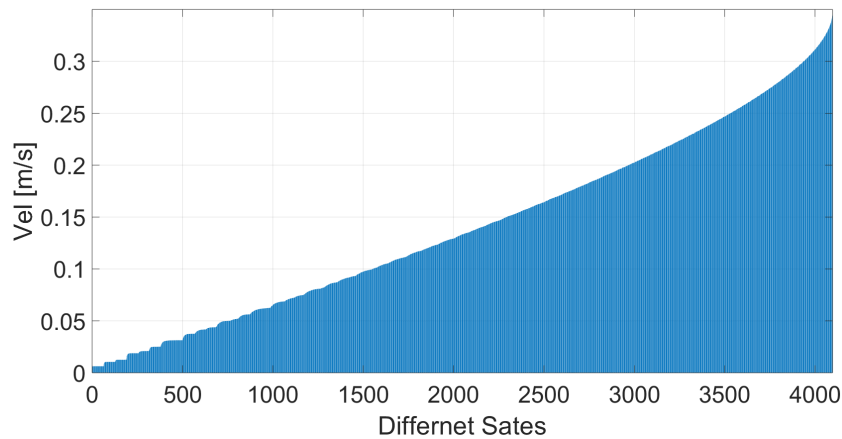


Figure 4.10: View on cylinder velocity controllability

Assuming it is wanted to control the pressure in chamber B to be close to 55 bar during a positive motion with a negative load of -10000 N. All the different velocities possible with a pressure in the range 50-60 bar can be plotted as shown in **Figure 4.11**, and the corresponding pressure in chamber B in **Figure 4.12**.

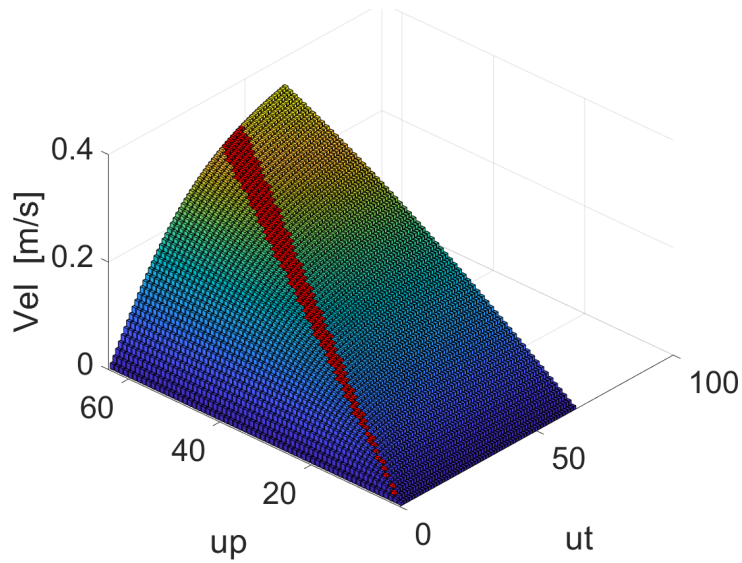


Figure 4.11: Possible velocities with $p_p = 120$ bar $p_t = 4$ bar and $F = -10000$ N when chamber B pressure is wanted to be kept between 50-60 bar

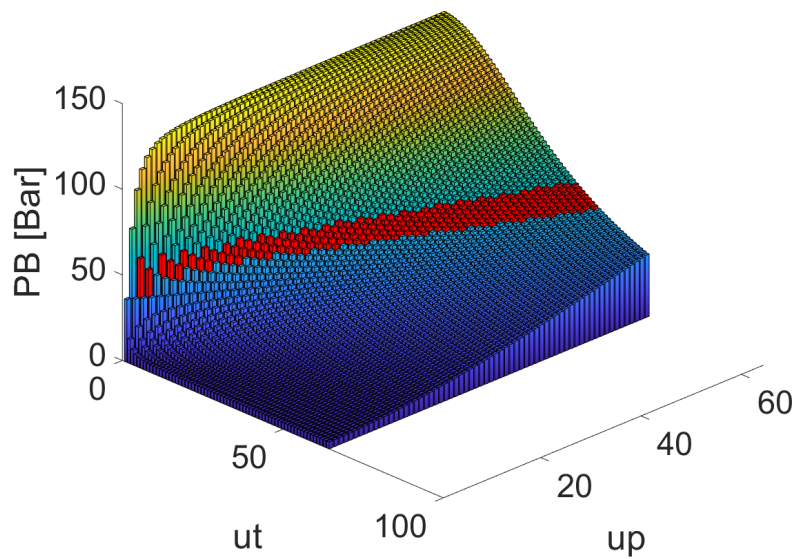


Figure 4.12: Pressures in chamber B within the range of 50-60 bar with $p_p = 120$ bar $p_t = 4$ bar and $F = -10000$ N

The resolution of the velocities is presented in **Figure 4.13** where the 50 first states has a velocity under 150 mm/s which is the maximum velocity for the system cylinder. As it can be seen here the controllability is very limited in the lower velocity range.

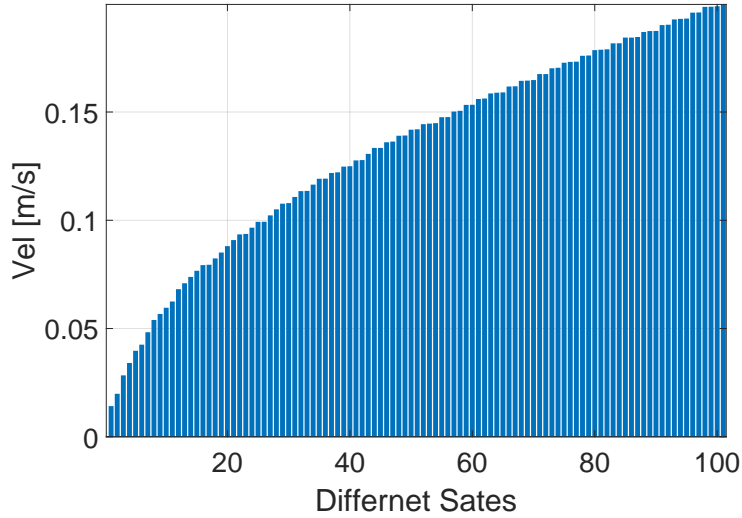


Figure 4.13: Velocity resolution with $p_p = 120$ bar $p_t = 4$ bar and $F = 10000$ N and chamber B pressure kept within 50-60 bar

This shows that it should be possible to control the pressure and velocity independently to some degree. It should then be possible to select a opening state from the reference velocity that will keep the pressure as close to 55 bar as possible. An example could be if the reference velocity is 0.1m/s all the combinations in the range $v_{ref} \cdot 0.9 \rightarrow v_{ref} \cdot 1.1$ can be looked at called v_{range} . Then the combination that minimizes a given cost function including the calculated pressures PA, PB and the calculated velocity can be used. **Eq.(4.5)** shows a cost function that calculates the error between the calculated pressures and the reference pressures, and the calculated velocity and reference velocity with weighting factors K. K can be changed to change the weighting of the different errors.

$$J = abs(PB_{calc} - PB_{ref}) \cdot K_{PB} + abs(PA_{calc} - PA_{ref}) \cdot K_{PA} + abs(v_{calc} - v_{ref}) \cdot K_v \quad (4.5)$$

This function can be further improved by a adding position error factor to v_{range} . When the combination that minimizes the cost function is found, the control signal to the valves is the row and column index of the 64×64 matrix. For the valves to be in the 0 - 0 state a condition has to be satisfied. The velocity reference has to be below the 1 - 1 state velocity and the position error has to be below a given threshold. The switching between **Eq.(4.2)** and **Eq.(4.3)** is done by the same switch function as in the two previous control strategies. The feedback signals used were also filtered the same way as in the previous controls.

The control algorithm was more advanced for this method than the simpler control methods used. There is also the possibility of adding additional penalty functions to the cost function. These can include reduction of valves switchings and energy losses.

4.3.2 Four Edge Control

For more advanced control strategy, the general **Eq.(4.3)** is used. A analytical solution to this version is more complex than the previous version, therfor a numerical solver is used for this case. According to [19] the Ridders method has a much higher convergence rate than the standard Newton-Raphson method and thus is much better numerical solver for this controller. A visualization of the flows is also much more complicated as there are 4 control variables. Therefore, no plots of the velocity and chamber pressures with different valve combinations are show in this section.

$$\begin{aligned}
 Q_a &= Q \cdot U_{pa} \cdot \sqrt{p_p - p_a} - Q \cdot U_{at} \cdot \sqrt{p_a - p_t} = A \cdot v \\
 Q_b &= Q \cdot U_{pb} \cdot \sqrt{p_p - p_b} - Q \cdot U_{bt} \cdot \sqrt{p_b - p_t} = -A_r \cdot v \\
 F &= A \cdot p_a - A_r \cdot p_b
 \end{aligned} \tag{4.6}$$

This method will give a much better velocity controllability especially in the lower velocity region. This is shown in [20] where the two different control methods are used on a cylinder. However only 4 valves for each DFCU is used in this case to reduce the number of combinations. **Figure 4.14** shows two plots of the different velocities achievable. However, this is also within a specific pressure rage. Meaning the pressure in one of the cylinder chambers is also controlled within a given range, between 7 and 11 bar in the case of this figure.

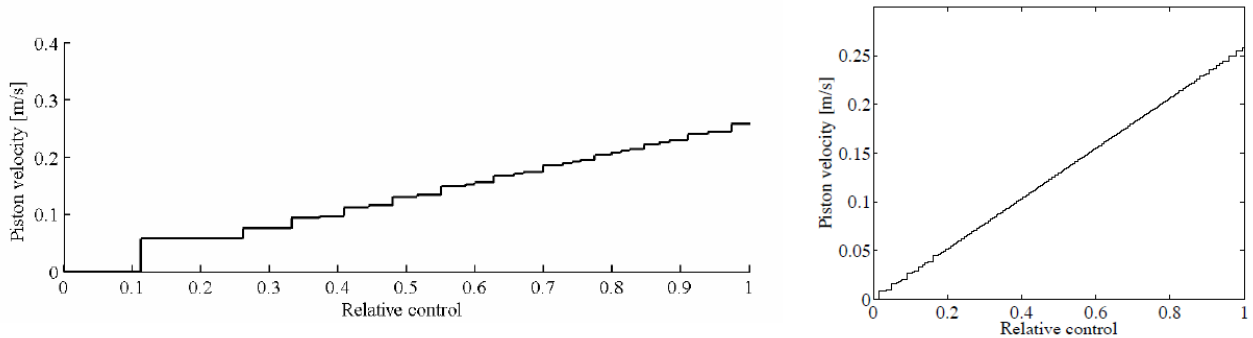


Figure 4.14: Difference in low velocity controllability between two and four edge control with 4-valves DFCU [20]

This approach is presented in this thesis only as a possible improvement of the two edge controller. It is not discussed further or used.

5 | System Modelling

The most essential hydraulic components are analysed in this section. The formulas used in the simulation models are presented and described. All assumptions taken are pointed out.

5.1 Valves

The relationship between the flow and pressure drop over the valve is normally described by the general orifice equation. In the case of ON/OFF valves, the discharge area A_d and the displacement of spool/seat x_v are switching between zero and the maximum value. These are not varying in the same way as servo/proportional valves. To simplify the model, the constants, discharge area A_d , discharge coefficient C_d and oil density ρ are reduced to one constant K_v . To avoid imaginary values for the flow, the square root of the pressure drop Δp is rewritten by the absolute value and the sign of the pressure drop. The following equation is used as a model for the valves in the project.

$$Q = x_v \cdot \Delta p_{sign} \cdot A_d \cdot C_d \cdot \sqrt{\frac{2}{\rho} |\Delta p|} \rightarrow x_v \cdot \Delta p_{sign} \cdot K_v \cdot \sqrt{|\Delta p|} \quad (5.1)$$

A more accurate way to model the valves is discussed in [21] and the equation is presented in **Eq.(5.2)**. This method requires some experimentally measured data to optimize the parameters b_1 , b_2 , x_1 and x_2 . Where x_1 and x_2 is the exponent that with a value of 0.5 would result in the standard square root model. b_1 , b_2 is the critical pressure ratio. This will make the flow stop increasing if the pressure difference gets to high. **Figure 5.1** shows flow curves for three valves. The vales are the same for all the curves, however the orifice size is changed. It can be seen that the exponent x is increasing as the orifice area decreases. The effect of the b factor can also be seen where the flow in the three plots stops increasing.

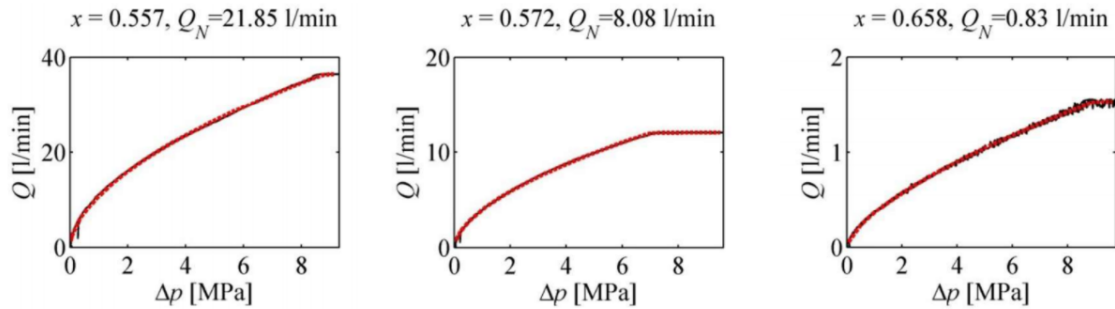


Figure 5.1: Flow curves for three different orifice sizes (2.6, 1.5, 0.5 mm left to right). [21]

This method gives a better representation of the real flow through a valve. However, because experimental work is not a part of this thesis the general orifice equation will be used in the modelling of the hydraulic system.

$$Q(p_{in}, p_{out}) = \begin{cases} K_{v1}(p_{in} - p_{out})^{x_1} & , b_1 p_{in} < p_{out} \leq p_{in} \\ K_{v1}[(1 - b_1)p_{in}]^{x_1} & , p_{out} \leq b_1 p_{in} \\ -K_{v2}(p_{out} - p_{in})^{x_2} & , b_2 p_{out} < p_{in} \leq p_{out} \\ -K_{v2}[(1 - b_2)p_{out}]^{x_2} & , p_{in} \leq b_2 p_{out} \end{cases} \quad (5.2)$$

$$p_{in} \geq 0, p_{out} \geq 0$$

5.1.1 Dimensioning of orifices for valves sizes adjustment

All digital valves used in this project are identical. This helps to achieve as similar behaviour as possible in the switching dynamics. All valves in PCM are now of the same size but the PCM method requires discrete valued sized valves based on 2^x where $x = [0, 1, 2, 3, \dots]$. This problem is solved by adding fixed orifices after each valve to achieve the desired equivalent sizes of valves.

According to the series flow orifices equation presented in **Eq.(5.3)** the equivalent discharge area A_d and coefficient C_d can be adjusted to the desired value by dimensioning a corresponding fixed orifice in series to the valve.

$$(C_d \cdot A_d)_{eff} = \frac{1}{\sqrt{\sum_{i=1}^N \frac{1}{C_{d,i}^2 \cdot A_{d,i}^2}}} \quad (5.3)$$

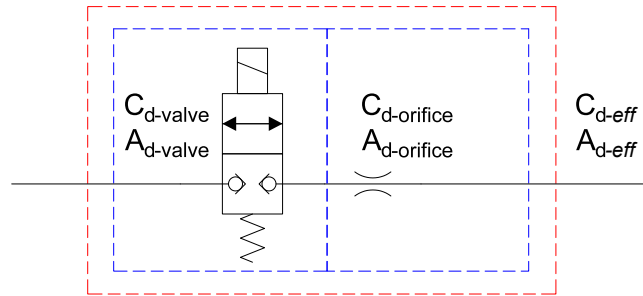


Figure 5.2: Orifice adjustment of valves

Typically, the data sheets of the valves do not provide the values of A_d and C_d . The values of nominal flow Q_N and nominal pressure drop Δp_N are used to calculate A_d and C_d for the selected valves according to the following equations:

$$K_v = Q_N \sqrt{\frac{1}{\Delta p_N}} \quad (5.4)$$

$$K_v = C_d A_d \sqrt{\frac{2}{\rho}} \quad (5.5)$$

$$C_d A_d = K_v \sqrt{\frac{\rho}{2}} \quad (5.6)$$

With the equivalent $K_{v_{eff}}$ for each valve arrangement, calculated from the flow requirement according to the PCM method, and $A_d C_d$ of the valve, calculated in **Eq.(5.6)**. The needed values of A_d and C_d for the adjustment orifice is found by **Eq.(5.3)** to achieve the desired overall $K_{v_{eff}}$ of the arrangement.

$$K_{v_{eff}} = (C_d A_d)_{eff} \sqrt{\frac{2}{\rho}} \quad (5.7)$$

Total flow through the parallel connected valve arrangements is calculated depending on which valves are open and closed.

$$Q_{tot} = \sqrt{\Delta p} \cdot (K_{v1} \cdot x_1 + K_{v2} \cdot x_2 + K_{vn} \cdot x_n) \quad (5.8)$$

Where:

Δp	- Pressure drop over valves	[Bar]
$x_1 \rightarrow x_n$	- 0 or 1 depending on if the valve is open or closed	
$K_{v1} \rightarrow K_{vn}$	- Flow coefficient of different orifice/valve combinations	$[m^3 \cdot \sqrt{\frac{m}{kg}}]$

5.1.2 Valve delay and response

The valve dynamic was modelled with a transfer function as shown in **Figure 5.3**. The valve delays also have to be modelled, these simply delay the on/off signal to the valves by a set time. A variable delay is not considered in the model, and thus there should not be any of the previously mentioned "bad" state transitions.

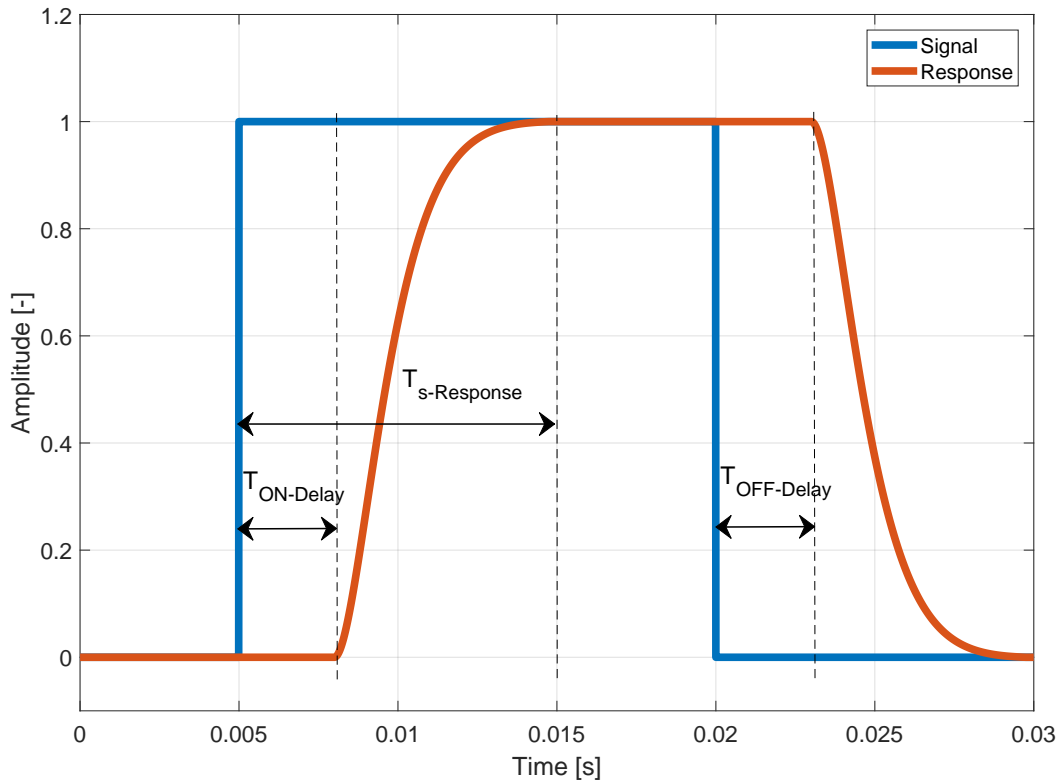


Figure 5.3: Simulated valve response with $T_s = 10ms$

Combining flow **Eq.(5.1)** and the adjusted K_v in **Eq.(5.7)** together with the transfer function presented in **Figure 5.3**. Resulted in a model representing size modified valves with opening and closing dynamics. **Figure 5.4** shows the applied model in Simulink for this case.

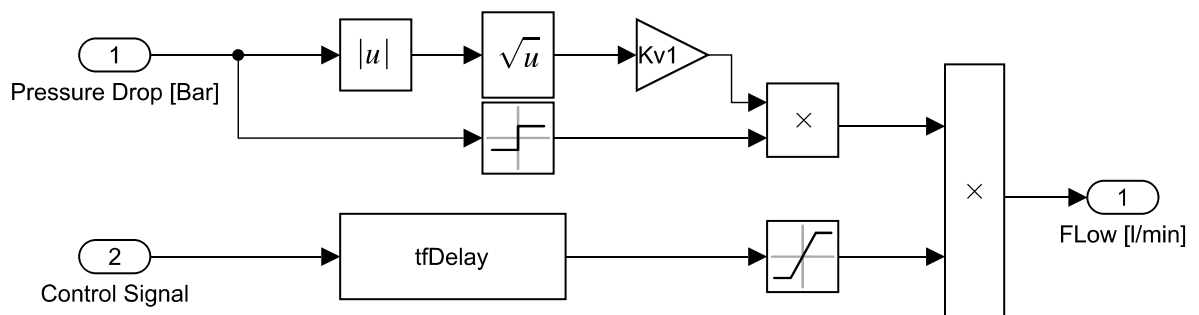


Figure 5.4: Simulink model for valve

The sampling time of the controller is set to the same time as the slowest valve response. This is to make sure all the valves can change their state before a new signal is received. The different response behaviours of the valve, depending on the signal length, are presented in **Figure 5.5**.

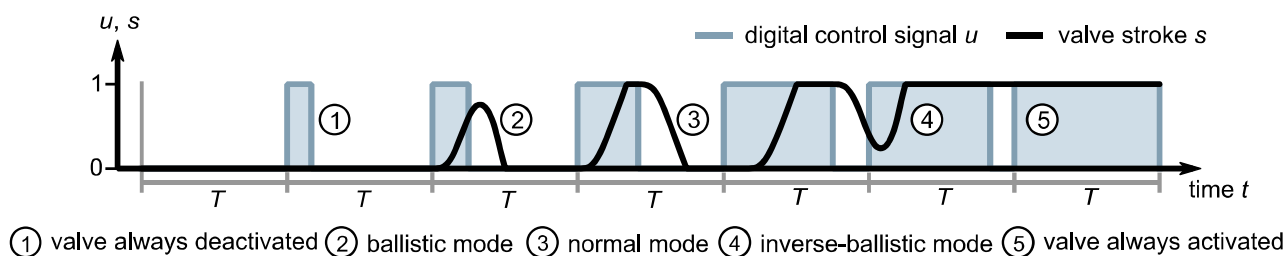


Figure 5.5: Operation modes of a switching valve in case of using digital control methods [22]

As shown in **Figure 5.5**, there are three different scenarios that can occur by different signal length.

1. Opening signal is too short to overcome the opening delay. In this case the valve remains closed.
2. Opening signal is shorter than the total response time. Here, the valve does not reach the full opening before it closes again.
3. Opening signal is equal to or longer than the response time. In this scenario, the valve reaches full opening.
4. Closing signal is shorter than response time. Here, the valve does not reach full closing before it opens again.
5. Closing signal is too short to overcome the opening delay. In this case, the valve remains open without any changes.

Not all the operation modes are suitable to be used in combination with a PCM coded DFCU. The reason for that is the difficulties to estimate the position of the valve and as a consequence, man can not rely on the flow calculation in the transient stage. In this thesis, only *mode 3* will be applied by setting the controller sampling time equal to the slowest valve response.

It should be noted that because of the ideal sizing and valve response time, the transient uncertainty between state switchings in the simulation will be closer to the behaviour of a PNM coded DFCU than a PCM one.

5.2 Cylinder

It is assumed no internal leakage in the cylinder. Possible leakage would be minimal and will not affect the system in a way to make it important to consider in the model. To find the position and velocity of the cylinder, **Eq.(5.9)** is applied. Forces acting on the cylinder shown in **Figure 5.6** are pressure differential force, external load and the friction force.

$$m\ddot{x} = p_a A - p_b A_r - F_f - F_{Load} \quad (5.9)$$

Where:

m	- Load mass	$[Kg]$
\ddot{x}	- Acceleration	$[\frac{m}{s^2}]$
p_a	- Pressure in piston side	$[Bar]$
A	- Area of piston side	$[m^2]$
p_b	- Pressure in rod side	$[Bar]$
A_r	- Area of rod side	$[m^2]$
F_f	- Friction force	$[N]$
F_{Load}	- Load force	$[N]$

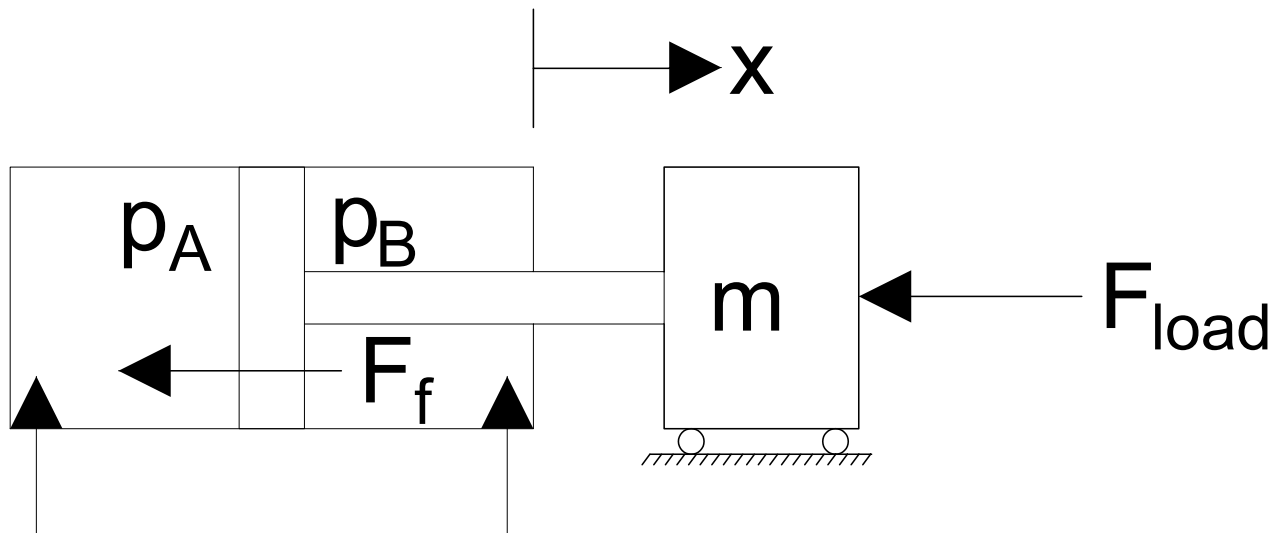


Figure 5.6: Cylinder load case

The friction force is modelled by the stribeck friction model, that is expressed in **Eq.(5.10)**. The parameters for the friction model are calculated to fit the measurements taken in [23] and plotted in **Figure 5.7**.

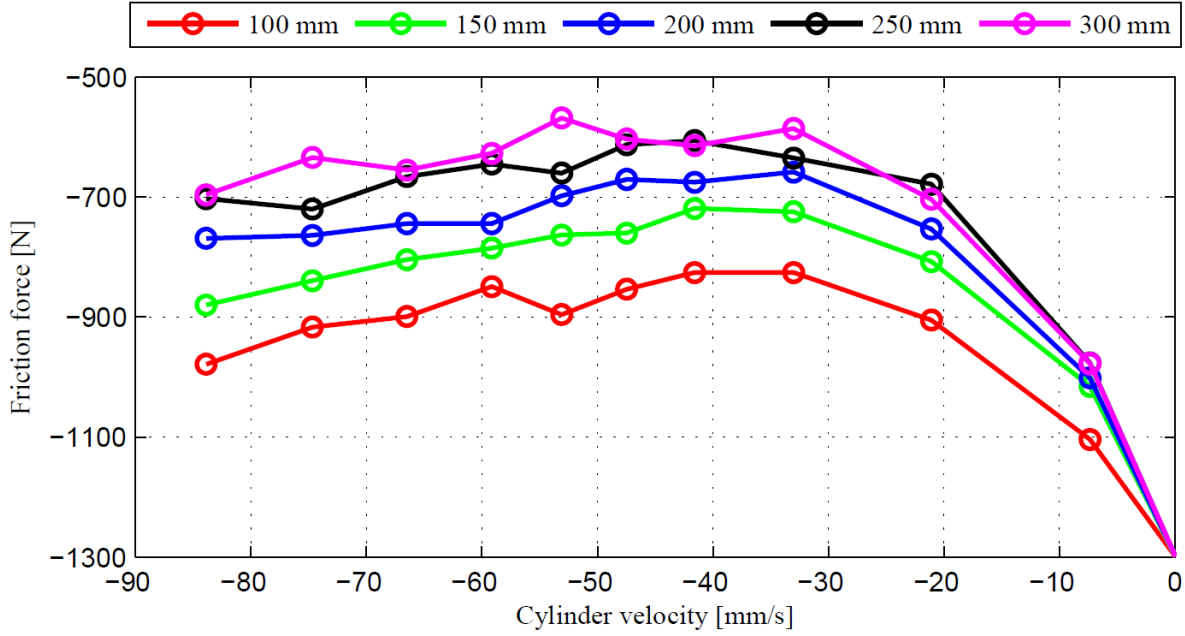


Figure 5.7: Measured friction force [23]

$$F_f = (f_s \cdot e^{-\frac{1}{\tau_s}|\dot{x}|} + f_c) \cdot (\tanh(\gamma \cdot \dot{x})) + f_v \cdot \dot{x} \quad (5.10)$$

Where:

f_v	- Coeff. of viscous friction for piston	$\left[\frac{kg}{s}\right]$
f_c	- Coulomb friction force	$[N]$
f_s	- Static friction time constant	$\left[\frac{s}{m}\right]$
\dot{x}	- Cylinder velocity	$\left[\frac{m}{s}\right]$
τ_s	- Static friction time constant	$\left[\frac{s}{m}\right]$
γ	- Approximation for friction force	$[-]$

The following **Figure 5.8** presents the friction forces from the simulated model based on measurements.

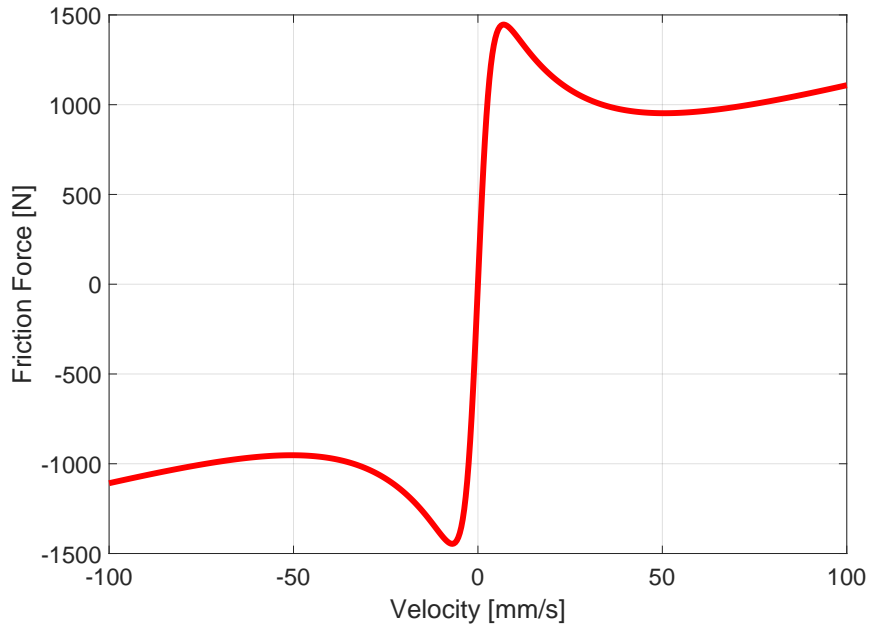


Figure 5.8: Modelled friction based on measured data

It is also important to model the additional forces on the cylinder if it is to move all the way to either the lower or upper bounds. This is modelled by **Eq.(5.11)**.

$$F_{endforce} = \begin{cases} x \cdot k_{lower} + \dot{x} \cdot c_{lower} & , x < 0 \\ x \cdot k_{upper} + \dot{x} \cdot c_{upper} & , x > L \\ 0 & , 0 < x < L \end{cases} \quad (5.11)$$

Where:

k_{lower}	- Lower Spring force	$[\frac{N}{m}]$
k_{upper}	- Upper Spring force	$[\frac{N}{m}]$
c_{lower}	- Lower Damper force	$[\frac{N \cdot s}{m}]$
c_{upper}	- Upper Damper force	$[\frac{N \cdot s}{m}]$
L	- Length of cylinder	$[m]$

To describe the pressure build-up in the cylinder, the continuity equation is used. In **Eq.(5.12)** the general form of the continuity equation is shown.

$$Q_{in} - Q_{out} = \dot{V} + \frac{V}{\beta} \dot{p} \quad (5.12)$$

If this is applied to the hydraulic cylinder and zero leakage is assumed it will result in **Eq.(5.13)**. For the cylinder moving in the positive direction.

$$\begin{aligned}
 Q_A &= v \cdot A + \frac{(A \cdot x + V_{A0}) \cdot \dot{p}_a}{\beta} \\
 -Q_B &= -v \cdot A_r + \frac{(A_r \cdot (L - x) + V_{B0}) \cdot \dot{p}_b}{\beta}
 \end{aligned} \tag{5.13}$$

Where:

Q_A	- Flow into cylinder chamber A	$[\frac{m^3}{s}]$
Q_B	- Flow out of cylinder chamber B	$[\frac{m^3}{s}]$
v	- Cylinder velocity	$[\frac{m}{s}]$
x	- Cylinder position	$[m]$
V_{A0}	- Dead volume chamber A	$[m^3]$
V_{B0}	- Dead volume chamber B	$[m^3]$
β	- Oil bulk modulus	$[Pa]$
\dot{p}_a	- Pressure gradient chamber A	$[\frac{Pa}{s}]$
\dot{p}_b	- Pressure gradient chamber B	$[\frac{Pa}{s}]$

This equation is then rearranged and solved for the pressure build up.

5.3 Accumulator

Accumulators are used in this thesis in some of the designed hydraulic systems. In the first application, the accumulator is used as pressure buffer. The system is set to keep the pressure in the accumulator within a specific range. It is referred to as the high pressure (HP) accumulator. This make it possible to unload the motor if the HP accumulator has sufficient pressure. The other application is where the accumulator is used as a closed tank. Due to the difference in cylinder chamber volumes a tank is required. This accumulator is referred to as the low pressure (LP) accumulator, this is pre-charged with a low pressure just to avoid vacuum in the suction pipes.

The capacitance based model for accumulators from [24] is used to model the accumulators according to **Eq.(5.14)**.

$$C = \frac{V_{lp}}{\beta} + \frac{V_0}{N} \frac{p_0^{\frac{1}{N}}}{p_{lp}^{\frac{N+1}{N}}} \tag{5.14}$$

Where:

C	- Capacitance based accumulator model	$[\frac{m^3}{bar}]$
V_{lp}	- Line volume	$[m^3]$
V_0	- Accumulator gas volume	$[m^3]$
p_{lp}	- Line pressure	$[bar]$
p_0	- Accumulator pre-charge pressure	$[bar]$
N	- Polytopic index	$[-]$

With the capacitance calculated, change in pressure of the accumulator can be found from **Eq.(5.15)**. Here, Q_{ac} is the flow flowing in/out of the accumulator. Adiabatic process is assumed where thermal exchange with the ambient is not considered.

$$\dot{p} = \frac{1}{C} \cdot Q_{ac} \quad (5.15)$$

Where:

$$\begin{aligned} \dot{p} & - \text{Change in pressure} & [Bar] \\ Q_{ac} & - \text{Flow to accumulator} & [\frac{l}{min}] \end{aligned}$$

5.4 Line losses

The pressure losses in the hose from the valves to the cylinder chambers are considered. First it has to be determined if the flow in the hose is turbulent or laminar. This can be done by calculating the Reynolds number.

$$Re = \frac{V_{line}^{max} \cdot D_{line}}{\nu} \quad (5.16)$$

Where:

$$\begin{aligned} Re & - \text{Reynolds number} & [-] \\ V_{line}^{max} & - \text{Maximum fluid velocity} & [\frac{m}{s}] \\ D_{line} & - \text{Inner diameter of pose} & [m] \\ \nu & - \text{Kinematic viscosity} & [\frac{m^2}{s}] \end{aligned}$$

From this the hose dimensions were selected to ensure a laminar flow at the maximum velocity of the system. This is done by making sure Reynolds number does not exceed 2300 at the maximum velocity. The pressure losses could then be modelled using the Hagen–Poiseuille equation shown in **Eq.(5.17)**. This equation is for an incompressible flow through a cylindrical pipe with laminar flow.

$$\Delta p = \frac{128 \cdot \mu \cdot L_{line} \cdot Q}{\pi \cdot D_{line}^4} \quad (5.17)$$

Where:

$$\begin{aligned} \mu & - \text{Dynamic viscosity of the oil} & [\frac{kg}{m \cdot s}] \\ L_{line} & - \text{Length of hose} & [m] \end{aligned}$$

5.5 Pump and electrical motor

All the designed hydraulic systems in this thesis are using constant speed electrical motors driving fixed displacement pumps. External gear pumps are recommended here due to its relatively stable flow without ripples compared to axial and radial piston displacement pumps.

Also, the main focus in this thesis is on the control components that are the ON/OFF valves. In the simulation model the pumps are represented with constant flow sources. The variation in efficiency is hereby not considered.

5.6 Pressure relief valve

In this thesis the pressure relief valves only serve as a safety component to protect the pump in case the control valve failure. This scenario is not considered and consequently the pressure relief valves are not modelled.

5.7 Cooler and filter

The thermal aspects are not considered in this thesis. Pressure drop over the cooler and filter is assumed negligible. Coolers and filters are not considered in the simulation models.

5.8 Bulk modulus

Bulk modulus depends on variation of pressure, fluid temperature, volume and the piping. In this thesis, variation in temperature is not considered. The piping is assumed to be relatively short and stiff since it will mainly consist of manifolds and steel pipes. This leads to the assumption of a constant bulk modulus of 15000 *Bar*. The main simulation is executed with the assumed Bulk modulus. Another comparison simulation is executed with lowered Bulk modulus down to 10000 *Bar* to simulate the impact of variation in Bulk modulus.

5.9 Power

Since the electrical motor and pumps are not modelled, the input power is calculated by the pump flow and pump pressure as in **Eq.(5.18)**. Output power is calculated from the mechanical work exerted by the hydraulic cylinder applying **Eq.(5.19)**.

$$P_{IN} = \frac{p_p \cdot Q_p}{\eta_{Combined}} \quad (5.18)$$

$$P_{OUT} = F \cdot v \quad (5.19)$$

Where:

P_{IN}	- Input power	[<i>Watt</i>]
p_p	- Pump pressure	[<i>Pa</i>]
Q_p	- Pump flow	[$\frac{m^3}{s}$]
$\eta_{Combined}$	- Combined efficiency of motor and pump	[-]
P_{OUT}	- Output power	[<i>Watt</i>]
F	- Cylinder force	[<i>N</i>]
v	- Cylinder velocity	[$\frac{m}{s}$]

6 | Results

Simulation Results of System Combinations

The modelling and simulation is performed in MATLAB Simulink. The model is built from MATLAB code, MATLAB function blocks and basic Simulink blocks to make customized components possible. The simulations were solved by a fix step solver ode3 "Bogacki-Shampine" with a step size of 0.1 *ms*.

Considering the ready to market valves [11] and its response time, it is assumed that a response time of 10 *ms* is a reasonable start value. The main simulation will be executed with 10 *ms* and later reduced and increased to study the impact of response time on the different systems. Bulk modulus is assumed to be 15000 *Bar* in the main simulation. Another simulation is executed with lowered Bulk modulus down to 10000 *Bar* to analyse its impact.

6.1 Load case

To have a study covering most of the load scenarios, the load case is consisting of two stages. In both stages a mass of 1000 *Kg* is attached to a vertical mounted cylinder. In the first stage, the cylinder is mounted over the mass so that gravity is acting in the same direction as cylinders extraction. The second stage is opposite to the first so that the gravity is acting in retraction direction of the cylinder. **Figure 6.1** gives an overview over the studied case.

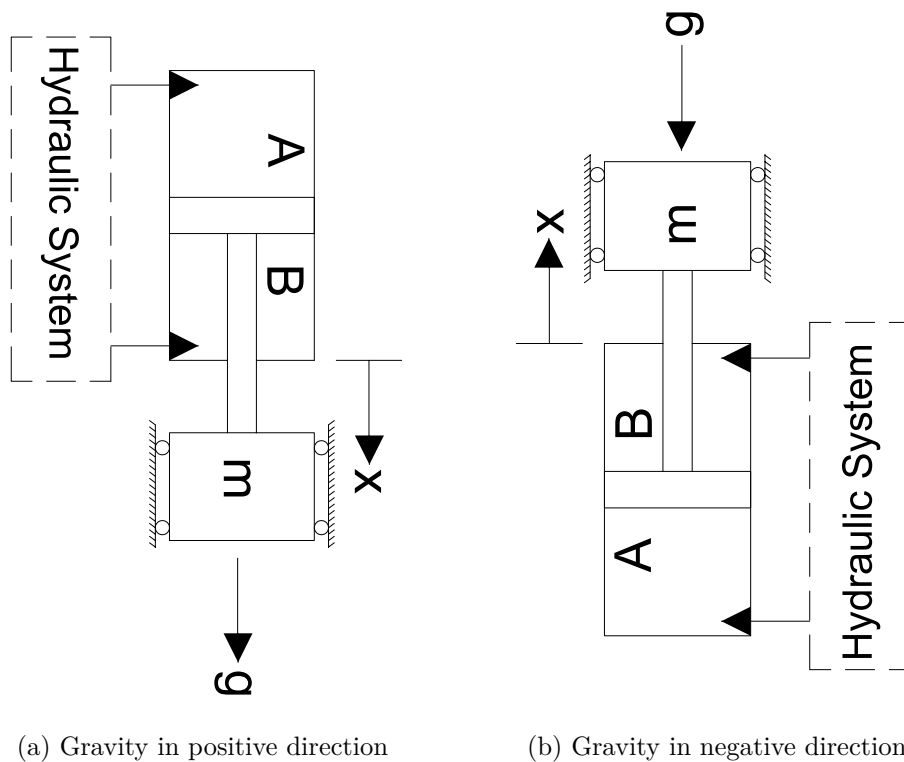


Figure 6.1: Study load case

The motion requirements are set to 0.5 mm accuracy and a maximum velocity of $150 \frac{\text{mm}}{\text{s}}$. The selected reference path can be seen in **Figure 6.2**. During the first two cycles the system will be subjected to a positive external load and during the two later a negative load. From the velocity reference it is seen the second and fourth cycle will require a velocity close to the maximum of the system.

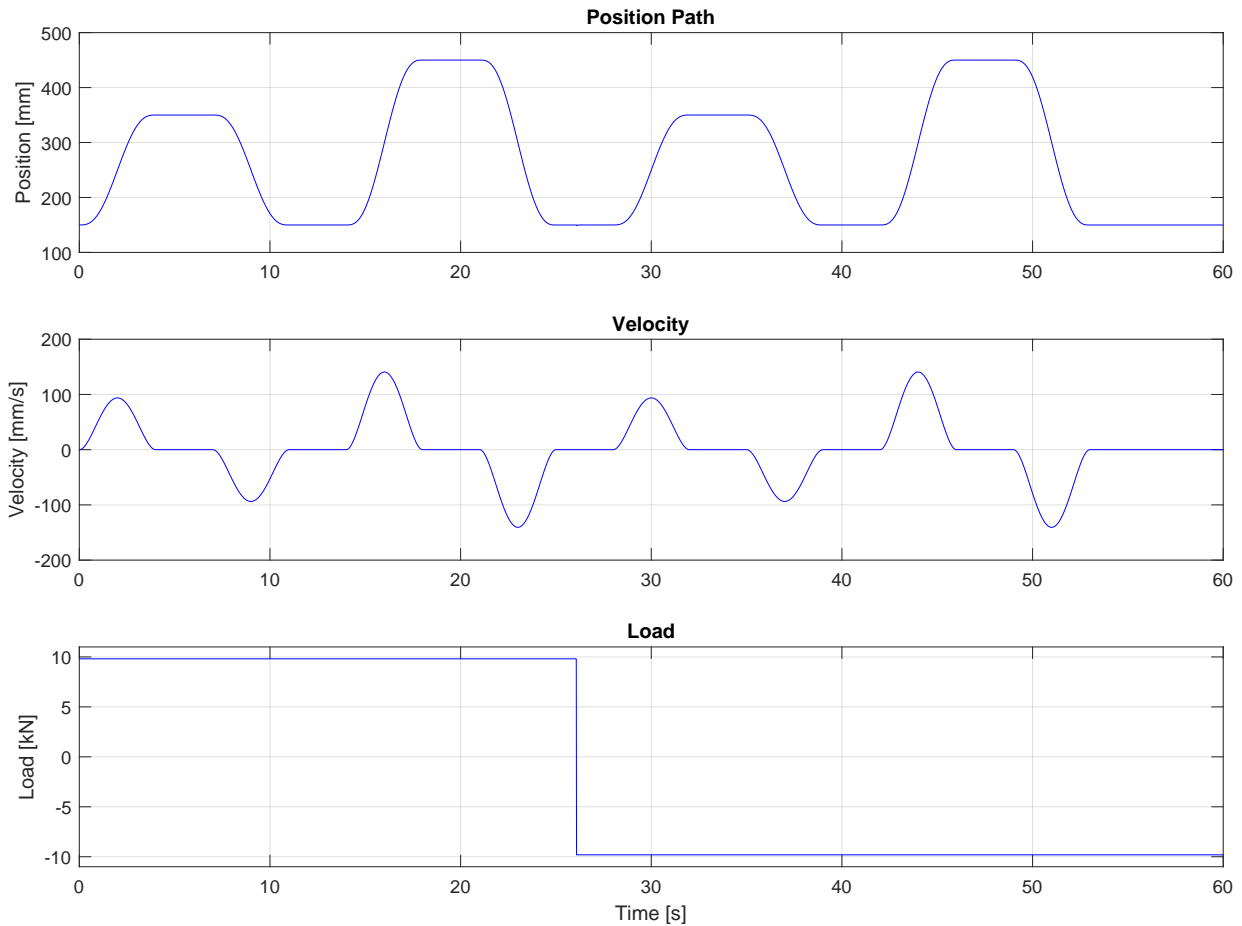


Figure 6.2: Position reference and load case

6.2 System simulation and analysis

With the three designed control systems and the four designed hydraulic architectures, many combinations can be achieved. However, the goal in this section is to examine the functionality of each control and hydraulic system. For this reason, each control system is combined and simulated with at least one hydraulic system. The same is applied for the hydraulics where each system is combined with at least one control system.

The result will cover all the hydraulic and control systems despite several possible combinations for each system. **Table 6.1** shows the selected combination to be simulated. Further in this chapter the results of the simulated combinations are presented. It is assumed that the not simulated combinations are possible to implement and give sufficient results, if all the selected combinations covering all the systems give good results.

Table 6.1: Selected and Simulated Combinations

CONTROL \ HYDRAULIC	HYD 1	HYD 2	HYD 3	HYD 4
	CTRL 1	-	SIMULATED 6.2.3	SIMULATED 6.2.4
CTRL 2	SIMULATED 6.2.1	-	-	-
CTRL 3	SIMULATED 6.2.2	-	-	-

6.2.1 Combination 1 Hydraulic 1 Control 2

The following plots are the results for the 4 DFCU system in combination with the position and velocity control presented in 4.2. The path and load case of the system is the one presented above.

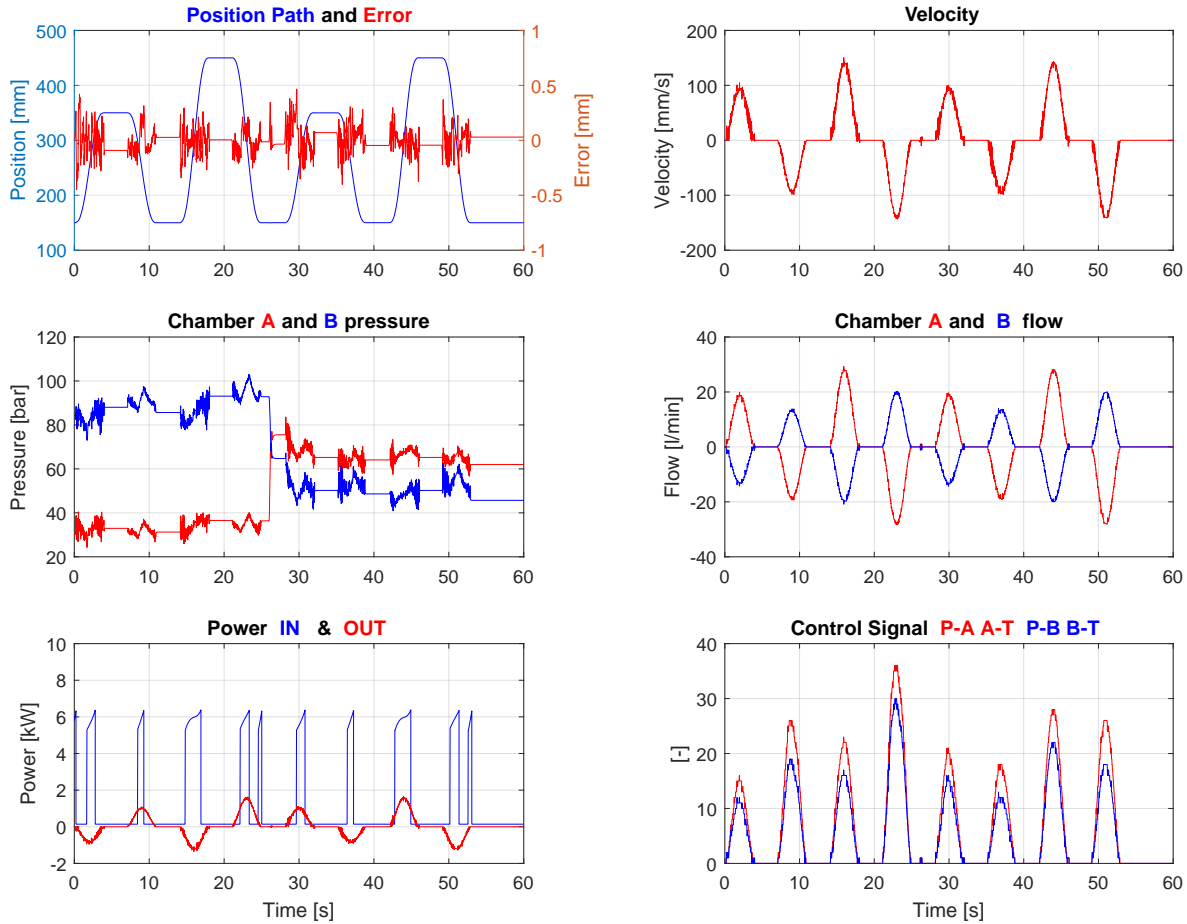


Figure 6.3: Plots of system response to the 4 DFCU system

Position and Accuracy

The first plot presents the error between the reference position and actual position. The error here is kept within $\pm 0.5 \text{ mm}$.

Velocity and Flow

The second and forth plots is the velocity and flow. The velocity should be proportional to the flow, and this is verified by the simulation. Negative flow means flow from the cylinder to the tank and a positive is from the pump to cylinder.

Pressure

The third plot is the pressure plot. This is very important for digital hydraulics as a big challenge is the pressure peaks. For this simulation the pressure does have some peaks but assumed to be less in a physical model that might have more damping factors. The two large pressure differences between A and B side are where the cylinder is retracting with a positive load. Here the pressure on the smaller area rod-side must overcome the load and a pressure to push the cylinder down at the reference velocity. The maximum pressure in this simulation is slightly over 100 *Bar* where the high pressure accumulator is set to vary between 110 & 130 *Bar*.

Power

The large power requirements happen when the pressure in the high pressure accumulator falls under the limits. The plot of output power indicates the possibility of recovering energy and improvement of efficiency.

Control Signals

Here in the last plot the control signals going to the four DFCU are plotted. By looking at the flow diagram above it is easy to tell if the control signal is to P-A or A-T. If the A-flow is positive the red control signal is the pump, and if the A-flow is negative the control signal is to the tank. Similarly for the B-side. It can also be seen that only the 5 smallest valves are used for most of the path. The largest valves are only opening when the cylinder is retracting at maximum velocity.

Impact of Response Time

To investigate the limitation of valve response time, the system is simulated with 4 different settings, 1, 10, 30 & 50 *ms*. **Figure 6.4** presents the impact of these on position error. The two smallest response time values can keep the error within the set limit. The two highest are generating to large values exceeding the acceptable limit.

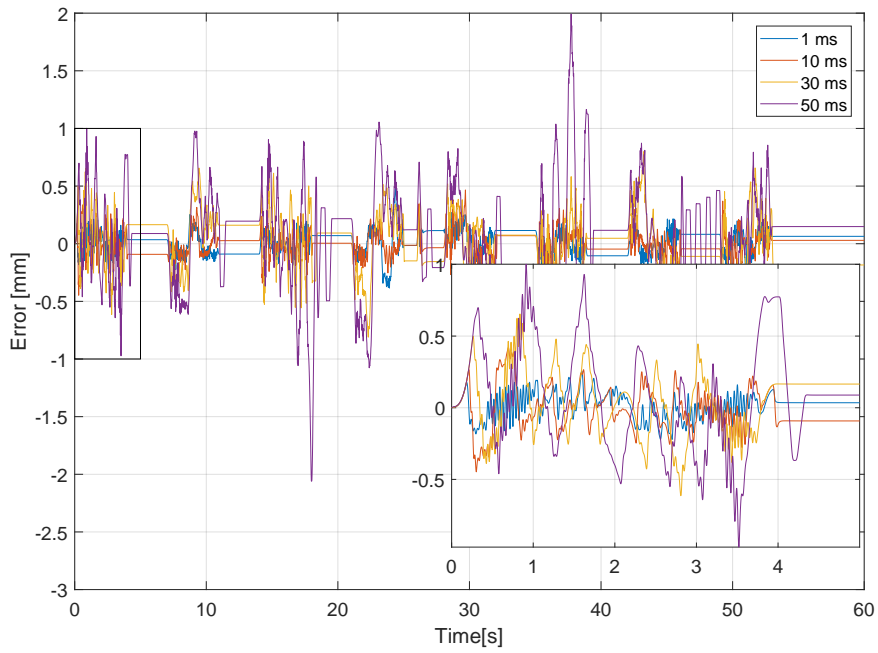


Figure 6.4: Position error by different valve response times in combination 1

Impact of Bulk modulus

Reduced Bulk modulus from 15000 down to 10000 *Bar* increased the oscillation in the system and consequentially the position error is slightly increased as shown in **Figure 6.5**.

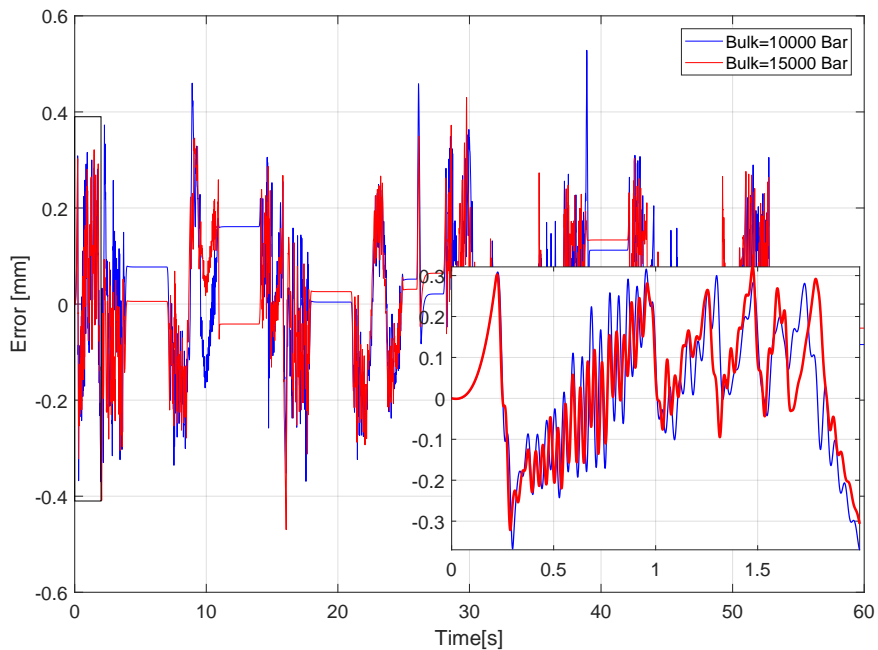


Figure 6.5: Position error by different Bulk modulus in combination 1

6.2.2 Combination 2 Hydraulic 1 Control 3

This is hydraulic system 1 in combination with CTRL 3. This will need the same type of measurements as CTRL 2. One cost function was tested for the system. The different reference pressures are presented in **Table 6.2** where the reference pressure depends on the direction of the load and if the cylinder is extracting or retracting.

Table 6.2: Reference pressure for the load case with cost function (4.5)

Direction of Load	Direction of Motion	Reference Pressure
+	+	$P_b = 40 \cdot 1.4$
+	-	$P_a = \text{abs}(F/A_A) \cdot 10^{-5} + 40$
-	-	$P_a = 40$
-	+	$P_b = \text{abs}(F/A_B) \cdot 10^{-5} + 30 \cdot 1.4$

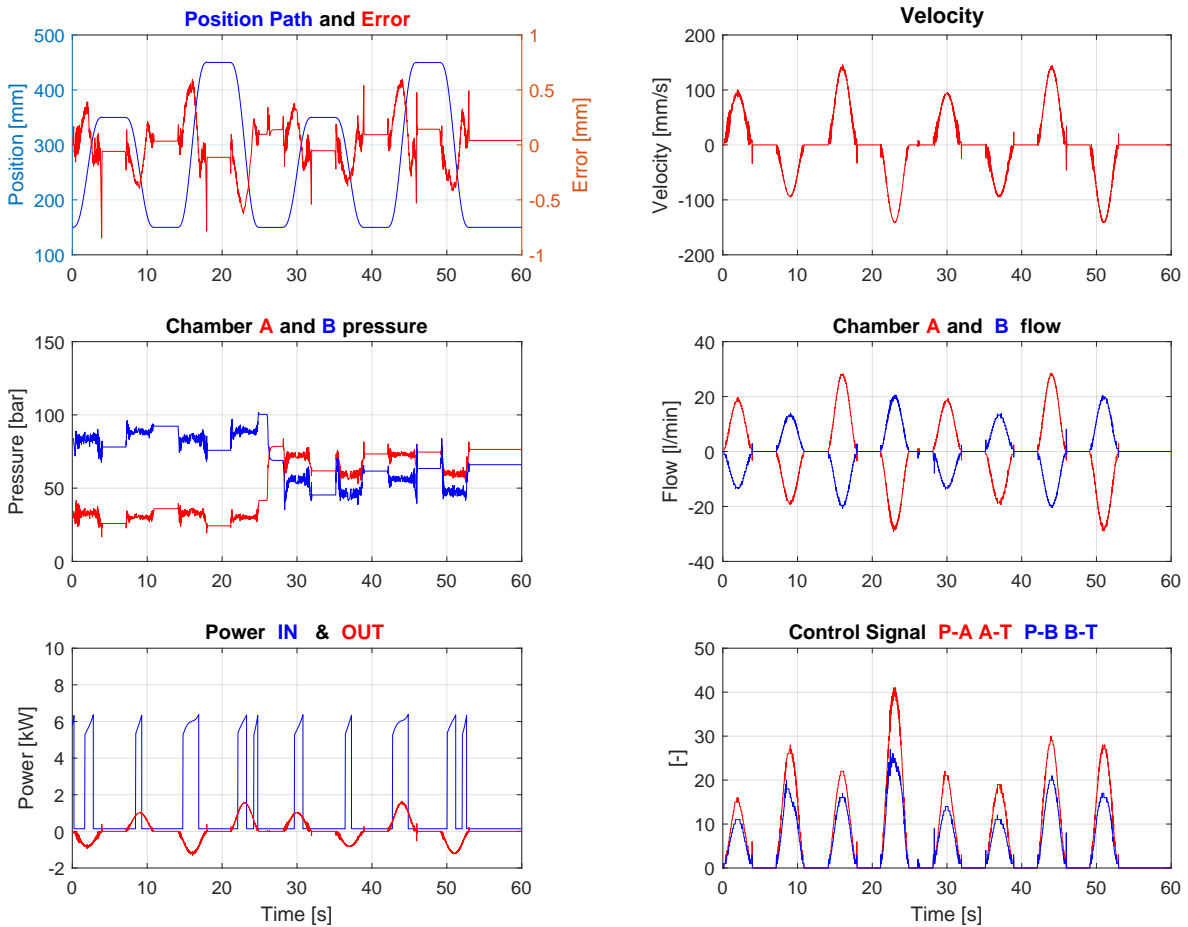


Figure 6.6: Plots of system response to the 4 DFCU system with CTRL 3 with cost function (4.5)

Position and Accuracy

The first plot in **Figure 6.15** shows that the error is kept within the limit most of the time. Peaks at around 4 & 18 s are exceeding the limits. This might be eliminated in physical system due to possible additional damping factors. A further optimization of the controller is needed to meet the error limitation and reduce the peaks.

Velocity and Flow

Flow and velocity are affected by the large peaks in the position error. Other than that, the flow and velocity are progressing as expected and desired.

Pressure

The pressure is not varying too much when the cylinder is changing direction. It is kept around the reference values calculated in **Table 6.2**. In the second stage of load case the highest pressure value is moved from B- to A-side due to load direction. The highest value reached in the whole cycle is about 100 *Bar*.

Power

Very similar to the previous combination, the motor is resting when the required pressure is reached in the accumulator. In the idle time the motor has only to put in power enough to overcome the valve to tank.

Control Signals

The control signal has deformed shape compared to reference velocity. This is due to error peaks that need to be corrected. The noise in some areas is not good for the life time of the valves. This could possibly be reduced by improvement to the tuning and optimization of the controller parameters.

Impact of Response Time

Figure 6.7 clearly shows the impact of valve response time and position error. With the smallest value of 1 *ms*, the system is performing best and keeping the error within the accepted range. Response time of 10 *ms* is performing relatively good with slightly overrun of the set limit. This might be solved by further optimization of control system parameters. The largest values of 30, & 50 *ms* are unable to keep the error limit and the highest error is above the limit. Such slow valves could be used for applications where accuracy is less critical.

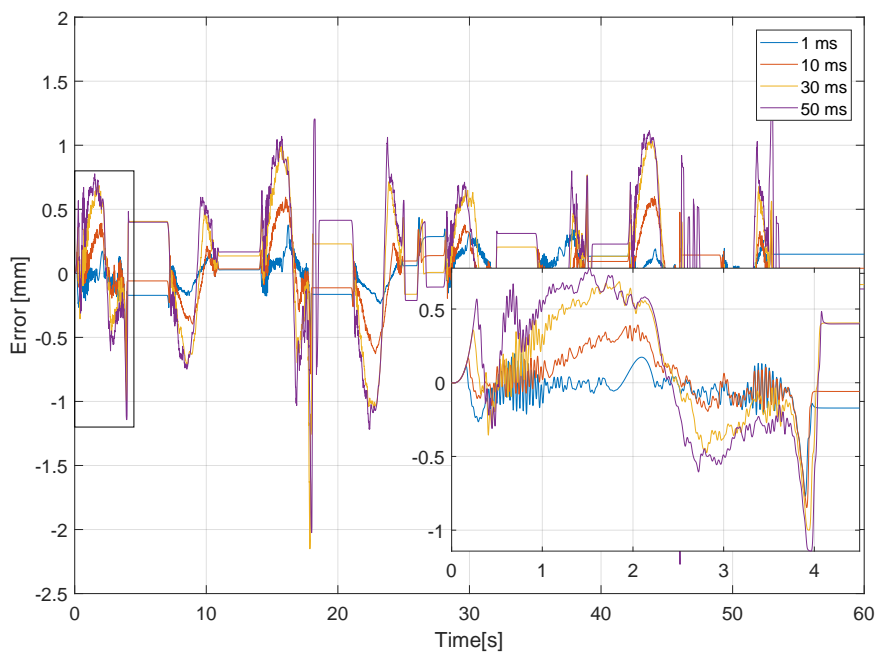


Figure 6.7: Position error by different valve response times in combination 2

Impact of Bulk modulus

Reduced Bulk modulus from 15000 down to 10000 *Bar* increased the oscillation in the system and consequentially the position error is slightly increased as shown in **Figure 6.8**.

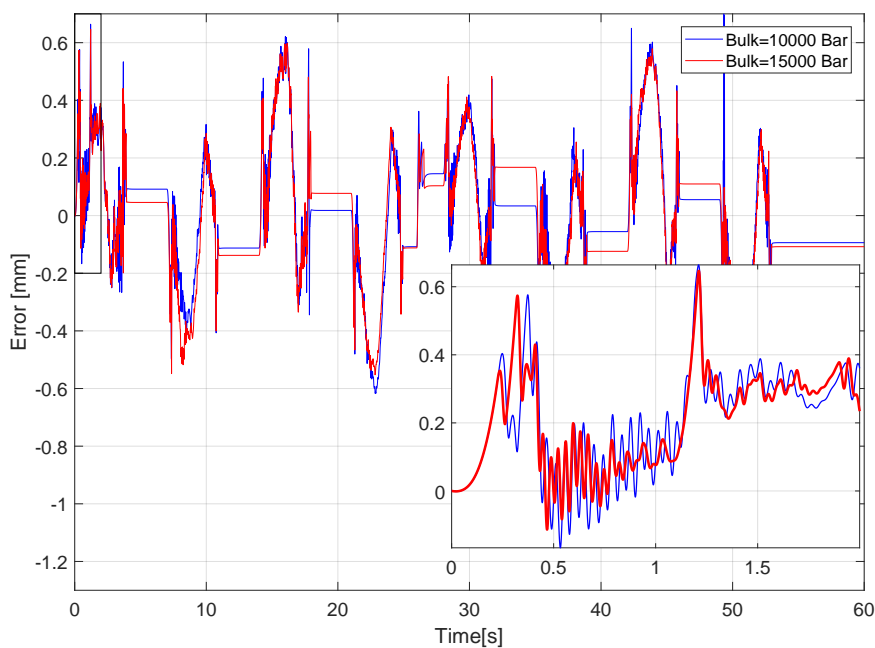


Figure 6.8: Position error by different Bulk modulus in combination 2

6.2.3 Combination 3 Hydraulic 2 Control 1

This system is not using any pressure transducers. It only needs the position feedback for the control system. A challenge is then faced when the load is changing direction. The system has no possibility to discover changes in load because of lack in pressure feedback. With fixed parameters in the controller, the system will be able only to perform one load case and struggle when the load is changing direction. This is solved in this simulation by adjusting control parameters when the load changes direction.

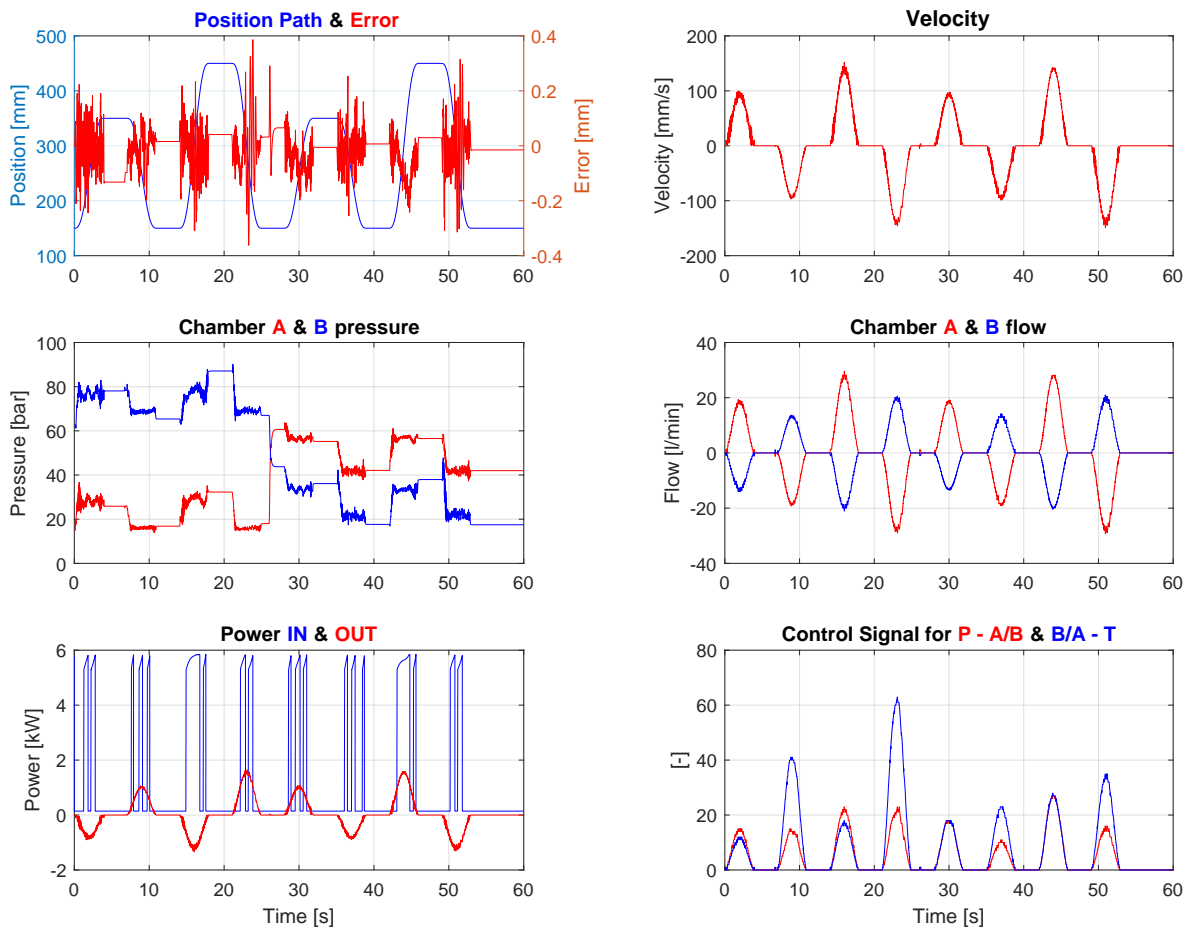


Figure 6.9: Plots of system response to the 2 DFCU system

Position and Accuracy

Despite fewer components in this system compared to system 1 with four DFCU, accuracy is still in an acceptable range. Maximum error is within $\pm 0.4 \text{ mm}$. It is important to notice that the error becomes smaller when the cylinder is acting in the opposite direction of the load.

Velocity and Flow

The flow is corresponding as expected to the velocity. No large peaks or rough transitions occurs which is important to reduce vibration and fatigue issues. However small peaks are existing but considered as acceptable.

Pressure

In the first load phase, the maximum pressure is higher than in the second phase. This is mainly because of difference in the effective pressure area that acts opposite to the load direction in both cases. Sloping transitions and not too noisy behaviour are good signs that the system is not too far from a conventional system with proportional valves. Keeping in mind that the high pressure accumulator is set between 110 *Bar* and 120 *Bar*, the system is only reaching 87 *Bar* at 18 *sec*. This gives an indication that the system might be further optimized to reduce the supply pressure. At the same time, this buffer might be used for a higher load case.

Power

Very similar to system 1. The pump is resting when the high pressure accumulator has sufficient pressure. At this idle time, the pump only need to overcome the pressure drop over the accumulator controlling valve. This valve is set to be larger than the ones used in the DFCU to reduce energy losses by standby run. The red plot for the output power indicating the possibility of energy recovering specially that it has a negative value in some areas. The input power might be reduced if a regenerative hydraulic system is implemented.

Control Signals

Avoiding noisy signals and large transitions has a direct connection to the durability of the valves. The plots shows a smooth and slowly stepped signal. This will be reflected by the lower switching frequency of the valves and in the non-pulsating pressure.

Impact of Response Time

The system is simulated with several valve response times. **Figure 6.10** shows position error with different response times. The results show a clear impact of response time on the accuracy. It has a proportional relationship with the error. The valves with 1 *ms* & 10 *ms* response time keep the error within the set range of ± 0.5 *mm*. However, the error exceeds the error limits when the time response is increased to 30 *ms* & 50 *ms*.

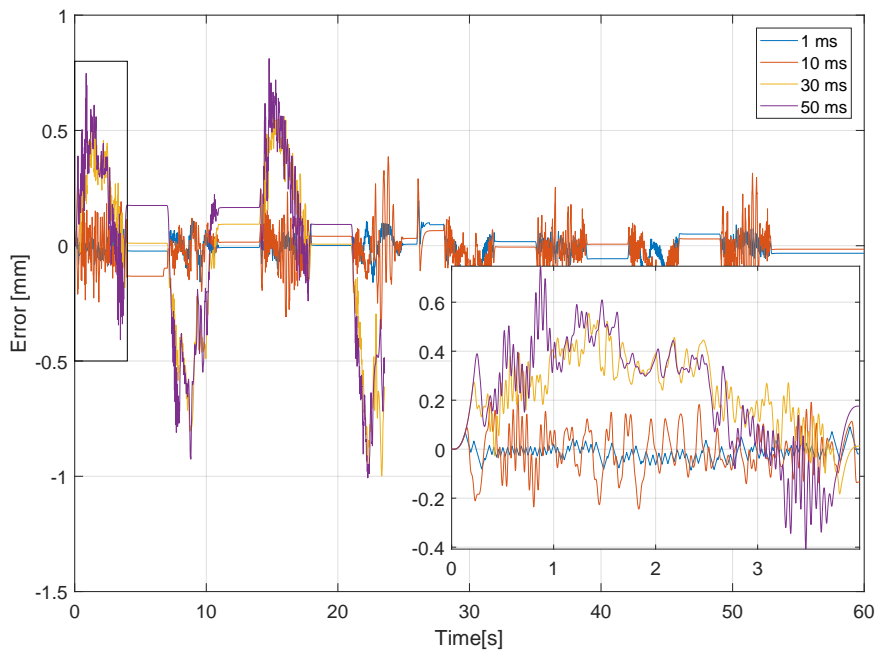


Figure 6.10: Position error by different valve response times in combination 3

Impact of Bulk modulus

Reduced Bulk modulus from 15000 down to 10000 *Bar* increased the oscillation in the system and consequentially the position error is almost doubled as shown in **Figure 6.11**.

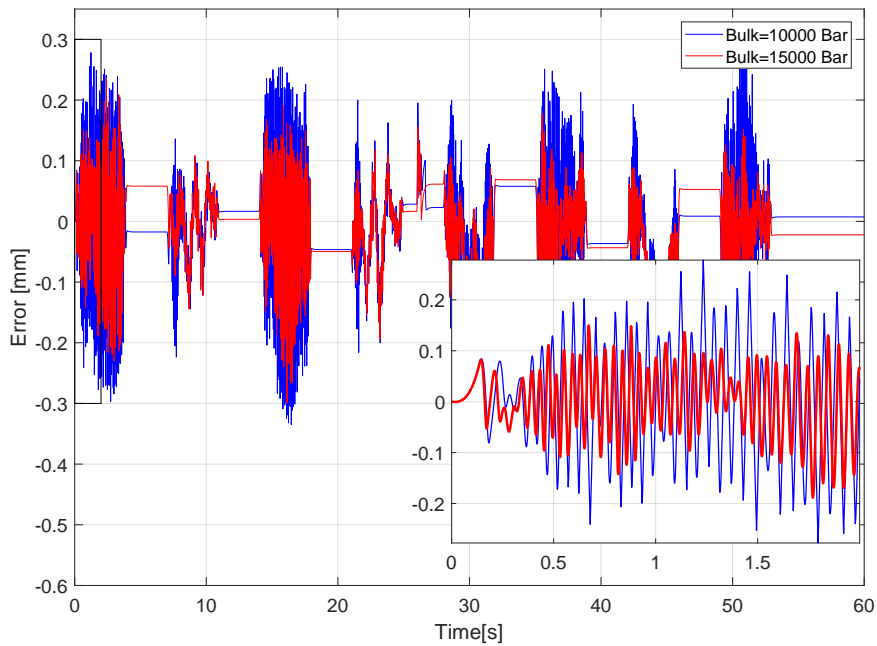


Figure 6.11: Position error by different Bulk modulus in combination 3

6.2.4 Combination 4 Hydraulic 3 Control 1

The control system used for this combination is similar the one used in combination 3 in **Section 6.2.3**. Here also there is no need for pressure transducers. Only position feedback is required. The main difference is that parameters are not changed when the load is varying. The six pumps are controlled in the same way the DFCU is controlled in combination 3. The control signal is split into pump and tank signal. Each signal is controlling the ON/OFF valves to control the inflow from the pumps and the outflow by the DFCU.

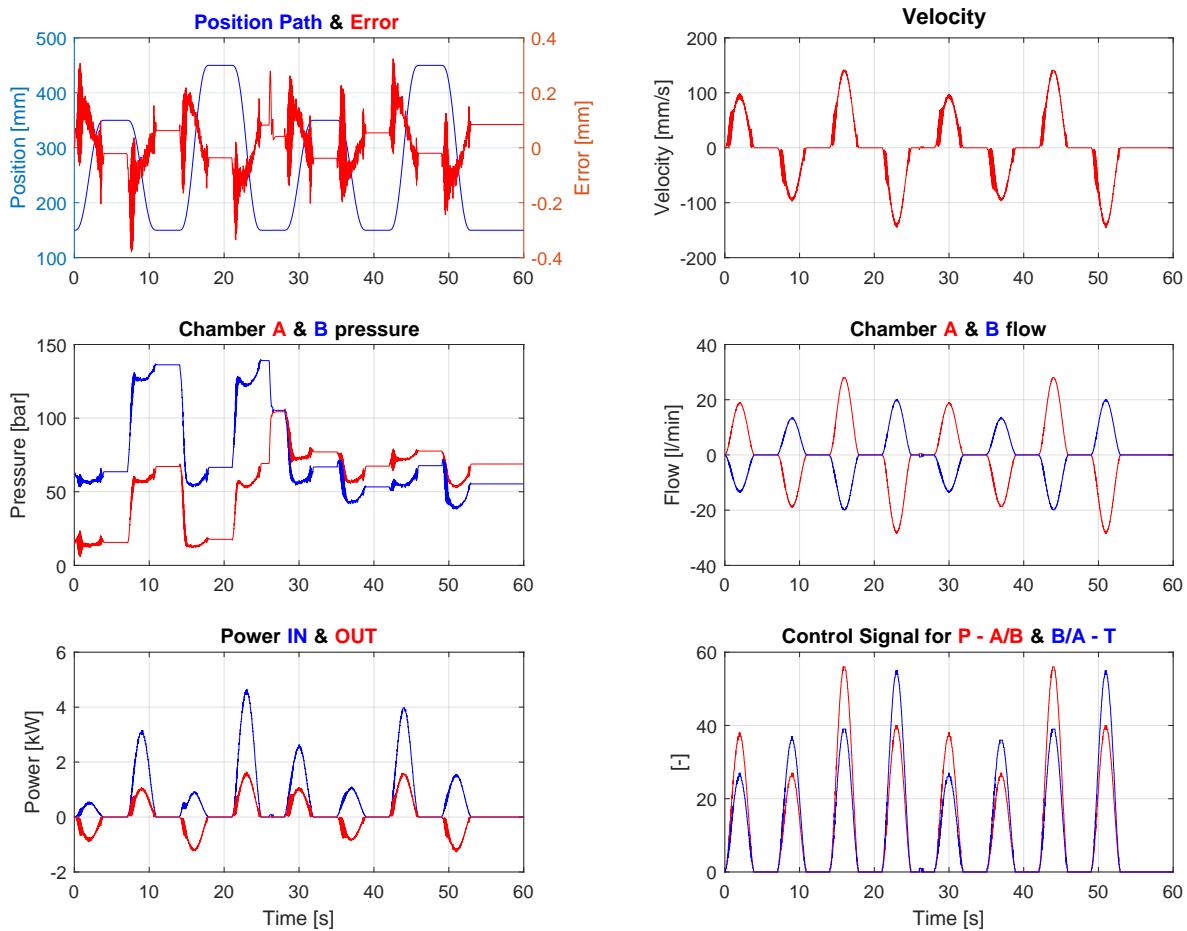


Figure 6.12: Plots of system response to the DDP system

Position and Accuracy

The inflow in this system is very stable and predicted. The reason for that is that the pumps are delivering the same flow independent of the pressure drop over the valves. Consequently, the position error is not so noisy and is varying between ± 0.5 mm.

Velocity and Flow

Because of the small and non-noisy position error, the velocity and flow have a good behaviour without peaks or rough transitions.

Pressure

The pressure in this system is completely not controlled. How high the pressure becomes depends only on the load and the opening ratio of the outflow DFCU. In the first phase of the load case the pressure in rod side reaches around 160 *Bar*. In the second phase, the maximum pressure in piston side is around 100 *Bar*.

Power

Comparing the power in and power out plots in **Figure 6.15**, improved efficiency can be observed compared to the previous combination. By only loading the pumps need to deliver the flow required, the power loss is reduced significantly and the motor driving the pumps is less exposed to shock loads.

Control Signals

The control signals have a similar shape as the velocity. Since the position error is not noisy and not large at the same time, the main contribution in the control signal is generated by the reference velocity. This results in low switching frequency in the valves and less vibration in the system.

Impact of Response Time

For this system it was not possible to run a full simulation with 50 *ms* valve. With 30 *ms* valve it was possible to run the simulation completely. However the error became too large and way over the limit. Valves with 1 *ms* & 10 *ms* resulted in acceptable and less noisy position error. The fact that the simulation gave bad results with 30 *ms* & 50 *ms* might be caused by the controller itself. Adjustment of the used controller is assumed to enhance the results.

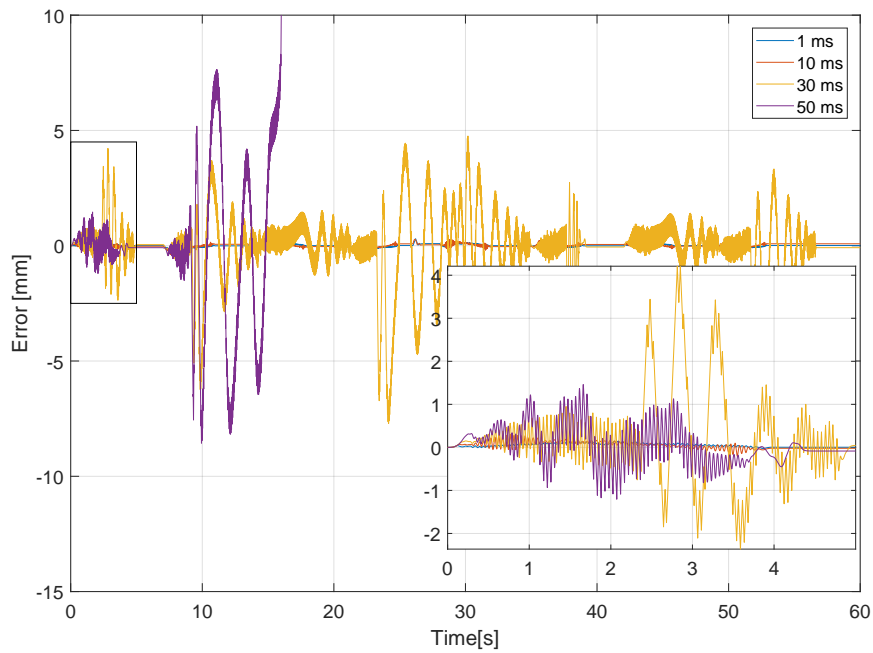


Figure 6.13: Position error by different valve response times in combination 4

Impact of Bulk modulus

Reduced Bulk modulus from 15000 down to 10000 *Bar* increased the oscillation in the system and consequentially the position error is increased as shown in **Figure 6.14**.

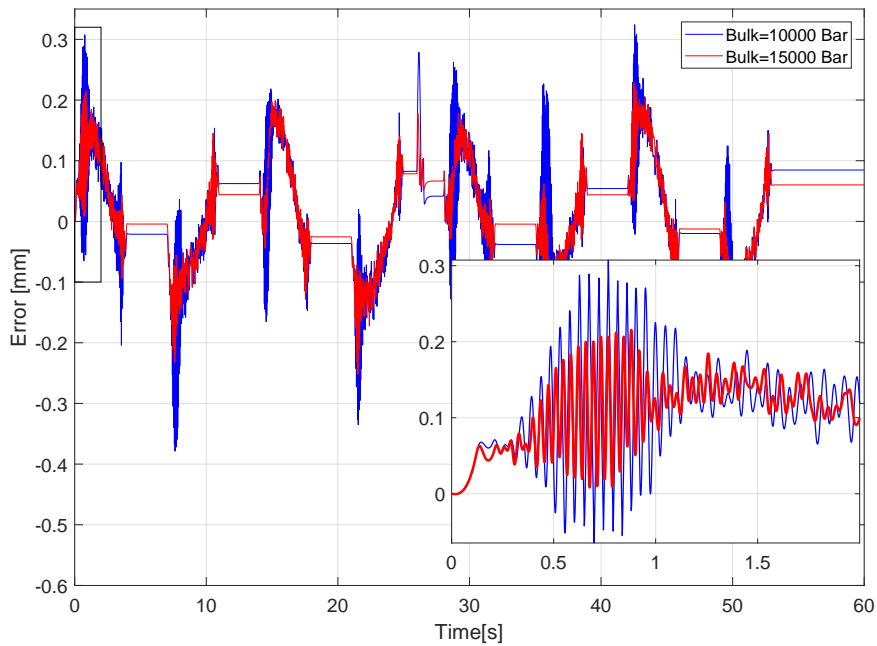


Figure 6.14: Position error by different Bulk modulus in combination 4

6.2.5 Combination 5 Hydraulic 4 Control 1

This combination is similar to hydraulic load sensing systems. It measures the pressure in the chamber directed to pump and sets the pump pressure 15 *Bar* higher. This gives more predicted flow through the valves all the time. The rest of the system is controlled by the velocity feed forward for main signal value and position feedback for correction.

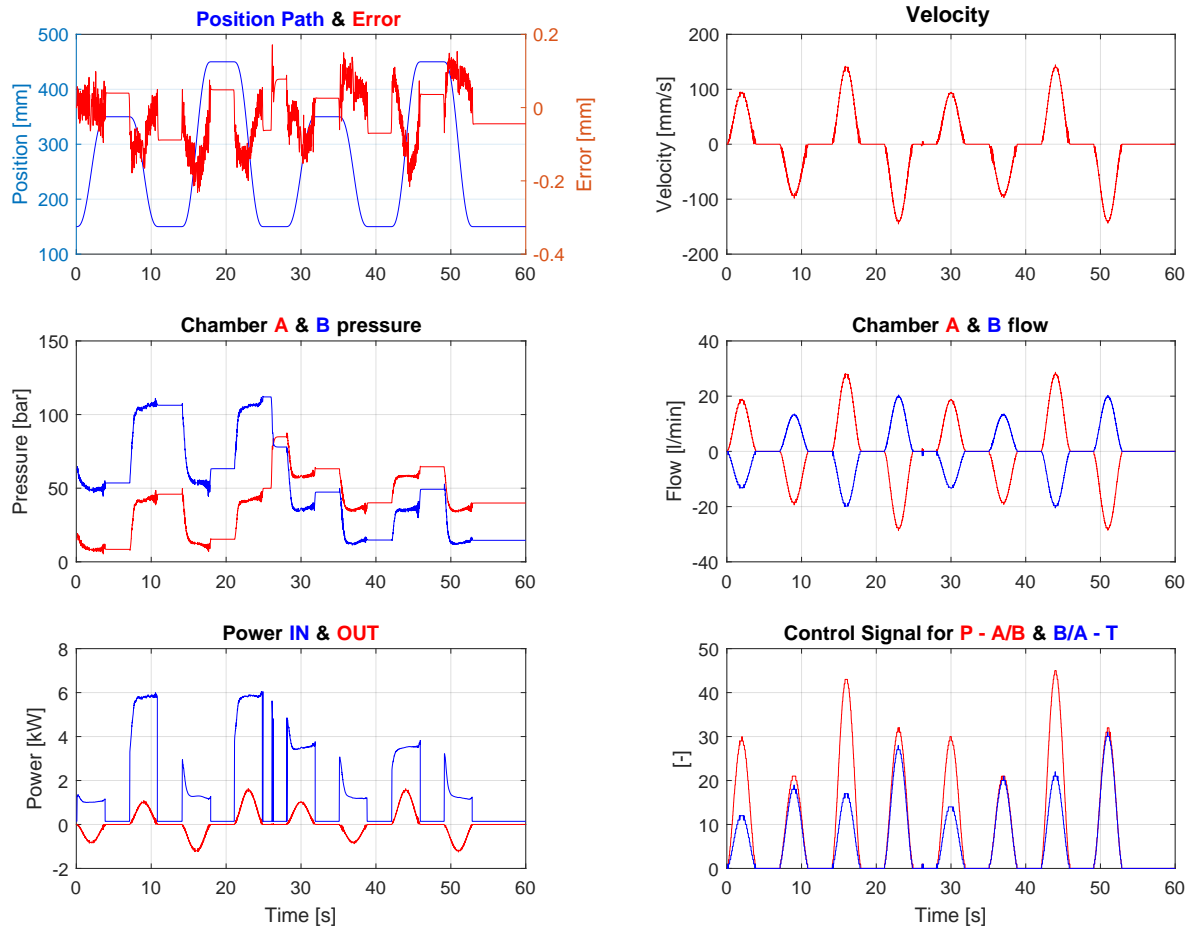


Figure 6.15: Plots of system response to the DDP system

Position and Accuracy

Position accuracy is very satisfying. It is only reaching $\pm 0.2 \text{ mm}$. Another good feature is that error is not varying around zero at each stage. It is either under or over. This results in less noise and less flow and pressure peaks.

Velocity and Flow

The flow and velocity have a smooth progression without high noise or too large steps. It is in practice reflected in smooth motions which again reduce the impact of vibration and fatigue on the system.

Pressure

Due to relatively stable error sign and smooth flow progression, the pressure became less noisy without any rough peaks. The highest value is 110 *Bar* at 24 *s*. In the second stage of the load case the maximum pressure is only reaching about 65 *Bar*.

Power

The maximum power is directly connected to the load pressure. The plot shows the motor will not be fully loaded when high pressure is not required. It indicates possibility for increased efficiency specially when combined with a regenerative system.

Control Signals

Stable signal with logical stepped progression indicates absence of unnecessary switching of valves which will be reflected in higher life time of the valves.

Impact of Response Time

The impact of response time is clearly seen in **Figure 6.16**. The higher the response time is, the larger the position error becomes. All four tested values were able to hold the error limitation of ± 0.5 *mm*. However, the smallest values gave the best and least noisy results.

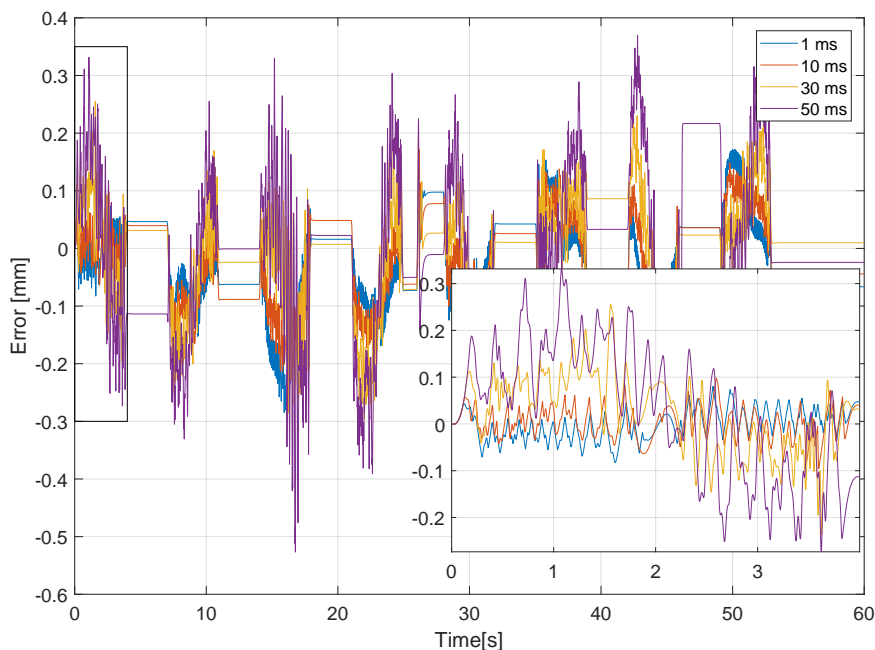


Figure 6.16: Position error by different valve response times in combination 5

Impact of Bulk modulus

Reduced Bulk modulus from 15000 down to 10000 *Bar* increased the oscillation in the system and consequentially the position error is increased as shown in **Figure 6.17**.

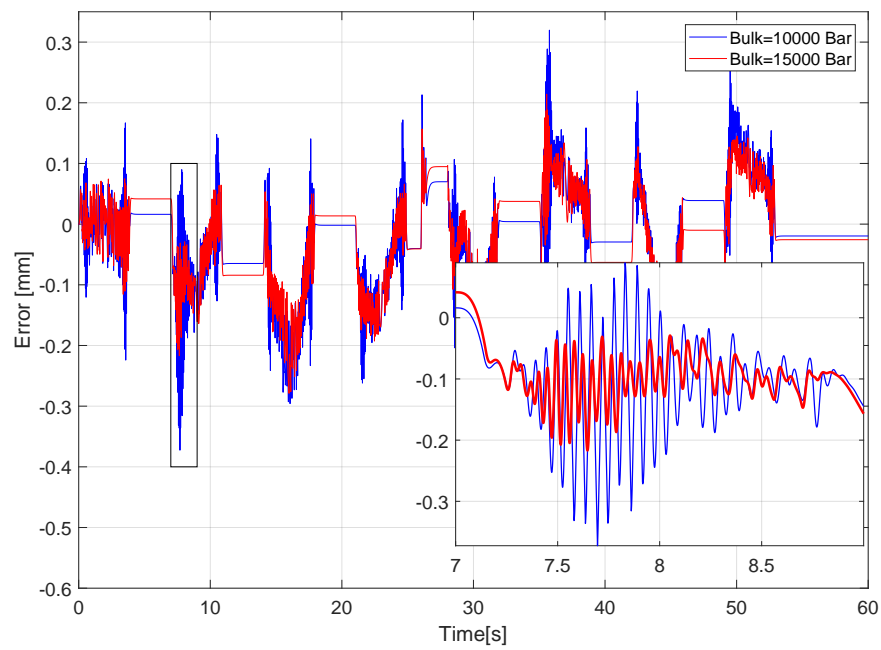


Figure 6.17: Position error by different Bulk modulus in combination 5

6.3 Simulation of a single-boom crane

In the last week of the project, a kinematic model of a crane located in the laboratory at University of Agder . Real measurement data from this crane were provided from [25]. The measurements were of four different cycles, however a load sensing hydraulic system was used for these data.

6.3.1 Crane kinematic model

The model provided a dynamic load case different than the previously used load case of $\pm 10000\text{ N}$. This kinematic model was derived by Prof. Lasse Schmidt from Aalborg University and uses the terms G_{eq} (Equivalent Gravitational Load), C_{eq} (Equivalent Coriolis Force), and M_{eq} (Equivalent Inertial Load) to describe the kinematics of the crane. **Figure 6.18** presents a picture and the main components of the actual crane.

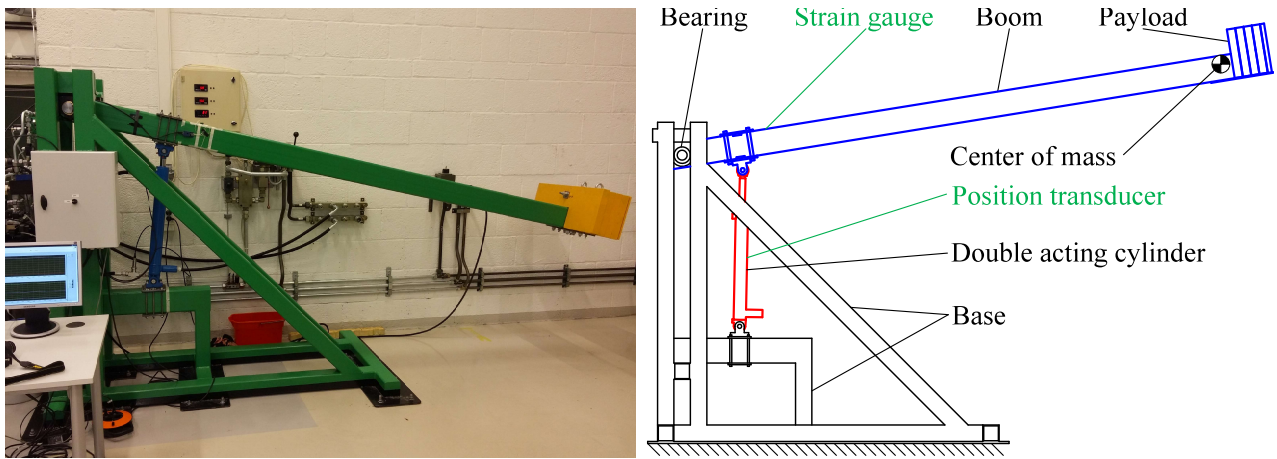


Figure 6.18: Picture and main components of test crane [26]

Figure 6.19 presents the main dimensions used to derivate the kinematic model.

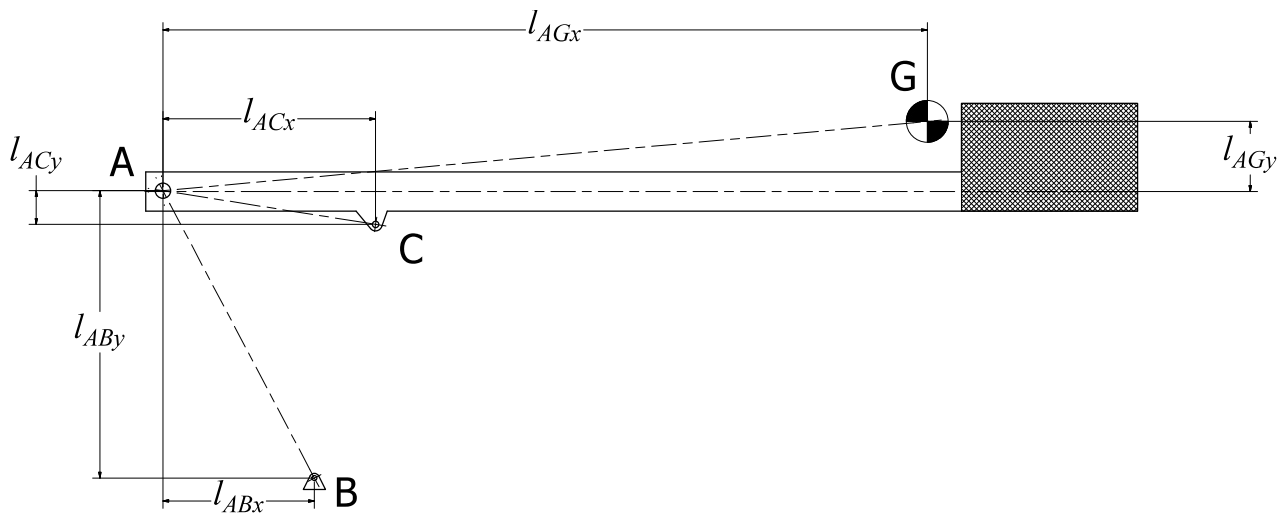


Figure 6.19: Main dimensions of test crane

Here also:

$$l_{AB} = \sqrt{l_{ABx}^2 + l_{ABy}^2} \quad (6.1)$$

$$l_{AC} = \sqrt{l_{ACx}^2 + l_{ACy}^2} \quad (6.2)$$

$$l_{AG} = \sqrt{l_{AGx}^2 + l_{AGy}^2} \quad (6.3)$$

The equivalent gravitational load, inertial load and Coriolis force are implemented in the cylinder force equation. The resulting formula for the cylinder force is presented in **Eq.(6.4)**. The derived expressions for C_{eq} , G_{eq} and M_{eq} are due to complexity presented in **Appendix C**. The equivalent load components are plotted for the length of the cylinder in **Figure 6.20**.

$$F_{Cyl} = F_f + G_{eq} + C_{eq} \cdot v^2 + M_{eq} \cdot a \quad (6.4)$$

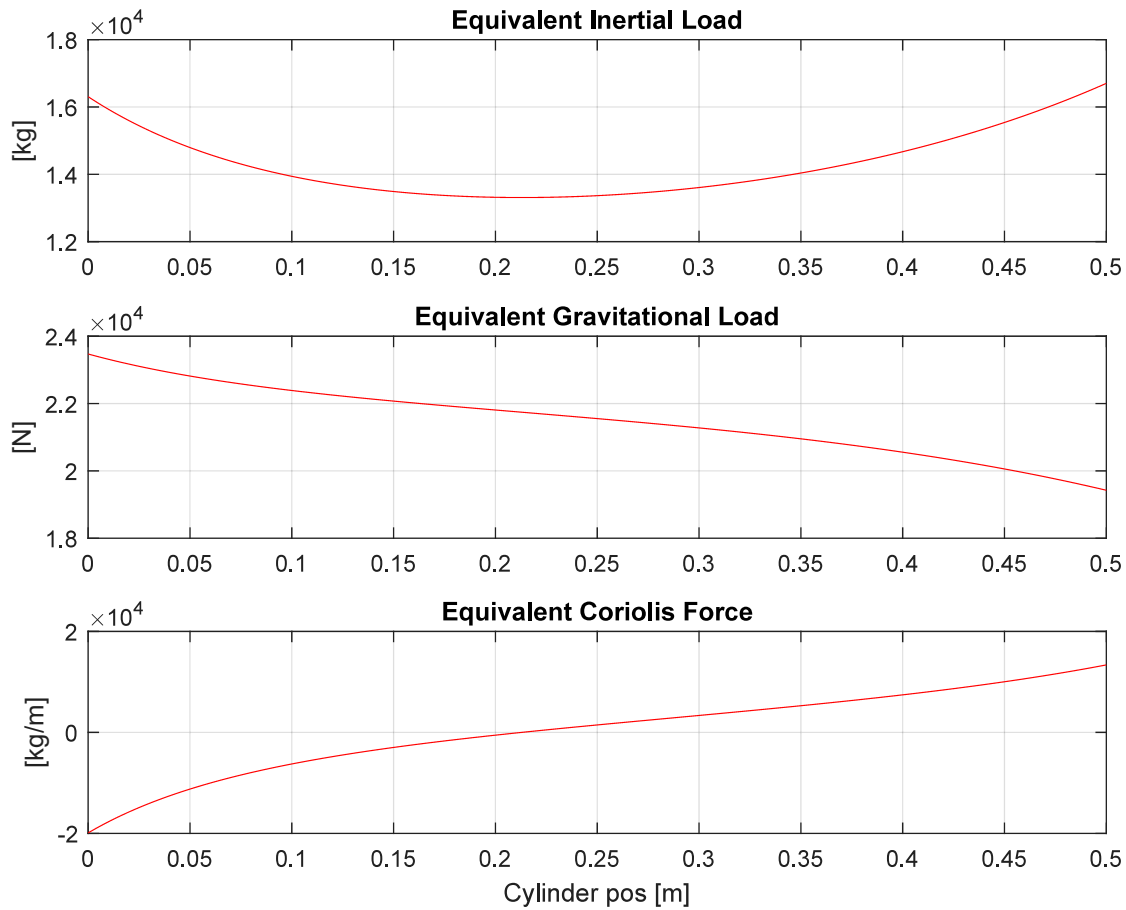


Figure 6.20: Equivalent load components over the length of the cylinder

The hydraulic load sensing system implemented in the test experiment is presented in **Figure 6.21**. Here, the opening of the proportional valve controlling the flow from the pressure source, is adjusted depending on the measured load pressure.

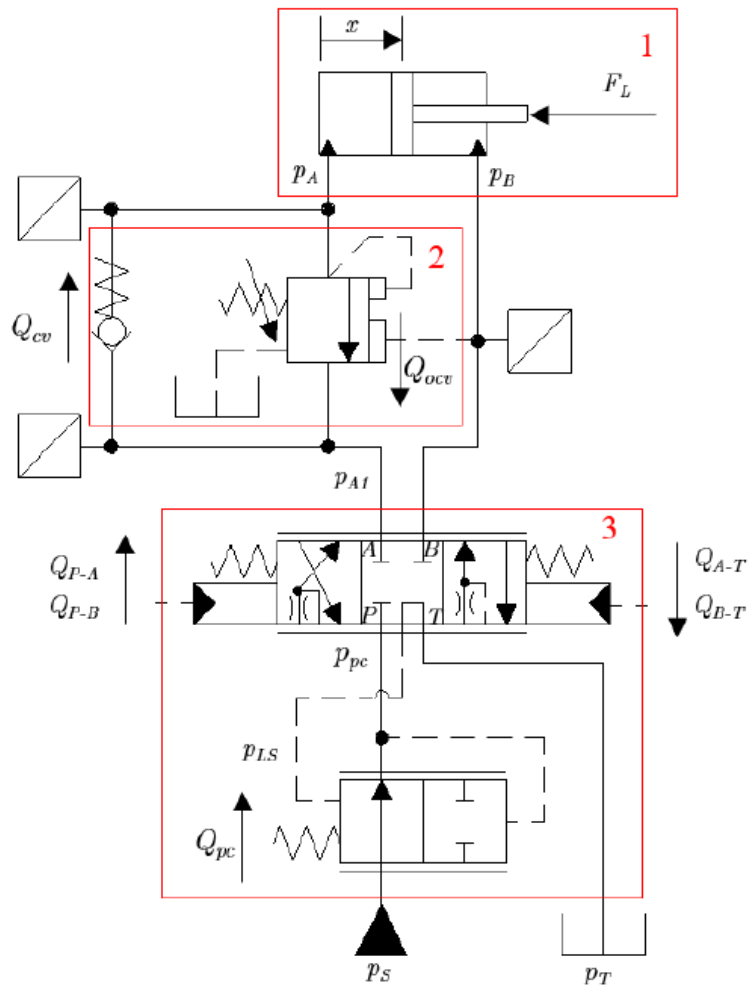


Figure 6.21: Hydraulic load sensing system used in the experiment [25]

6.3.2 Simulations results and comparison

The kinematic model of the test crane is implemented in simulation model of system combination 5 **6.2.5**. The reason for that is the similarity of working principle between combination 5 and the load sensing system. The simulation is executed in four different working cycles with the same parameters as in the previous section. **Figure 6.22** presents the four working cycles that were performed in the test experiment. The same cycles are used to simulate the selected system combination.

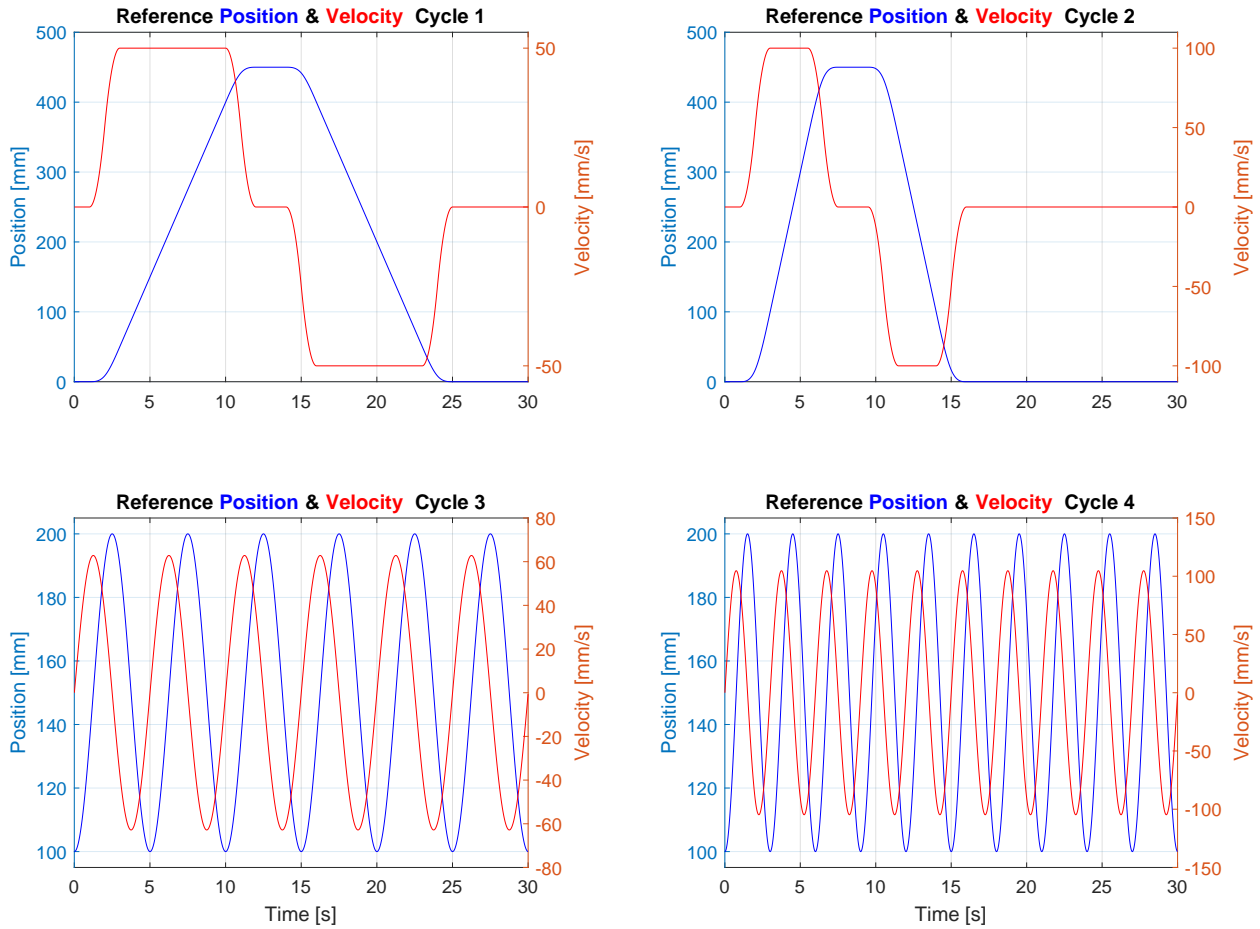


Figure 6.22: Performed working cycles

It is important to mention the comparison is not 100% fair since the digital hydraulic system is only simulated and due to time constrains not tested in practice. Basically the simulation on the crane model is executed to prove that the designed system is able to operate a mechanical system from real life with varying load.

Figures 6.23-6.26 present the measured data of the load sensing system in the left column and the simulated data from the digital hydraulic system in the right column. Each figure is presenting the results for one working cycle. The simulation results show the ability of the digital hydraulic system to operate a real crane. It manages mostly to keep the position error within acceptable values. The measured results from the test experiment are oscillating a lot due to the combination of pressure compensator and over-center valve in the load sensing system.

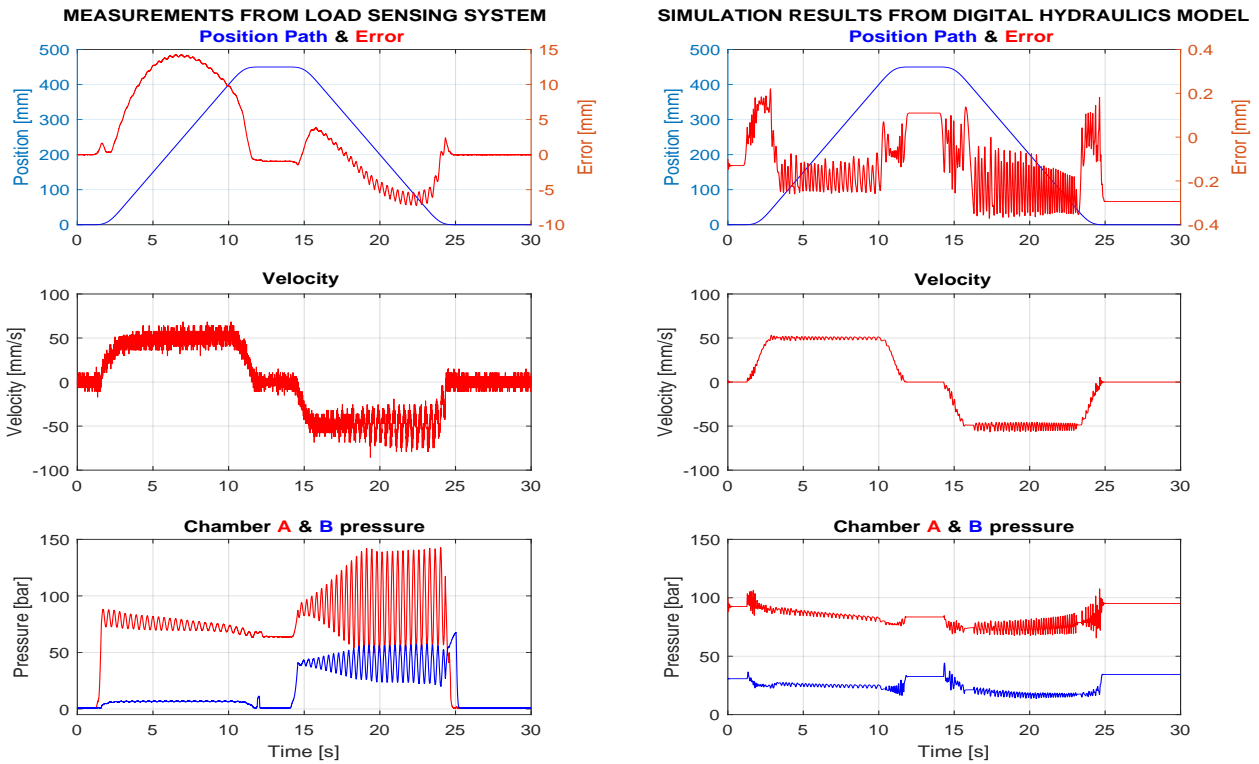


Figure 6.23: Results comparison for working cycle 1

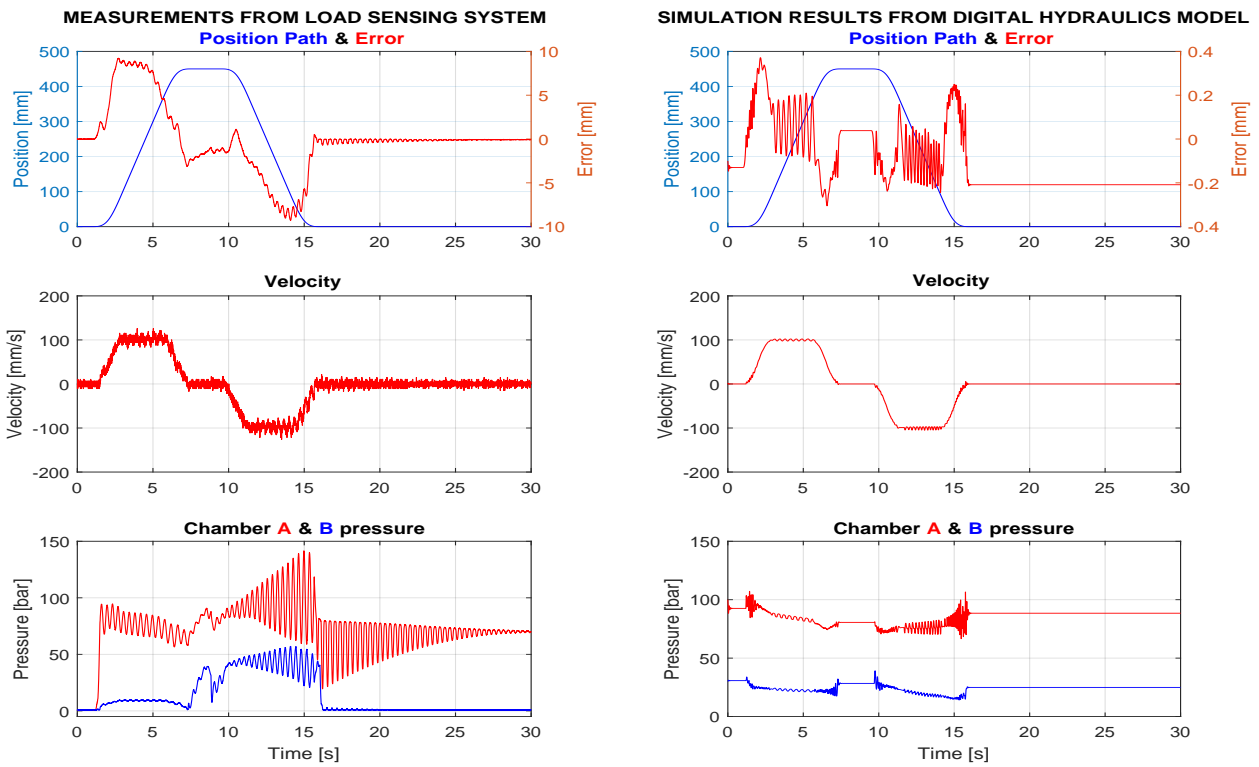


Figure 6.24: Results comparison for working cycle 2

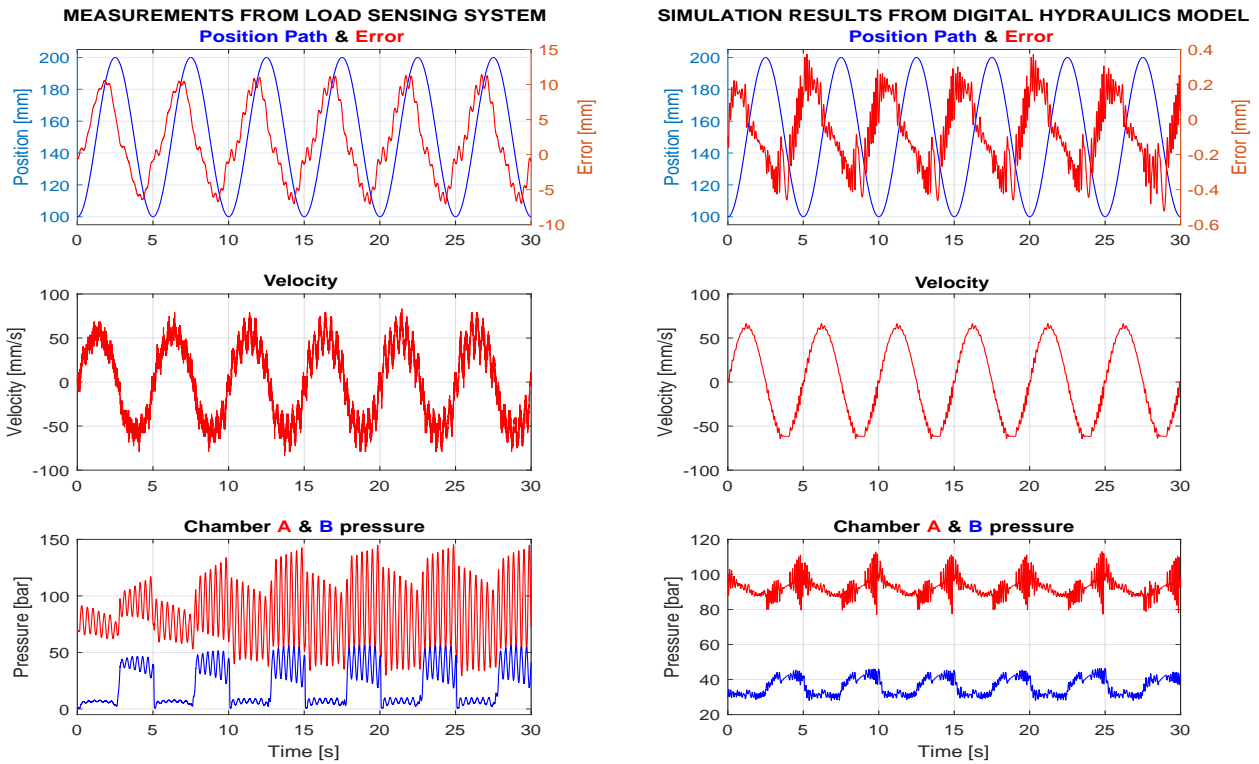


Figure 6.25: Results comparison for working cycle 3

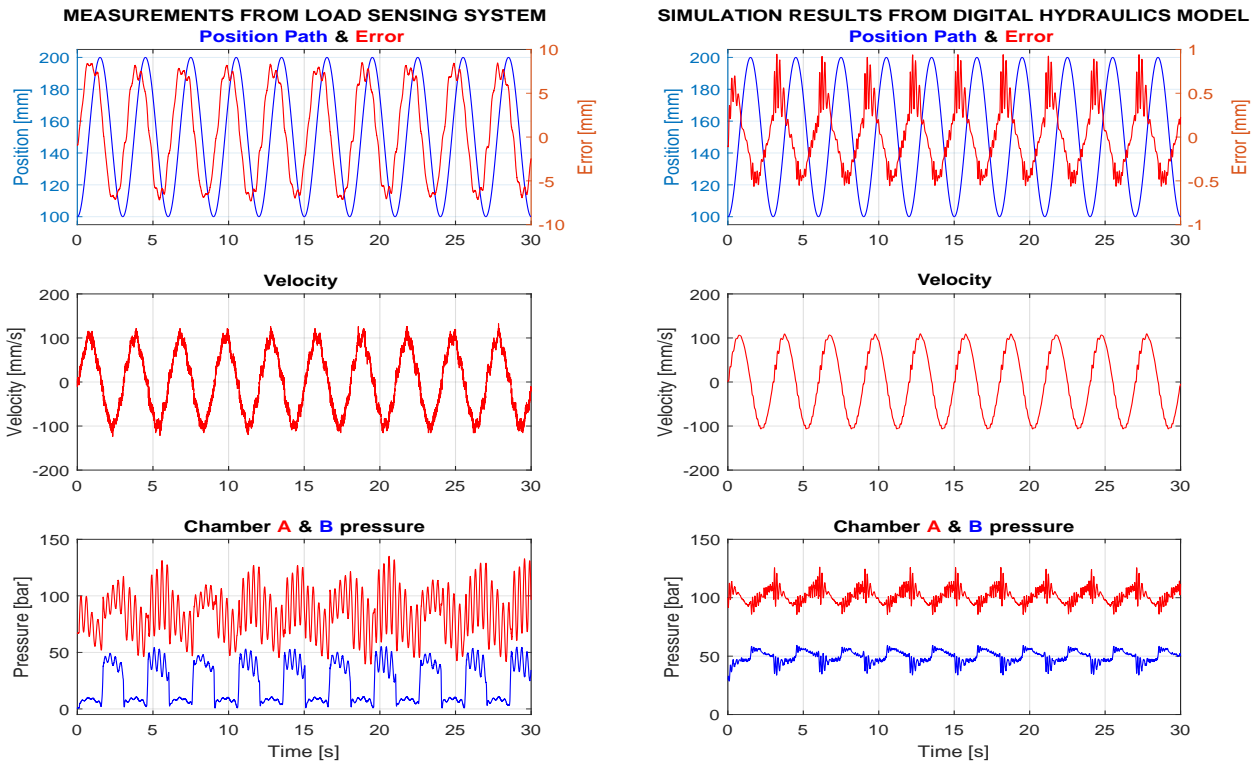


Figure 6.26: Results comparison for working cycle 4

7 | Discussion

The five different combinations selected in **Table 6.1** of hydraulic architectures and control algorithms based on PCM coded DFCU and DDP resulted in different behaviours. Each combination has its strengths and weaknesses. To highlight these, all simulated systems are weighted against each other for different criteria. **Table 7.1** presents the five simulated systems weighted according to different criteria. A score of 5 is best and 1 is worst. The scores are summarized to give an indication for which combination performed best and worst.

Table 7.1: System combinations results weighting

Specification \ Combination	Comb. 1	Comb. 2	Comb. 3	Comb. 4	Comb. 5
Accuracy	2	1	3	4	5
Number of valves	1	1	3	4	2
Valves durability	4	3	2	3	3
Response time sensitivity	3	2	4	1	5
Load holding capability	5	5	5	5	5
Fault robustness	5	5	4	2	3
Control robustness	4	3	2	3	2
Power	2	2	2	4	3
Cost	3	3	4	1	4
Size	3	3	4	2	5
SUM	32	28	33	29	37

After analysing the five combinations in **Table 7.1** some conclusions related to the given criteria can be drawn. For example:

- **Accuracy**
Combination 5 is performing best here. However, it demands the load is not changing direction. If the load is changing direction the best system is combination 4.
- **Power**
Combination 4 is using the least power and assumed to be the most efficient system.
- **Durability**
Combination 1 & 2 are switching less than the other three because of the doubled number of flow controlling valves.
- **Feasibility**
Combination 5 is the least sensitive to valves response time and assumed to be feasible with the conventional ON/OFF valves.
- **Load robustness**
Combination 1 & 2 have pressure measurements in the cylinder and can detect changes in the load. It is assumed that these fits best when the load is changing.
- **Controller optimization**
It is important to note that although combination 2 gave the poorest results it does have the controller with the most room for optimization.

The achieved result from the provided crane kinematic model are very promising. The system performed as expected in the simulation. The position error is held within acceptable range. The pressure is not too noisy and the flow has a stepped progression. Assumed a real model of combination 5 would perform similarly to the simulation, it would be a potential and beneficial alternative to the load-sensing system.

Considering performed simulations results and the designed hydraulic systems and control systems presented in this thesis, gained advantages and faced challenges can be drafted in the following two sections.

7.1 Advantages

Digital hydraulics implementation in this thesis represented by ON/OFF valves and digital displacement pumps has led to new benefits in addition to the benefits gained by the self-contained design. Some of the most significant advantages are:

- **Load holding capability**
The biggest part of the ON/OFF valves are zero leak or close to zero leak compared to conventional servo and proportional valves. This leads to both enhanced safety in the system and reduction of cost by cutting of the use of extra load loading valves.
- **Valves robustness**
The use of ON/OFF valves reduces the sensitivity of the system for external influential factors. Normally the tuning of the servo valves is demanding and challenging part of designing a control system. This problem is not present at all in digital hydraulics and the control system can perform independent of the changing environment.

- **Simple interface**

Digital valves can be easily connected direct to for example a PLC unit. The need for signal amplifier and converter is reduced significantly.

- **Cost**

Despite relatively limited existing ready to market digital hydraulic components, the idea has a large potential of cutting the cost by replacing the normally expensive servo valves.

7.2 Challenges

There are some challenges with the implementation of digital hydraulics. By analysing the results plots in the previous chapter and the hydraulic architecture, the following challenges can be noticed:

- **Components availability**

Since the interest for digital hydraulics still relatively new, it is a challenge to all required components from manufacturer without the need of some modifications. Especially pumps that are binary sized, are difficult to find.

- **Vibration and fatigue**

Stepwise flow progression leads to pressure peaks and consequently to vibration in the mechanical system. The different systems in this thesis are exposed to vibration in different rates. However, all systems are at this point worse than systems with servo or proportional valves.

- **Size**

The design of an self-contained system faces a problem related to size of the required components compared to the size of the cylinder itself. Nowadays, ON/OFF valves and DDP are relativity large. However, there are many promising developments in this area that will reduce the size of the components.

8 | Conclusion & Future Work

8.1 Conclusions

The novelty of the designed solution in this thesis, is a result of combining two major new trends in hydraulics; Self-contained approach and digital hydraulics. The components needed for digital hydraulics are becoming more compact, easily available, less complex and profitable. The possibility of designing a digital electro-hydraulic cylinder (DEHC) based on the two mentioned new trends is proven by modelling and simulation of the designed systems. Practical tests and experiments are due to time constraints not performed.

Literature review and some market investigation gave the indication of the possibility to acquire all needed components to build hydraulic architectures for a DEHC. Based on that, four different hydraulic architectures are designed with the intention to exclusively use digital hydraulics. The main focus is set on the flow control. Power regeneration is not considered in this thesis.

There are many ways to control a hydraulic system. Three different control approaches are proposed in this thesis. The first is a position controller based on position feedback and velocity feed forward. The second is similar to the first but with pressure feedback in addition. The third and last is based on the steady states equations of the system.

Based on the assumption that each proposed control approach can be implemented on each designed hydraulic architecture, five combinations are modelled and simulated to test and cover all designed hydraulic architectures and control approaches. A common generic load case and, where possible, identical simulation parameters are used.

The five simulated system combinations resulted different outcomes. However, the common characteristic between the five results is, that it is possible and beneficial to design a self-contained electro-hydraulic cylinder based on digital hydraulics, called in this thesis DEHC. The impact of valve response time is also clear and reasonable, the faster the valves the better accuracy the system can achieve. This conclusion is based only on simulation results but is still a good motivation to start practical experiments.

To couple this work more to reality, a simulation of a selected combination is performed where the load was a kinematic model of a single boom crane from the laboratory at the University of Agder. Again, the results here were satisfying and give an extra motivation to start practical experiments.

8.2 Future Work

By performing practical experiments for one of the systems it would be interesting to see the difference in behaviour between the theoretical simulations and the real world. The valve **WS22GD** from **BUCHER Hydraulics** is recommended to be used in this context. It has a nominal flow of $14 \frac{l}{min}$ at 10 Bar. All the designed hydraulic architectures in this thesis are consisting of the same components except the system with DDP. Therefore, many approaches can be tested if the components are acquired.

A practical experiment would also give the possibility for optimization work to the control algorithms. Especially, controller 3 by the implementing and upgrading to a four edge control.

The systems should also have a better possibility of energy recovery when the load force can do the work. Considering the study made about hybrid actuator in [27], the following **Figure 8.1** present a proposed hydraulic architecture to increase efficiency by recovering energy.

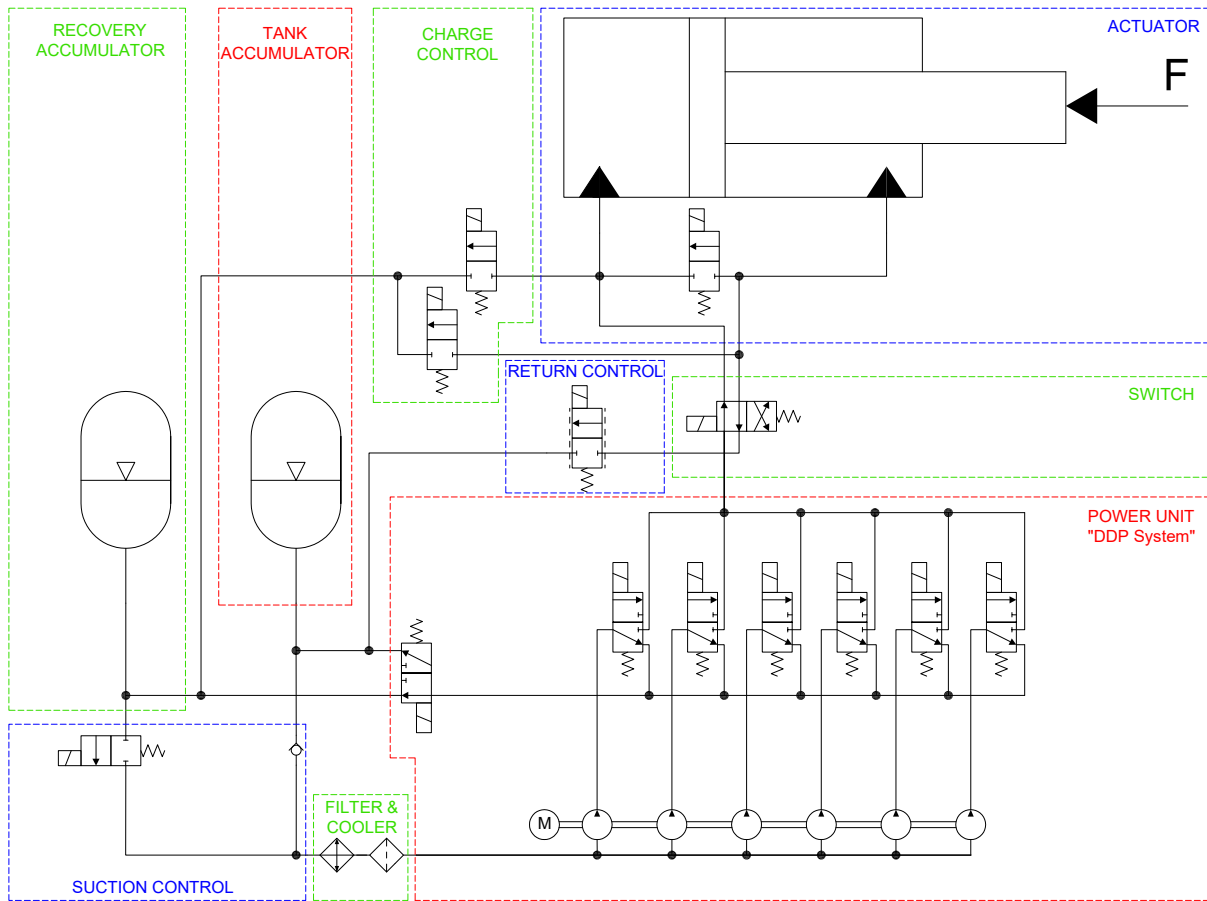


Figure 8.1: Proposed hybrid system based on 6 binary sized pumps

Figure 8.2 shows the working principals of the proposed system. The symbols for the valves are removed to simplify the figures and increase readability of the recovery modes. By moderate restricting load, the outflow from the rod side is used to reduce the need of flow delivered by the pump in extraction mode. In retraction mode, the pump is connected to rod side and the piston side is connected directly to tank. The same approaches is used by a large restricting load. The difference here is that the suction port of the pump is connected to the accumulator used to save energy. By reducing the pressure drop over the pump, the needed power is also reduced.

Overrunning load gives the possibility to recover energy. By moderate overrunning load and extraction mode, the outflow from rod side is connected to the accumulator to charge it with the pressure created by the load and the effective area ratio. If the cylinder here is in retracting mode, the outflow from piston side is connected to the suction port and the accumulator at the same time. This results in a charged accumulator and reduced pressure drop over the pump.

In case of large overrunning load, the accumulator is connected to the outflow both during extraction and retraction. Meter-out flow control might be necessary here to avoid cavitation.

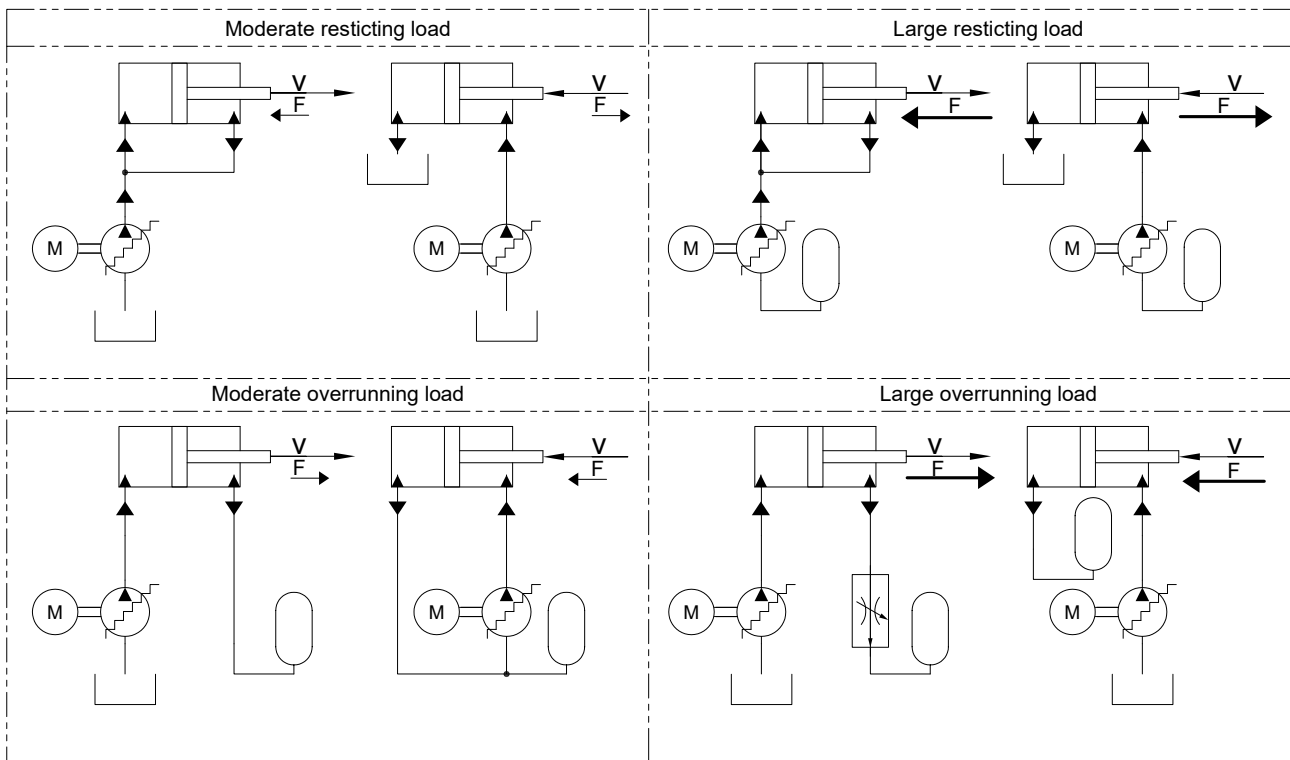


Figure 8.2: Proposed driving and energy recovery modes

Bibliography

- [1] B. Rexroth. (27.03.2018) Intelligent self-sufficient systems for powerful drive tasks. [Online]. Available: <https://www.boschrexroth.com/en/xc/company/press/index2-16194>
- [2] Servi. (27.03.2018) Servi hybrid drive. [Online]. Available: https://www.servi.no/media/wysiwyg/servi_hybrid.png
- [3] B. Rexroth. (27.03.2018) Servo-hydraulic actuator. [Online]. Available: https://dc-corp.resource.bosch.com/media/general_use/products/industrial_hydraulics_1/systems_1/Technical_Information_RD_08137.pdf
- [4] Available at https://www.nov.com/uploadedImages/Content/Segments/Rig_Systems/Marine_and_Construction/Lifting_and_Handling/Cranes/Knuckle_Boom_Cranes/Knuckle%20Boom%20Crane%2013_1200x650.png?n=2714 (2018/04/09).
- [5] M. Linjama, “Digital fluid power: State of the art,” in *12th Scandinavian International Conference on Fluid Power, Tampere, Finland, May, 2011*, pp. 18–20.
- [6] M. Linjama and M. Vilenius, “Digital hydraulics-towards perfect valve technology,” in *In: Vilenius, J. & Koskinen, KT (eds.) The Tenth Scandinavian International Conference on Fluid Power, May 21-23, 2007, Tampere, Finland, SICFP’07, 2007*.
- [7] M. Linjama, M. Paloniitty, L. Tiainen, and K. Huhtala, “Mechatronic design of digital hydraulic micro valve package,” *Procedia engineering*, vol. 106, pp. 97–107, 2015.
- [8] “Digital hydraulic manifold,” <http://www.tut.fi/en/digital-fluid-power/index.htm>, accessed: 2018-05-07.
- [9] T. Lantela and M. Pietola, “High-flow rate miniature digital valve system,” *International Journal of Fluid Power*, vol. 18, no. 3, pp. 188–195, 2017.
- [10] M. Paloniitty, M. Linjama, and K. Huhtala, “Equal coded digital hydraulic valve system—improving tracking control with pulse frequency modulation,” *Procedia engineering*, vol. 106, pp. 83–91, 2015.
- [11] B. Winkler, “Recent advances in digital hydraulic components and applications,” in *Proc. of The Ninth Workshop on Digital Fluid Power, Aalborg, Denmark, 2017*.
- [12] A. Laamanen, M. Linjama, and M. Vilenius, “On the pressure peak minimization in digital hydraulics,” in *The Tenth Scandinavian International Conference on Fluid Power, May 21-23, 2007, Tampere, Finland, SICFP’07*. Citeseer, 2007.
- [13] M. Huova and A. Plöckinger, “Improving resolution of digital hydraulic valve system by utilizing fast switching valves,” in *In: Laamanen, A. & Linjama, M.(eds.). Proceedings of the Third Workshop on Digital Fluid Power, October 13-14 2010, Tampere, Finland, 2010*.
- [14] A. Plöckinger, C. Gradl, and R. Scheidl, “High accuracy sensorless hydraulic stepping actuator,” in *Proceedings of The Eight Workshop on Digital Fluid Power, May 24-25, 2016, Tampere, Finland*.
- [15] M. Linjama, A. Laamanen, and M. Vilenius, “Is it time for digital hydraulics?” in *In: Koskinen, KT & Vilenius, M.(eds.) The Eight Scandinavian International Conference on Fluid Power, Proceedings of the Conference, May 7-9, 2003, Tampere, Finland, SICFP’ 03, 2003*.

BIBLIOGRAPHY

- [16] Rexroth. (20.05.2018) Rexroth external gear pump. [Online]. Available: https://www.boschrexroth.com/ics/cat/?cat=Industrial-Hydraulics-Catalog&m=XC&u=si&o=Desktop&p=p944845&pi=FB13814B-D996-2402-61AB28FED21545FD_IC_S_82
- [17] artemis. (20.05.2018) artemis. [Online]. Available: http://artemis.armadillojam.co.uk/wp-content/uploads/2015/09/4485646_orig.gif
- [18] M. Linjama, K. T. Koskinen, and M. Vilenius, "Accurate trajectory tracking control of water hydraulic cylinder with non-ideal on/off valves," *International Journal of Fluid Power*, vol. 4, no. 1, pp. 7–16, 2003.
- [19] M. Linjama. (07.03.2018) On the numerical solution of steady-state equations of digital hydraulic valve-actuator system. [Online]. Available: https://www.researchgate.net/profile/Matti_Linjama/publication/303663151_On_the_numerical_solution_of_steady-state_equations_of_digital_hydraulic_valve-actuator/links/5757a89308aef6cbe35f58ef/On-the-numerical-solution-of-steady-state-equations-of-digital-hydraulic-valve-actuator.pdf
- [20] M. Linjama and M. Vilenius, "Improved digital hydraulic tracking control of water hydraulic cylinder drive," *International Journal of Fluid Power*, vol. 6, no. 1, pp. 29–39, 2005.
- [21] M. Linjama, M. Huova, and M. Karvonen, "Modelling of flow characteristics of on/off valves," in *The 5th Workshop on Digital Fluid Power*, 2012.
- [22] M. Flor, S. Scheller, R. Heidenfelder, and B. R. AG, "Digital hydraulics at bosch rexroth—a trend evolves to real applications," in *The fifth workshop on digital fluid power, Tampere, Finland*, 2012.
- [23] T. Børseth and C. H. Solvik, "Stabilization of hydraulically actuated boom using pressure feedback - theoretical and experimental investigation," 2015.
- [24] J. D. Zimmerman, "Toward optimal multi-actuator displacement controlled mobile hydraulic systems," Ph.D. dissertation, Purdue University, 2012.
- [25] J. A. Olsen, G. M. Tesfaghiorghis, and Z. Osinkas, "Implementation of a self-contained electro-hydraulic actuator drive on a single-boom crane," 2018.
- [26] J. K. Sørensen, M. R. Hansen, and M. K. Ebbesen, "Numerical and Experimental Study of a Novel Concept for Hydraulically Controlled Negative Loads," *Modeling, Identification and Control*, vol. 37, no. 4, pp. 195–211, 2016.
- [27] M. Linjama, M. Huova, M. Pietola, J. Juhala, and K. Huhtala, "Hydraulic hybrid actuator: theoretical aspects and solution alternatives," *The 14th*, 2015.

A | Simulations Parameters

Parameter	Description	Value	Unit
m	Load mass	1000	[kg]
d_p	Piston Diameter	65	[mm]
K_v	Flow coefficient of valves	$\frac{\sqrt{12}}{15}$	$[m^3 \cdot \sqrt{\frac{m}{kg}}]$
d_r	Rod Diameter	35	[mm]
V_{A0}	Dead Volume at A-side	0.2	[l]
V_{B0}	Dead Volume at B-side	0.25	[l]
A_A	Effective Area at A-side	3318	[mm ²]
A_B	Effective Area at B-side	2356	[mm ²]
L	Stroke Length	500	[mm]
ρ_c	Area Ratio	1.4083	[-]
p_{max}	Maximum System Pressure	200	[Bar]
ρ	Oil density	870	$[\frac{kg}{m^3}]$
β	Bulk modulus	$1 \cdot 10^4$	[Bar]
ν	Kinematic oil viscosity	$5.1 \cdot 10^{-5}$	$[\frac{m^2}{s}]$
μ	Dynamic oil viscosity	$4.44 \cdot 10^{-2}$	$[\frac{kg}{m \cdot s}]$
f_s	Cylinder static friction	1250	[N]
f_c	Cylinder coulomb friction	600	[N]
f_v	Coeff. of viscous friction for piston	5000	$[\frac{kg}{s}]$
τ_s	Static friction time constant	$\frac{1}{50}$	$[\frac{s}{m}]$
γ	Approximation for friction force	250	[mm]
t_{on}/t_{off}	Valve delay	3	[ms]
t_s	Valve response time	10	[ms]
C_s	Controller sample time	10	[ms]
L_{line}	Hose length	1	[m]
D_{line}	Hose diameter	10	[mm]
V_{lp}	Volume transmission line to accumulator	0.00001	[m ³]
V_{LP}	Low pressure accumulator volume	1	[l]
P_0^{LP}	Low pressure accumulator pre charge	1.8	[bar]
V_{HP}	High pressure accumulator volume	2	[l]
P_0^{HP}	High pressure accumulator pre charge	99	[bar]

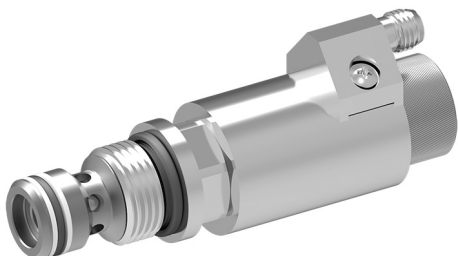
B | Sample valve data sheet

2/2 Cartridge Seat Valve, Size 5

$Q_{\max} = 30 \text{ l/min}$, $p_{\max} = 350 \text{ bar}$

Digital valve, bidirectional seat-valve shut-off, direct acting

Series WS22GD.../ WS22OD...



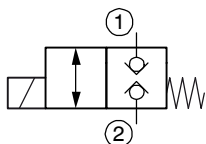
- For use in digital hydraulics
- With bidirectional seat-valve shut-off
- Compact construction for cavity type ALM – M20x1.5
- High switching performance
- Short response times
- All exposed parts with zinc-nickel plating
- High pressure wet-armature solenoids
- The slip-on coil can be rotated, and it can be replaced without opening the hydraulic envelope
- Can be fitted in a line-mounting body

1 Description

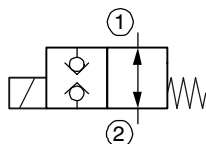
These direct acting 2/2 solenoid operated directional seat valves, series WS22GD... / WS22OD..., are screw-in cartridges with a M20x1.5 or 3/4-16 UNF mounting thread. They are designed on the poppet/seat principle, and are therefore virtually leak-free in both directions of flow (bidirectional seat-valve shut-off). Over-excitation, preferably through an electronic switching device (booster), is required to operate the solenoid. Combined with the low mass of the moving parts, this results in short response times and high switching performance in a compact package. "De-energised closed"

and "de-energised open" functions are available. The straightforward design delivers an outstanding price/performance ratio. The valves are used in applications in digital hydraulics, where fast response and long life with minimum size are vitally important. All external parts of the cartridge are zinc-nickel plated to DIN 50 979 and are thus suitable for use in the harshest operating environments. The slip-on coils can be replaced without opening the hydraulic envelope and can be positioned at any angle through 360°.

2 Symbol



WS22GD...



WS22OD...

3 Technical data

General characteristics	Description, value, unit
Designation	2/2 cartridge seat valve
Design	digital valve, bidirectional seat-valve shut-off, direct acting poppet/seat design (pressure balanced)
Mounting method	screw-in cartridge M20x1.5 or 3/4-16 UNF
Tightening torque	50 Nm \pm 10 %
Size	nominal size 5, cavity type ALM M20x1.5 cavity type AL 3/4-16 UNF please contact BUCHER
Weight	0.20 kg

General characteristics	Description, value, unit
Mounting attitude	unrestricted
Ambient temperature range	-25°C...+80 °C

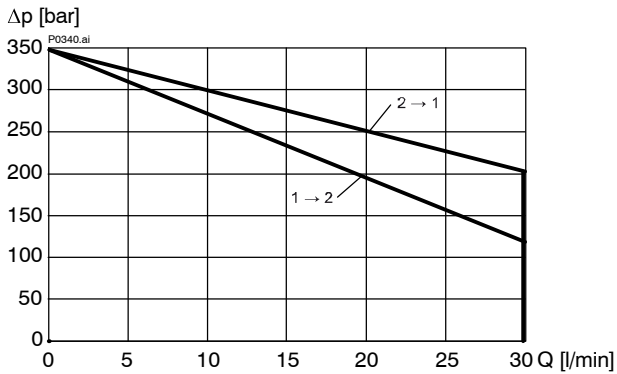
Hydraulic characteristics	Description, value, unit
Maximum operating pressure (ports 1 and 2)	350 bar
Maximum flow rate	30 l/min
Flow direction	1 → 2 / 2 → 1, see symbols
Hydraulic fluid	HL and HLP mineral oil to DIN 51 524; for other fluids, please contact BUCHER
Hydraulic fluid temperature range	-25 °C ... +80 °C
Viscosity range	10...500 mm ² /s (cSt), recommended 15...250 mm ² /s (cSt)
Minimum fluid cleanliness Cleanliness class to ISO 4406 : 1999	class 20/18/15

Electrical characteristics	Description, value, unit								
Excitation voltage	48 V DC (standard)								
Length of over-excitation	4...5 ms								
Supply voltage	12 V DC (standard)								
Voltage tolerance	± 5 % (at ambient temperature < 60°C : ± 10 %)								
Nominal power consumption	15 W at 12 V DC								
Switching time	<table border="0"> <tr> <td style="padding-right: 20px;">- model WS22G...</td> <td>6 ... 20 ms (energising)</td> </tr> <tr> <td></td> <td>10 ... 30 ms (deenergising)</td> </tr> <tr> <td style="padding-right: 20px;">- model WS22O...</td> <td>6 ... 30 ms (energising)</td> </tr> <tr> <td></td> <td>5 ... 20 ms (deenergising)</td> </tr> </table> <p style="font-size: small; margin-top: 5px;">These times are strongly influenced by fluid pressure, flow rate and viscosity, as well as by the dwell time under pressure.</p>	- model WS22G...	6 ... 20 ms (energising)		10 ... 30 ms (deenergising)	- model WS22O...	6 ... 30 ms (energising)		5 ... 20 ms (deenergising)
- model WS22G...	6 ... 20 ms (energising)								
	10 ... 30 ms (deenergising)								
- model WS22O...	6 ... 30 ms (energising)								
	5 ... 20 ms (deenergising)								
Relative duty cycle	- static 100 %								
Duty cycle / switching frequency	- dynamic see characteristics								
Protection class to ISO 20 653 / EN 60 529	IP 65								
Electrical connection:	3-pin plug M8x1								
- PIN 1	48 / 12 V DC								
- PIN 3	0 V								
- PIN 4	not used								

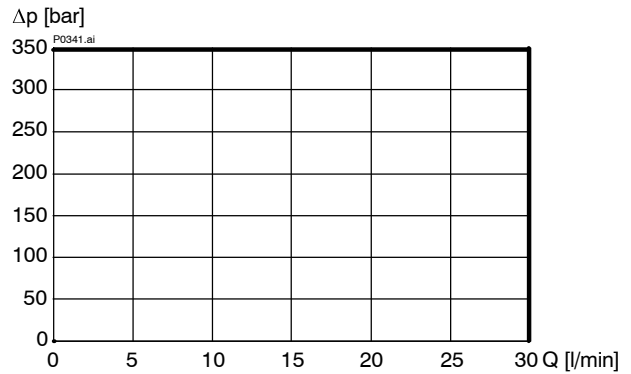
4 Performance graphs

measured with oil viscosity 33 mm²/s (cSt), coil at steady-state temperature and 10 % undervoltage

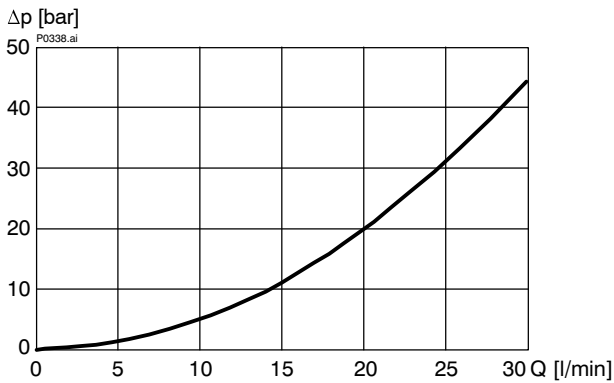
$p = f(Q)$ Performance limits
[WS22GD...]



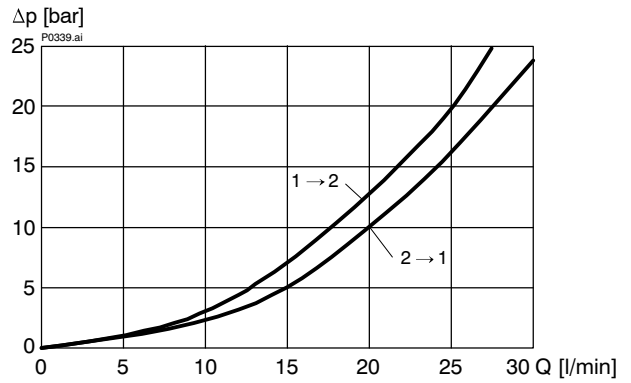
$p = f(Q)$ Performance limits
[WS22OD...]



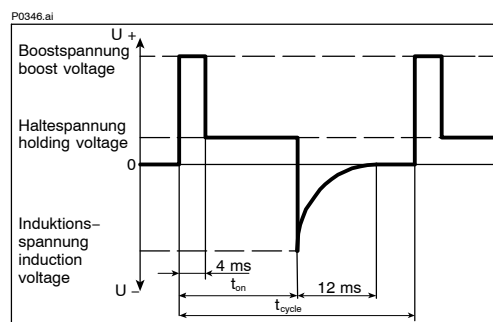
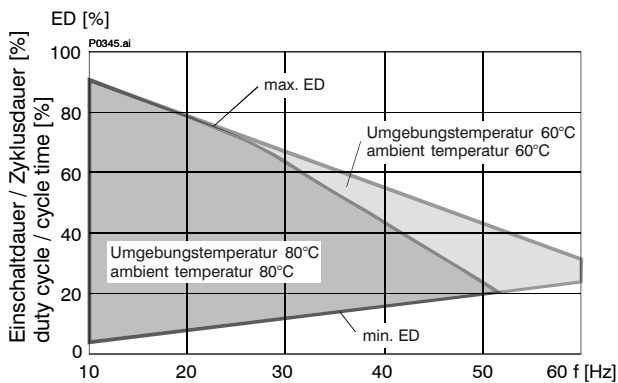
$\Delta p = f(Q)$ Pressure drop - Flow rate characteristic
[WS22GD...]



$\Delta p = f(Q)$ Pressure drop - Flow rate characteristic
[WS22OD...]



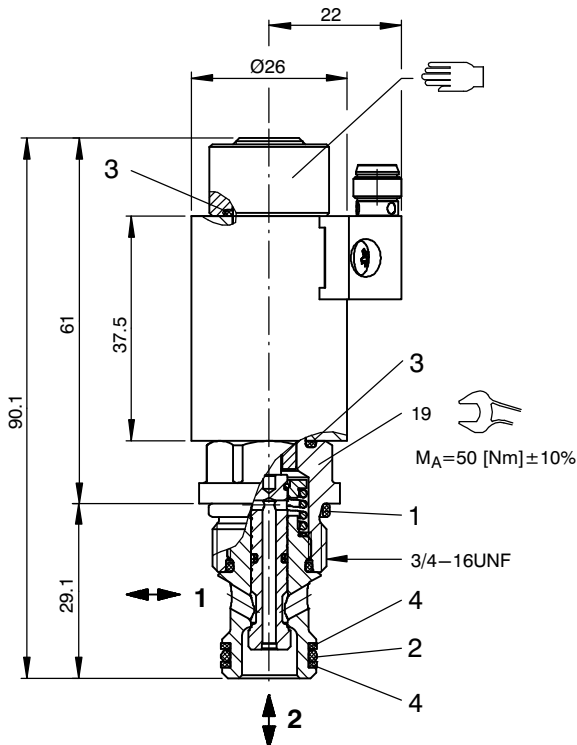
ED = f(f) duty cycle - switching frequency - characteristic [at steady-state coil temperature]



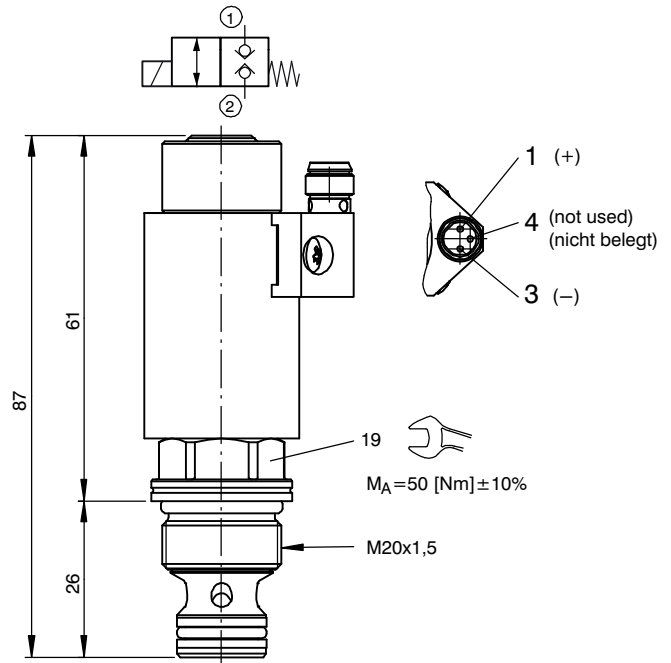
$$ED [\%] = \frac{t_{on}}{t_{cycle}} \times 100$$

5 Dimensions & sectional view

5.1 "Normally closed" design WS22GD...

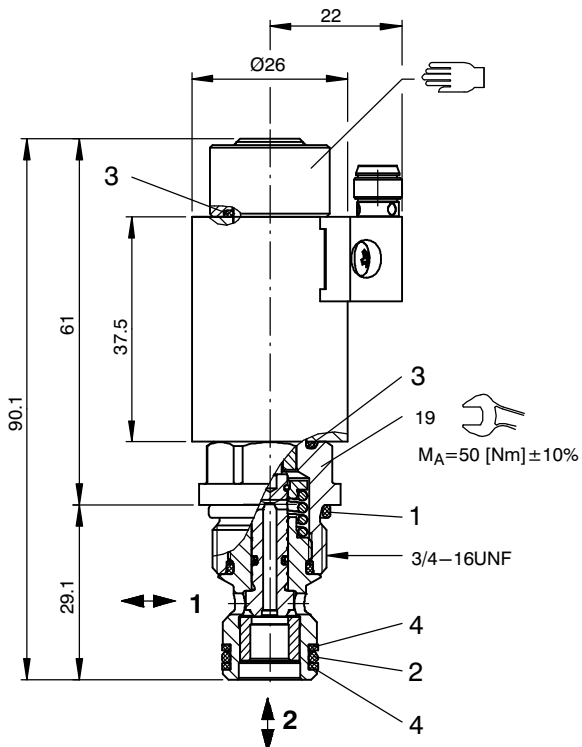


with 3/4-16 UNF thread – cavity type AL
please contact BUCHER

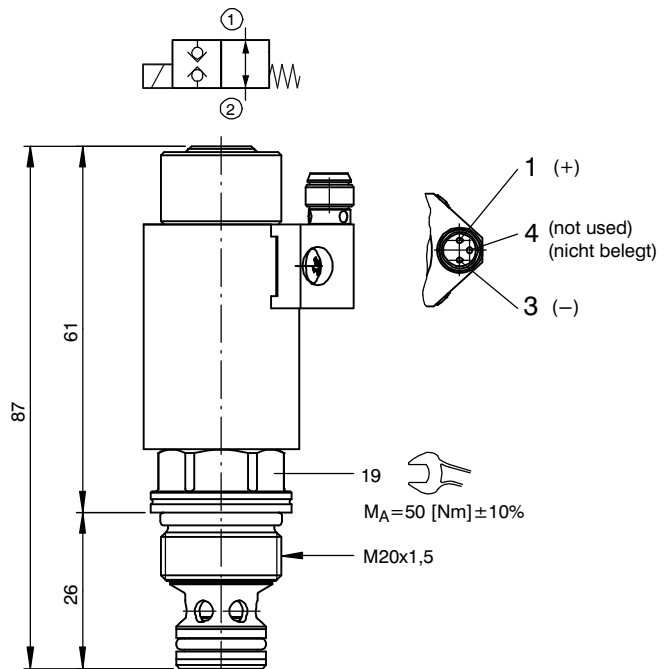


with M20x1.5 thread – cavity type ALM

5.2 "Normally open" design WS22OD...



with 3/4-16 UNF thread – cavity type AL
please contact BUCHER



with M20x1.5 thread – cavity type ALM

6 Installation information



IMPORTANT!

When fitting the cartridges, use the specified tightening torque. No adjustments are necessary, since the cartridges are set in the factory.



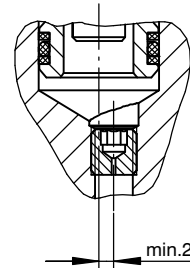
ATTENTION!

Only qualified personnel with mechanical skills may carry out any maintenance work. Generally, the only work that should ever be undertaken is to check, and possibly replace, the seals. When changing seals, oil or grease the new seals thoroughly before fitting them.



ATTENTION!

If an orifice is fitted directly in port 2 close to the valve, and if the flow direction is from 2 to 1, it is important to ensure that the axis of the orifice drilling is offset from the valve axis by at least 2 mm!



3/4-16 UNF "A" – NBR seal kit no. DS-435-N ¹⁾

Item	Qty.	Description
1	1	O-ring no. 017 \varnothing 17,17 x 1,78 N90
2	1	O-ring no. 014 \varnothing 12,42 x 1,78 N90
3	2	O-ring \varnothing 12.00 x 1.50 Viton
4	2	Backup ring \varnothing 10.70 x 1,45 x 1,0 FI0751



IMPORTANT!

¹⁾ Seal kit with FKM (Viton) seals, no. DS-435-V

M20x1.5 "Z" - NBR seal kit no. DS-436-N ¹⁾

Item	Qty.	Description
1	1	O-ring no. 017 \varnothing 17,17 x 1,78 N90
2	1	O-ring no. 013 \varnothing 10,82 x 1,78 N90
3	2	O-ring \varnothing 12.00 x 1.50 Viton
4	2	Backup ring \varnothing 9.90 x 1,45 x 1,4 FI0751



IMPORTANT!

¹⁾ Seal kit with FKM (Viton) seals, no. DS-436-V

7 Ordering code

Ex.

W S 22G D Z 5 - 1 12 D

- W = directional valve
- S = seat valve, direct acting
- 22G = 2/2 function, de-energised closed
- 22O = 2/2 function, de-energised open
- D = digital valve
- Z = special features - with M20x1.5 thread (standard)
- A = standard model - with 3/4 - 16 UNF thread (please contact Bucher)
- 5 = nominal size 5
- (blank) = NBR (Nitrile) seals (standard)
- V = FKM (Viton) seals (special seals - please contact BUCHER)
- 1 ... 9 = design stage (omit when ordering new units)
- ... = voltage e.g. 12 (12 V)
- D = current DC
- (blank) = M8x1 male connector (standard)
- F = for flying leads (1000 mm), please contact Bucher

8 Related data sheets

Reference	(Old no.)	Description
400-P-040011	(i-32)	The form-tool hire programme
400-P-040171	(i-33.10)	Cavity type AL
400-P-040201	(i-33.13)	Cavity type ALM
400-P-720101	(G-4.10)	Line-mounting body, type GALA (G 3/8")
400-P-720105	(G-4.11)	Line-mounting body, type GALMA (M20 x 1.5)

info.ch@bucherhydraulics.com

www.bucherhydraulics.com

© 2015 by Bucher Hydraulics AG Frutigen, CH-3714 Frutigen

All rights reserved.

Data is provided for the purpose of product description only, and must not be construed as warranted characteristics in the legal sense. The information does not relieve users from the duty of conducting their own evaluations and tests. Because the products are subject to continual improvement, we reserve the right to amend the product specifications contained in this catalogue.

Classification: 430.300.-.305.305.300

APPENDIX B. SAMPLE VALVE DATA SHEET

C | Expressions for load components

```

1 % Equivalent Gravitational Load [N]
2 Geq = -0.2e1*sqrt(-(x-L_AB+L_min+L_AC)*(x+L_min-L_AC-L_AB)*(x+L_AB+...
3     L_min-L_AC)*(x+L_AB+L_min+L_AC))*g*m_cm*(cos(acos((L_AB^2+L_AC^2-...
4     (x+L_min)^2)/L_AC/L_AB/0.2e1)-atan(L_ABy/L_ABx)+atan(L_ACy/L_ACx)+...
5     atan(L_AGy/L_AGx))*L_AGx-sin(acos((L_AB^2+L_AC^2-(x+L_min)^2)/L_AC
6     /...
7     L_AB/0.2e1)-atan(L_ABy/L_ABx)+atan(L_ACy/L_ACx)+atan(L_AGy/L_AGx))...
8     *L_AGy)*(x+L_min)/(x-L_AB+L_min+L_AC)/(x+L_min-L_AC-L_AB)/(x+L_AB+...
9     L_min-L_AC)/(x+L_AB+L_min+L_AC);
10 % Equivalent Inertial Load [kg]
11 Meq = -4*(L_AGx^2*(x+L_min)*m_cm+L_AGy^2*(x+L_min)*m_cm+(x+L_min)*J_cm)
12     ...
13     *(x+L_min)/(-x+L_AB-L_min-L_AC)/(-x+L_AB-L_min+L_AC)/(x+L_AB+...
14     L_min+L_AC)/(x+L_AB+L_min-L_AC);
15 % Equivalent Coriolis Force [N/(m/s)^2] = [kg/m]
16 Ceq = 4*((L_AGx^2+L_AGy^2)*m_cm+J_cm)*(x+L_min)*(-L_AB^2+L_AC^2+(x+...
17     L_min)^2)*(L_AB^2-L_AC^2+(x+L_min)^2)/(x+L_min-L_AC-L_AB)^2/(x-...
18     L_AB+L_min+L_AC)^2/(x+L_AB+L_min+L_AC)^2/(x+L_AB+L_min-L_AC)^2;

```